9-1-2001

Report on Field Measurements and Assessment of the I-64 Kanawha River Bridge at Dunbar, West Virginia

Robert J. Connor

John W. Fisher

LEHIGH
University

Report on Field Measurements and Assessment of the I-64 Kanawha River Bridge at Dunbar, West Virginia

Final Report

by

Robert J. Connor

and

John W. Fisher

ATLSS Report No. 01-14

September 2001

ATLSS is a National Center for Engineering Research on Advanced Technology for Large Structural Systems

117 ATLSS Drive
Bethlehem PA, 18015-4729

Phone: (610)758-3525
Fax: (610)758-5553

http://www.atlss.lehigh.edu
Email: inatl@lehigh.edu

Report on Field Measurements and Assessment of the I-64 Kanawha River Bridge at Dunbar, West Virginia

Final Report

by

Robert J. Connor
Research Engineer
ATLSS Engineering Research Center

and

John W. Fisher
Co-Director
ATLSS Engineering Research Center

ATLSS Report No. 01-14

Prepared for:
T.Y. Lin International
and
The West Virginia Department of Transportation
September 2001

ATLSS is a National Center for Engineering Research on Advanced Technology for Large Structural Systems

117 ATLSS Drive
Bethlehem PA, 18015-4729

Phone: (610)758-3525
Fax: (610)758-5902

www.atlss.lehigh.edu
Email: inatl@lehigh.edu

TABLE OF CONTENTS

1.0 Introduction

This report discusses and summarizes the results of the field testing performed on portions of the I-64 bridge over the Kanawha River. These results are utilized in assessing the existing retrofits, the potential for further fatigue cracking and corrective measures to enhance service life.

The entire structure consists of several spans which cross railroad tracks, the Kanawha River, and local roads. The portion of the structure under investigation is the three-span continuous plate girder bridge over the Kanawha River shown in Figure 1.1. Instrumentation was concentrated in spans 10 and 11, which are approximately 440ft and 220ft long, respectively. The four plate girders vary from about 7'-7" to 16'-6" deep and are spaced 23'-3".

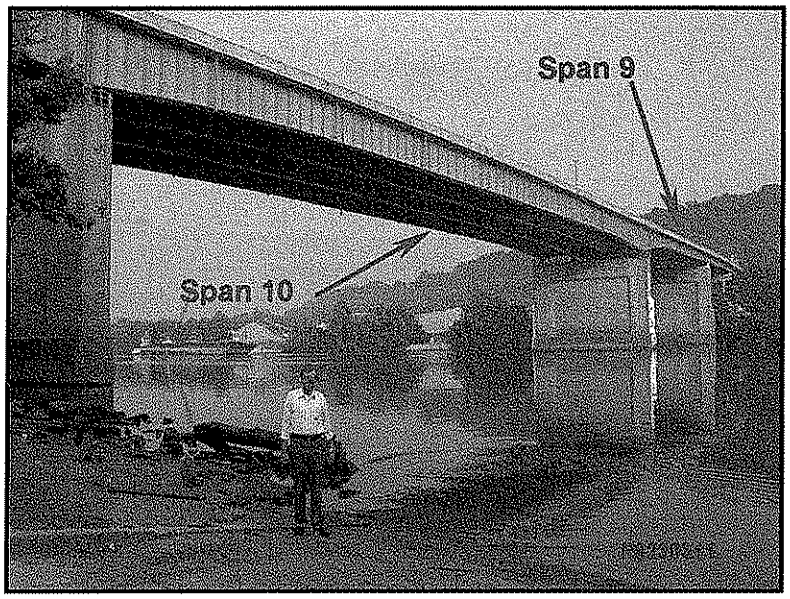

Figure 1.1 – Photograph of elevation view of upstream face of bridge

The structure was completed in 1974 and contains numerous fatigue sensitive details such as lateral gusset plates and transverse connection plate web gaps. The fatigue resistance of many standard details found on the bridge are adequately characterized by the existing AASHTO LRFD Bridge Design Specification [1]. However, several details, such as those susceptible to out-of-plane web gap cracking, were not specifically addressed in the AASHO Specification when the structure was designed and built.

Some fatigue cracking was observed in the 1980's at the top ends of the floorbeam-transverse connection plates on the main girders since none of the connection plates were welded to the top flanges between floorbeam FB2 and FB40. In the negative moment regions these plates were cut short 1 inch from the top tension flanges and fitted elsewhere. Cracks had been detected in all four girders between floorbeam FB6 and FB14 on each side of Pier 9 and between floorbeam FB28 and FB36 on each side of Pier 10. The detected cracks had retrofit holes drilled at the crack tips in 1989. Two retrofit angles

were also installed on each side of all transverse connection plates between FB2 and FB40 at that time. Eight A325 high strength bolts in single shear connected the angles to the top flanges and four A325 bolts in double shear connected the angles to the transverse connection plates.

At a number of locations (FB's 2 to 6, 16 to 26, and 36 to 40 in Bay 2), the lateral gusset plates were not connected by welds to the transverse connection plates. Instead the gusset plates were provided with 1-1/2 inch to 2 inch wide slots. Some cracks were detected in the web gap space between the ends of the lateral gusset plate and the transverse connection plate welds between floorbeam FB2 to FB6 and FB36 to FB40 in the side spans at girders G2 and G3. As a result, four holes were drilled in the girder webs above and below the gusset plate with two on each side of the transverse connection plate in the side spans. In addition, two pieces of small angle (3/8 in.) were bolted to the gussets and transverse connection plates with two bolts in each leg. No changes were made between floorbeam FB16 to FB26 in the main span where A514 steel girders were located. At their lateral gusset connections a smaller lateral gusset for the transverse strut at each floorbeam in bays 1 and 3 was welded to the web and the transverse floorbeam connection plate. This provided a "bridge" across the web gap, however its effectiveness was not known.

There was also concern with groove welds in the A514 steel main river span girders between Piers 10 and 11. These groove welds had been evaluated in the 1970's and 1980's because of concern with welded A514 steel members. A major fracture (Bryte Bend Bridge in Sacramento, CA) and the detection of many weld cracks and defects in other A514 steel bridge members (I-24 Bridges at Paducah, KY, Gulf Outlet Bridge in Louisiana, the Benecia-Martinez Bridge in CA, and the New Silver Bridge in WV). In addition, electroslag welds had been used in several A36 and A588 steel splices in the negative moment regions adjacent to Piers 9 and 10. Concern with electroslag welds had resulted from adverse experience in the 1970's when the I-79 plate girder span over the Ohio River in PA cracked in 1977 as a result of a large weld repair crack that extended in fatigue. The fatigue crack resulted in brittle fracture of the girder as a result of low toughness in the electroslag weld. Many structures were subsequently found to have crack-like defects requiring retrofits and FHWA placed a moratorium on the use of electroslag welds in tension components. Nondestructive tests were carried out between 1978 and 1987 using radiography, ultrasonic testing (UT) and acoustic emission (AE), These tests suggested that two areas had AE activity at defects. One was at an electroslag weld in the bottom compression flange of Girder G2 near FB33. The second location was at an A514 steel web groove weld in Girder G3 near FB18.

In order to accurately characterize the potential for future cracking, assess the effectiveness of the retrofit measures that were carried out in 1989, and to provide recommendations for any further retrofit procedures or other corrective action, measurements were made of in-service live-load stress ranges at selected locations. The measurements were used to assess the behavior and susceptibility for cracking of the various details identified as susceptible to fatigue. The effectiveness of the existing retrofits at the upper end of the transverse connection plates (i.e., at the top flange web gap) and for the lateral gusset plates in the side spans was also assessed. The measurements also permitted an assessment of defects in the groove welds of the main girders and their susceptibility for cracking under existing truck traffic.

All reported field work was conducted in August through November of 2000 by personnel from Lehigh University's Center for Advanced Technology for Large Structural Systems (ATLSS) located in Bethlehem, PA.

2.0 Instrumentation

The following section describes the instrumentation plan used during the field testing.

2.1 Strain Gage Plan and Details

Strain gages were placed at locations known to be fatigue sensitive or to provide global load distribution characteristics of the bridge. "As built" strain gage plans detailing the locations of all strain gages are provided in Appendix A

The original proposal indicated that up to 60 strain gages would be installed. This estimate was developed based on the design drawings, which were found to be different from actual field conditions. Due to limited clearance, several gages could not be installed and on-site modifications to the proposed gage plan were required. As a result, the total number of strain gages installed on the bridge was 47. This include eight strip gages each containing ten independent gages.

The only type of permanent sensors used were strain gages, of both the bondable and weldable type. All strain gages were wired as quarter-bridge circuits using a three-wire configuration. Excitation voltage varied from 2V, 5V or 10V, depending on the type of gage used.

All uniaxial weldable gages installed in the field were produced by Measurements Group Inc. and were 0.25 in. gage length type LWK-06-W250B-350. Weldable type strain gages were selected due to ease of installation in a variety of weather conditions. The "welds" are a point or spot resistance weld about the size of a pin prick. The probe is powered by a battery and only touches the foil that the strain gage is mounted on by the manufacturer. This fuses a small pin size area to the steel surface. It takes ten or more of these dots to attach the gage to the steel surface. There are no arc strikes or heat affected zones that are discernible. There is no preheat or any other preparation involved other than the preparation of the local metal surface by grinding and then cleaning before the gage is attached to the component with the welding unit. There has never been an instance of adverse behavior associated with the use of weldable strain gages including their installation on extremely brittle material such as A615 Gr75 steel reinforcing bars.

These gages are a temperature-compensated uniaxial strain gage and perform very well when accurate strain measurements are required over long periods of time (months to years). The gage resistance was 350Ω and an excitation voltage of 10 Volts was used. The gages where installed at locations where access was good and the effects of very high strain gradients were not a concern.

At locations where clearance was limited and strain gradients were expected to be high, smaller bondable uniaxial strain gages were utilized. These gages were also produced by Measurements Group Inc. and were 0.25 in. gage length type CEA-06-250UN-350 (350Ω). These gages are a general purpose resistance strain gage fully temperature compensated for use on structural steel. The gage resistance was 350Ω and the excitation voltage was 5 Volts.

At locations where clearance was restricted and some information pertaining the strain gradient was of interest, bondable "strip" gages where used. These were also produced by Measurements Group Inc. and were type EA-06-031MF-120. The strip gage consists of (up to) ten (10) evenly spaced gages in a line. The gage length of the individual gages is very short, about 0.031in. The total gage length is 0.79in (i.e., the

distance from gage 1 to gage 10). These gages were typically placed immediately adjacent to a weld toe in or adjacent to a web gap. Altogether, eight of these gages were installed. As stated above, each strip gage contains ten individual uni-axial gages. For this application, two of the ten gages were selected for monitoring which provided sufficient information pertaining to stress ranges and strain gradient adjacent to the weld toe. The gage resistance was 120Ω and an excitation voltage of 2 Volts was used.

All gages were protected with a multi-layer system and then sealed with a silicon type agent. Where required, wire connections were soldered, electrically insulated with heat shrink tube.

2.2 Summary of Strain Gage Installations

The following section summarizes the gage plan. The detailed gage plan, showing the locations of all gages is provided in Appendix A.

2.2.1 Gages on Main Girders

Strain gages were installed on the main girders at floorbeam 24 in the main span and floorbeam 35 in the side span. A single uniaxial strain gage was installed on the bottom flange of each main girder. In addition, a single uniaxial gage was installed on the top flange directly above the bottom flange gage on G1 and G2 at both cross-sections. These gages were used to gain information pertaining to transverse load distribution, lane position and the degree of composite action at these two sections. These gages were also used, along with the controlled load data, to estimate the GVW of heavy vehicles crossing the bridge. Figure 2.1 a shows a typical installation of these gages.

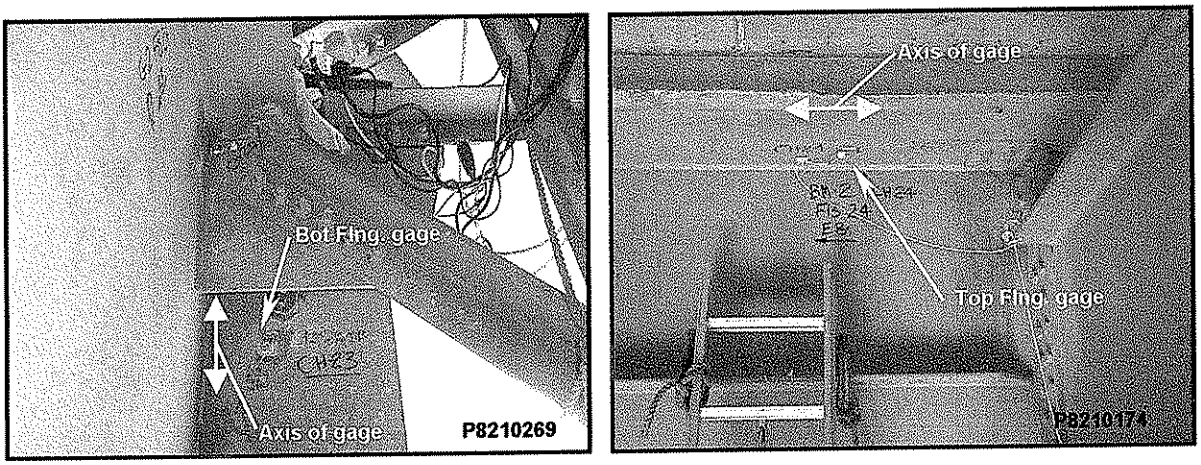

Figure 2.1 – Photographs of typical gage installation on top and flanges

2.2.2 Gages at Web Gaps, Gusset Plate Web Connections

Strain gages were installed at several web gaps in order to establish the stress range at these details. Both retrofitted and non-retrofitted details were instrumented in order to established the effectiveness of the retrofit details. A photograph of a typical installation is shown in Figure 2.2.

Gages were also installed adjacent to retrofit holes drilled in the web at a gusset plate connection. The gages were placed on the opposite side web where the gusset plate connects as shown in Figure 2.3a and 2.3b.

Figure 2.2 – Photograph of typical gage installation at a bottom web gap on the surface opposite a floorbeam connection plate.

Details of the strain gages located at the web gaps, gusset plates, and members framing into these locations are given on sheets three to eight of Appendix A.

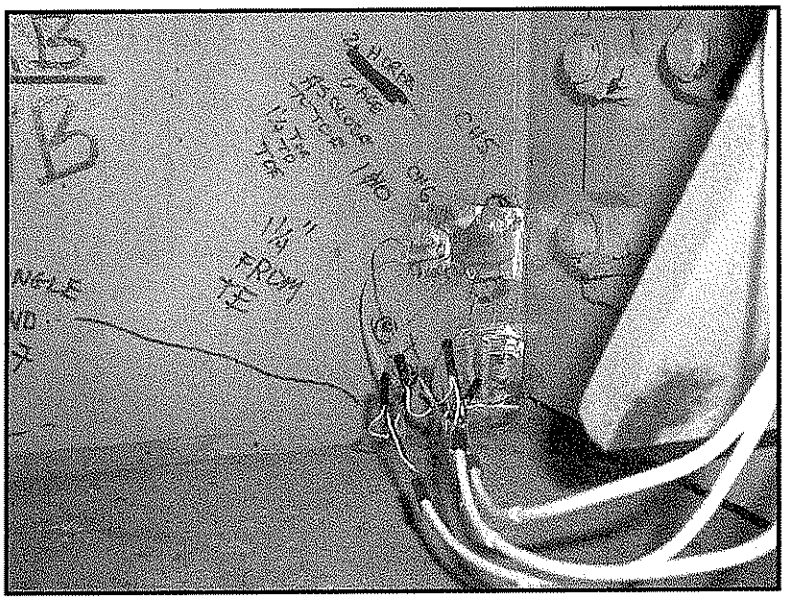

Figure 2.3a – South Face of Girder G3 at FB 37

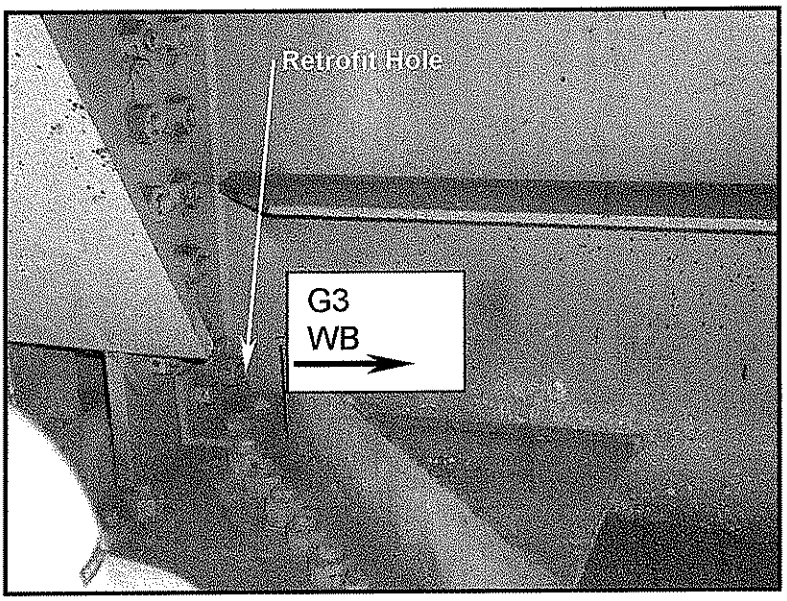

Figure 2.3b – North Face of Girder G3 at FB 37

Figure 2.3a & 2.3b – Photograph of gage installation at retrofit holes at bottom gusset plate/web connection at G3 FB37
Gages were also placed at the bottom web gap.

3.0 Test Program - Summary

The test program included controlled load tests and uncontrolled monitoring of random traffic. The controlled load tests utilized a standard, loaded vehicle that traveled across the structure at normal highway speeds in the traffic flow. During these tests, time history data were collected from all gages. Uncontrolled monitoring involved collecting time history data during the passage of *random* vehicles which began while ATLSS personnel were on site. In addition, a remote long-term monitoring program was initiated which covered the period from September 21, 2000 to November 20, 2000. During the remote monitoring program, time history data and stress range histograms were collected for selected gages.

3.1 Controlled Load Tests

A series of controlled load tests were conducted using a test truck of known load and geometry. Figure 3.1 is a photograph of the test truck parked under span 11. Details pertaining to the controlled load tests are summarized in Table 3.1. Each of the controlled-load crawl tests were repeated a minimum of three times.

Figure 3.1 – Photograph of test truck utilized during the controlled load tests

The gross vehicle weight (GVW) of the truck was 58,600 pounds. The truck was provided by the West Virginia DOT and was labeled as *Truck # 377-255*. Tables 3.1 and 3.2 summarizes the axle loads and geometry of the test truck. Table 3.3 summarizes the conditions for the sixteen test runs that were made with test truck. The column titled "test number" refers to the order at which the test was run. The test truck was positioned in lanes 1 through 4 on the bridge, as identified in Figure 3.2.

Due to the high volume of traffic on the bridge, it was not possible to close lanes during the controlled load tests. Thus, other traffic was on the bridge while the test truck crossed. Although attempts were made to ensure the test truck crossed while no other

vehicles were on the structure, this was not always possible. The position and configuration of other trucks were noted by an ATLSS engineer who rode with the driver. The speed of the test truck was also recorded. The controlled load tests are summarized in Table 3.3.

Test Description	Rear Axle Type	Front Axle Load (lb)	First Rear Axle Load (lb)	Second Rear Axle Load (lb)	GVW[1] (lb)	Date of Tests
Controlled Load Tests	Tandem[2]	16,600	21,100	21,000	58,600	Aug 25th, 2000

Notes
1. GVW=Gross Vehicle Weight
2. Rear axle of AASHTO design trucks actually represents a tandem.

Table 3.1 - Test truck axle load data

Rear Axle	L1 (in)	L2 (in)	Wf (in)	Wr (in)	A[1] (in)	B (in)	C (in)	D[1] (in)	E (in)
Tandem	171.5	55.5	79	72	-	10.5	22	-	9

Notes
1. This dimension was not measured.

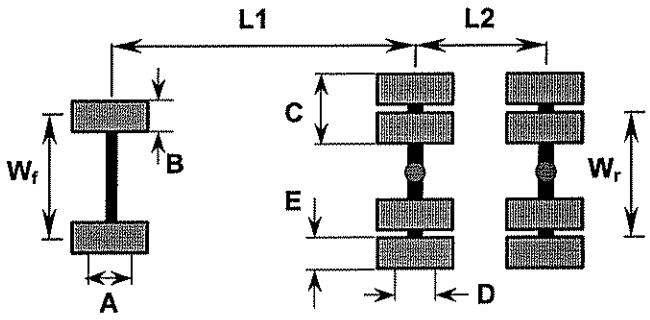

Table 3.2 – Geometry of test truck used for controlled load tests

Test #	File Name	Travel Direction	LANE	Speed (mph)	Comments
7	WB_L1_4.DAT	Westbound	1	45	HS truck ahead of test truck ~ 90 yards
5	WB_L1_3.DAT	Westbound	1	60	HS behind test truck
3	WB_L1_2.DAT	Westbound	1	50	Test truck adjacent to small HS
1	WB_L1_1.DAT	Westbound	1	45	Dump truck and HS behind test truck
15	WB_L1_5.DAT	Westbound	1	55	No other trucks on bridge
13	WB_L2_3.DAT	Westbound	2	60	HS truck on Eastbound side of bridge – passed at midspan span 10
11	WB_L2_2.DAT	Westbound	2	55	HS truck ahead of test truck ~ 100 yards
9	WB_L2_1.DAT	Westbound	2	60	No other trucks on bridge
14	EB_L3_3.DAT	Eastbound	3	60	3 HS trucks on Westbound side of bridge – passed at midspan span 10
12	EB_L3_2.DAT	Eastbound	3	55	No other trucks on bridge
10	EB_L3_1.DAT	Eastbound	3	50	No other trucks on bridge
8	EB_L4_4.DAT	Eastbound	4	60	No other trucks on bridge
6	EB_L4_3.DAT	Eastbound	4	60	No other trucks on bridge
4	EB_L4_2.DAT	Eastbound	4	50	Test truck passed by 2 HS trucks
2	EB_L4_1.DAT	Eastbound	4	50	Dump truck and HS behind test truck
16	EB_L4_5.DAT	Eastbound	4	55	Several HS trucks behind test truck

Notes:
1. "HS" refers to a typical 5-axle truck, i.e., a tractor trailer

Table 3.3 – Summary of controlled speed tests using test truck

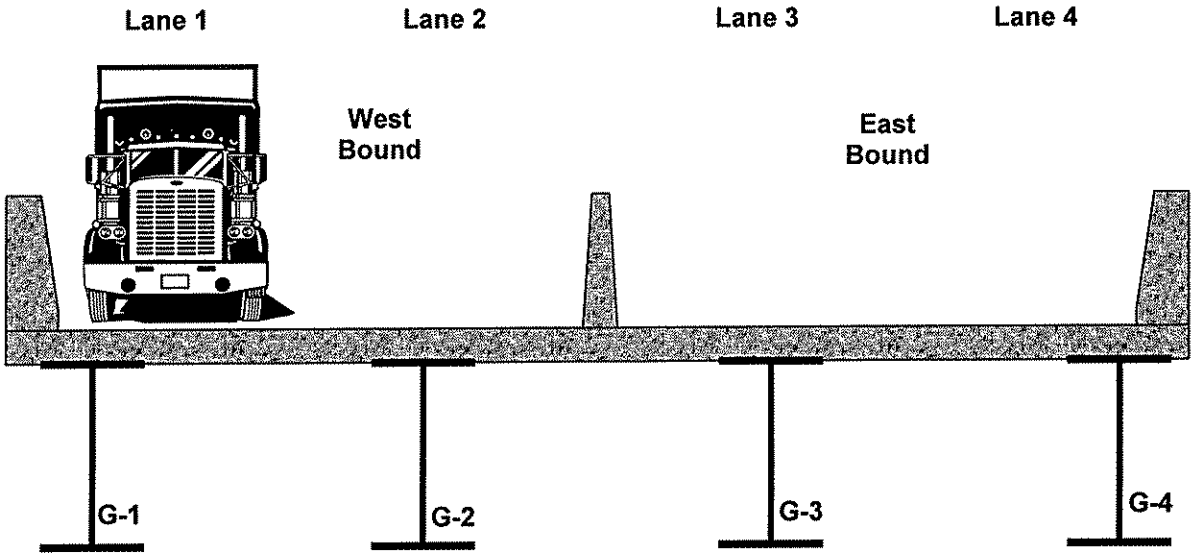

Figure 3.2 – Location of lane numbers as identified during controlled load testing (View looking eastbound)

3.2 Monitoring of Random Traffic

Continuous and triggered time history data were collected from all gages on August 24th and August 25th. These data were used to establish the appropriate trigger levels to be used during the remote long-term monitoring program (*for a discussion of "triggered" data, see Section 3.4.1*). After a review of these test data, a group of twenty gages were selected to be included in the remote monitoring program. Table 3.4 summarizes the data collected on these two days.

File Name	Start	Finish	Comments
824_MON.DAT	Aug 24th 6:35PM	Aug 24th 6:46PM	Continuous time history, S/R = 200Hz
824_PM.DAT	Aug 24th 8:24PM	Aug 25th 9:25AM	Trigger time history – Trig on CH_26
825_PM.DAT	Aug 25th 8:00PM	Aug 25th 11:00AM	Trigger time history – Trig on CH_31

Table 3.4 - Summary of data collected on site during on-site monitoring of random traffic

3.3 Out-of-Plane Displacement Measurements Under Random Traffic

Although not within the original scope of work, prior to beginning the field instrumentation program, it was decided to attempt to measure out-of-plane displacements at top and bottom web gaps. It has been shown that out-of-plane displacements of very small magnitude, (on the order of 0.001 to 0.005in) can produce large stress ranges within the web gap. Displacements were measured using very sensitive Linear (LVDTs) manufactured by Macro Sensors Inc. and were type GHSD-750-250 (See Figure 3.3). These sensors are an all welded stainless steel spring loaded LVDT specially designed to be used in harsh industrial environments where dirt, water and other contaminates are present. Hence, they were well suited for this application. These LVDTs had a stroke of ±0.25in displacement. LVDTs of this type theoretically have infinite resolution, however, in reality, the resolution of the measurements is limited by the data acquisition system. The resolution of the data acquisition system combined with this sensor had a resolution of about $8x10^{-6}$ in.

Displacements were measured at ten locations where out-of-plane displacements were expected in span 11. Measurements were also made at locations where retrofit angles were installed in order to assess their effectiveness in eliminating or reducing out-of-plane displacements.

The LVDT was secured in place using a 300lb magnetic base support. After data were collected, the LVDT was then removed and positioned in a different location and data collected. Due to limited time, data were only collected for periods of five to eight minutes at each location. Data were simultaneous collected from all gages during these tests. Although only a few minutes of data were collected at each location, the LVDT was not removed until at least one heavy truck crossed the bridge. The data collected during August 24th and 25th, and the long-term monitoring data can be used to project or estimate corresponding peak out-of-plane displacements under heavier loads.

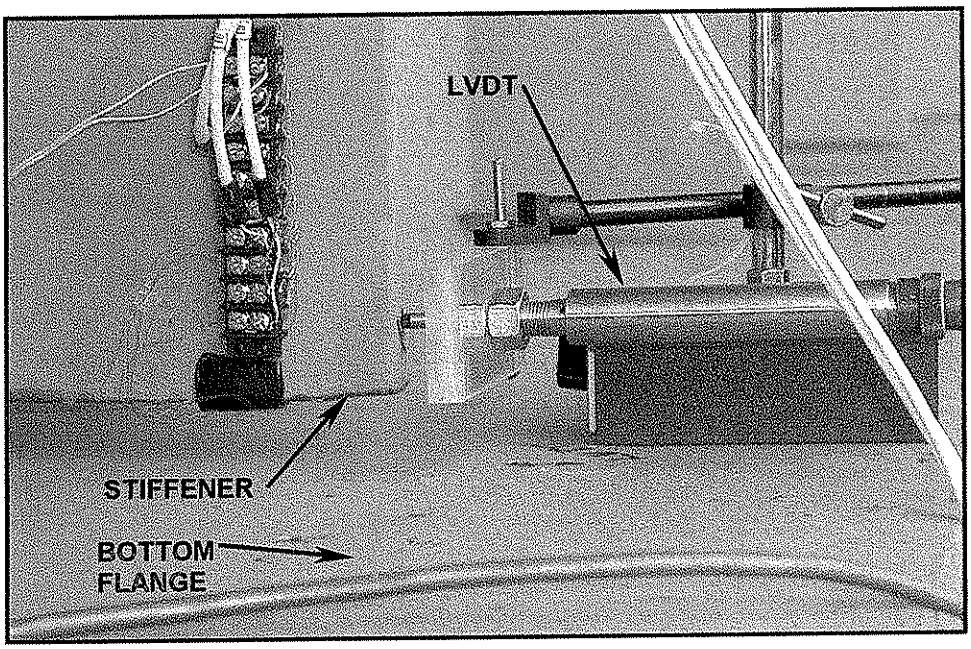

Figure 3.3 – Photographs of LVDT used to measure relative displacement between a stiffener and the bottom flange

3.4 Long-Term Remote Monitoring

Triggered time histories and stress-range histograms were developed for twenty gages located at various details. The channels included in the remote monitoring program were selected based on the results of the controlled load tests and the on site monitoring of random traffic. The channels included in the long-term monitoring program are summarized in Table 3.5. Data were collected for the period of September 21st, 2000 to November 20th , 2000 (i.e., two months). The "*Sheet #*" listed in Table 3.5 refers to the sheet on which the respective gage can be found on the gage plans in Appendix A.

Ref #	Channel Name	LOCATION			Sheet #
		G#	FB#	Description	
1	CH_31	G1	FB24	Bottom Flange - 24in West of FB24	2
2	CH_26	G4	FB24	Bottom Flange - 24in West of FB24	2
3	CH_19	G2	FB24	S. East side of Bottom G.P. Perp. To Weld Toe	3
4	CH_21	G2	FB24	N. West side of Bot. Conn. Plate Gage is Perp. to Weld Toe (Opp. CH_20)	3
5	CH_34	G3	FB34	Gage on Bot. N. East Lateral Strut	4
6	CH_35	G3	FB34	N. East Conn. Plate for Lateral Strut – Gage is Perp. to Vert. Stiffener (Opp. CH_36)	4
7	CH_36	G3	FB34	N. West Conn. Plate for Lateral Strut – Gage is Perp. to Vert. Stiffener (Opp. CH_35)	4
8	CH_41	G3	FB34	S. East Top Web Gap – Retrofit Angle is Present	5
9	CH_43	G1	FB34	Bottom Flange - 24in West of FB35	2
11	CH_47	G4	FB35	Bottom Flange - 24in West of FB35	2
14	CH_20	G2	FB24	S. West side of Bot. G.P. Perp. To Weld Toe (Opp. CH_21)	3
15	CH_4	G1	FB35	Weld toe at @ S. West Longit. Stiffener	6
16	CH_5	G3	FB37	Adj. to Web/Stiffener Weld between Repair Holes (S. W. Repairs 5" above Bot. Flng., Opp. CH_8)	6
17	CH_7	G3	FB37	S. West Bottom Vertical Web Gap	6
18	CH_8	G3	FB37	Adj. to Web/Stiffener Weld between Repair Holes (S. E. Repairs 5" above Bot. Flng., Opp. CH_5)	6
19	CH_10	G3	FB37	S. East Bottom Vertical Web Gap	6
20	CH_11	G3	FB37	0.16 inches above CH_10	6

Table 3.5 – Channels included in remote long-term monitoring program

3.4.1 Triggered Time Histories

During the long-term monitoring period, time histories were recorded when the stresses induced by live loads exceeded predetermined levels or "triggers". Once the predetermined stress levels were exceeded, time history data were collected for all 20 gages.

Separate triggers and data files were written for both the eastbound and westbound lanes. In order to ensure a heavy truck was producing the trigger event, thresholds for two gages on either the eastbound or westbound sides of the bridge had to be exceeded. For example, a portion of a triggered time history is presented in Figure 3.4. For westbound traffic, channels CH_31 and CH_43 were selected as trigger channels. The value of the

thresholds were varied throughout the monitoring program as more data became available. For Figure 3.4 the triggers were set at +1.75ksi and –0.5 ksi for channels CH_31 and CH_43, respectively. In order to capture the entire event, data were recorded prior to the trigger event for a specified interval. In Figure 3.4, this time was set to six (6) seconds, (i.e., an six second buffer was maintained). The data acquisition system recorded for seven additional seconds and then stopped only if the triggers were no longer satisfied.

All gages were automatically re-zeroed every 15 minutes using a digital balance algorithm. The appropriate intervals for the pre- and post-triggers and the trigger threshold stress magnitudes were based on the uncontrolled monitoring of random traffic. Recording times and threshold stresses are not the same for the eastbound and westbound lanes.

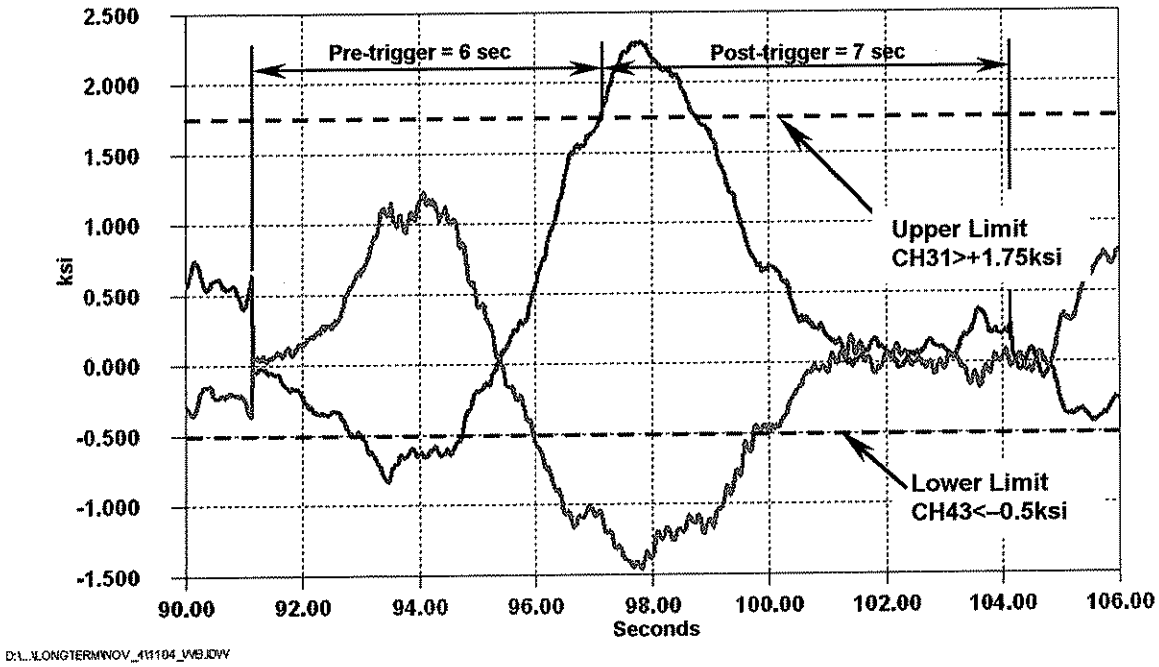

Figure 3.4 – Details of typical triggered time history for westbound traffic

3.4.2 Stress-Range Histograms

Data for stress-range histograms were collected concurrently, but independently of the triggered time histories, using the rainflow cycle counting method. The stress-range histograms were generated continuously and did not operate on triggers, thus all cycles were counted. Stress-range bins were divided into 0.5ksi intervals and stress cycles less than 0.25ksi were ignored. The stress-range bins were updated every 10 minutes.

4.0 Results of Controlled Load Tests and On-site Monitoring

Results of the controlled load tests are discussed in this section. All controlled load tests were conducted on August 25, 2000. As previously discussed, the test truck was "mixed in" with normal traffic in order to avoid lane closures and impact to the motoring public. Hence, other vehicles were crossing the bridge during the test. As indicated in Table 3.3, the presence and configuration of other heavy vehicles were noted as accurately as possible.

Although the gross vehicle weight (GVW) of the test truck was 58.6 kips, the measured data indicated that the test truck was lighter than most other vehicles crossing the bridge during the time of the test. Nevertheless, the controlled load data can be used to estimate the GVW of heavy vehicles crossing the bridge.

Data collected during the on-site monitoring and remote long-term monitoring program will be discussed in order to aid in the interpretation of results as necessary.

4.1 Response of Main Girders

4.1.1 Effect of Transverse Position of Test Truck

Strain gages were installed on the bottom flanges of all four main girders at floorbeams 24 in Span 10 and 35 in Span 11. In addition, gages were installed on the top flanges of girders G1 and G2 at both floorbeams. The gages installed on the main girders can provide information related to the transverse load distribution characteristics of the bridge.

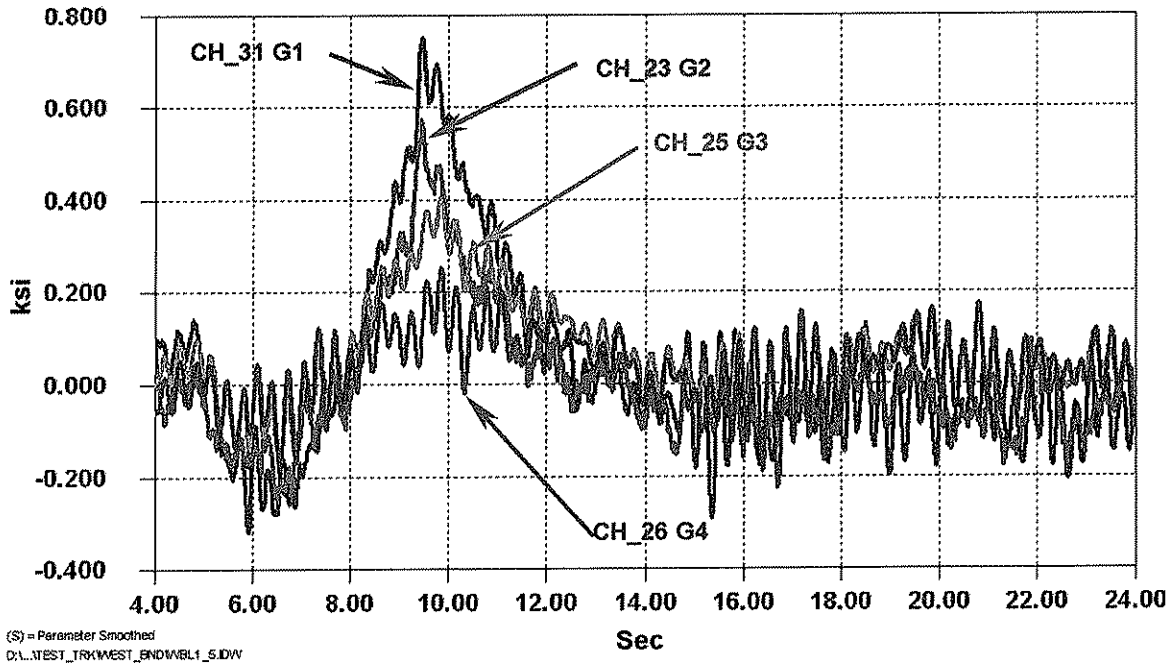

Figure 4.1 – Span 10 main girder bottom flange response near FB24 – Test truck headed westbound in lane one (Test #15)

Figures 4.1 and 4.2 illustrate the response of each of the main girders at floorbeams FB24 and FB35 for gages mounted on the bottom flange for spans 10 and 11

respectively. During this test, the test truck was headed westbound in lane one. There were no other trucks in the immediate area (eastbound or westbound) during this test run. In this position, the truck is located between G1 and G2, but is slightly closer to G2. As expected, the greatest stress ranges are produced in girders G1 and G2 and less in girders G3 and G4.

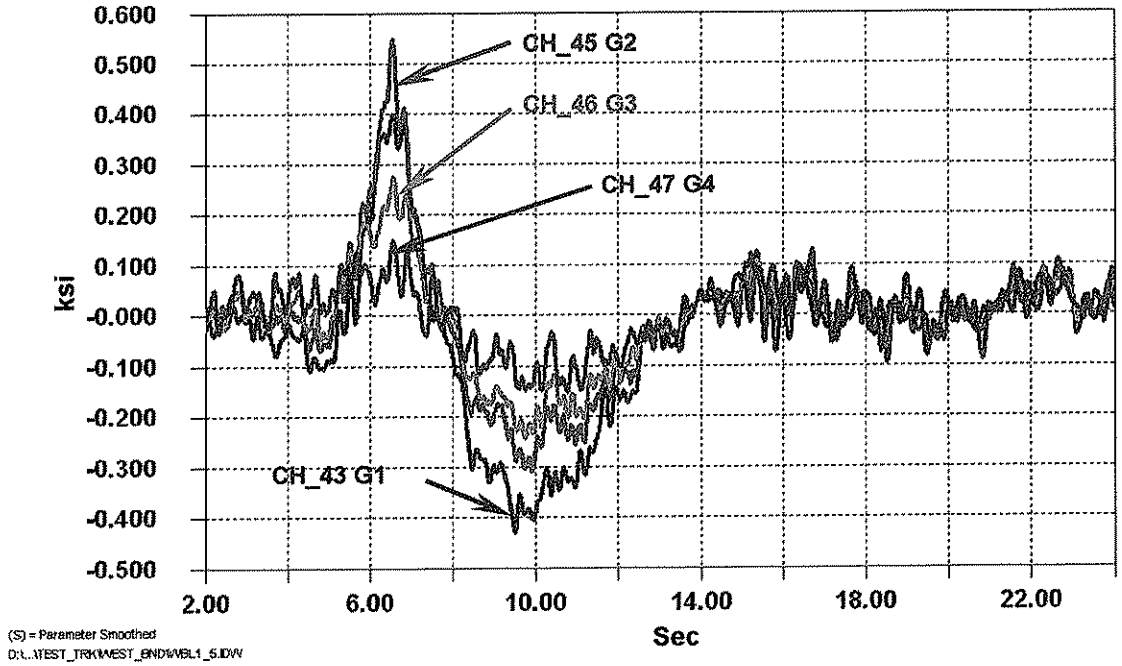

Figure 4.2 – Span 11 main girder bottom flange response near FB35 – Test truck headed westbound in lane one (Test #15)

Table 4.1 summarizes the maximum measured stress range in each gage mounted on the bottom flange for all lane positions from the controlled load tests. Note that the gages installed on the bottom flange were placed on the top surface of the bottom flange. Hence, stress ranges on the bottom of the flange would be greater, but only by a few percent.

Gage	Location	Measured Stress Range (ksi)			
		Lane Position			
		1	2	3	4
CH_31	FB24 G1	1.1	0.8	0.6	0.6
CH_23	FB24 G2	1.1	0.8	0.7	0.5
CH_25	FB24 G3	0.6	0.6	0.8	0.8
CH_26	FB24 G4	0.4	0.5	0.7	1.0
CH_43	FB35 G1	0.8	0.6	0.5	0.4
CH_45	FB35 G2	0.9	0.8	0.7	0.6
CH_46	FB35 G3	0.5	0.5	0.9	0.8
CH_47	FB35 G4	0.3	0.3	0.6	1.0

Table 4.1 - Bottom flanges stress ranges measured at floorbeams 24 and 35

Table 4.1 indicates that the test truck produced low stress ranges in the main girders, as expected. The controlling load case for strength design of long spans such as these is driven by lane loads and not individual trucks. The test truck is also lighter than the legal limit.

It is important to note that the data in Table 4.1 are stress ranges, and not absolute stresses. Since the tests were conducted at normal highway speeds, the data also include any dynamic effects. The most obvious is a sinusoidal vibration of about 3Hz observed throughout the time histories. This vibration was produced by the test truck as well as other trucks which recently crossed the bridge and is the natural frequency of the bridge. Note that this vibration continues after the test truck passed. Although no crawl tests were conducted, the data suggest that for the most heavily loaded girders, (i.e., G1 and G2 for tests with the test truck in lane 1 or 2) a dynamic amplification factor of 1.1 to 1.2 seems reasonable.

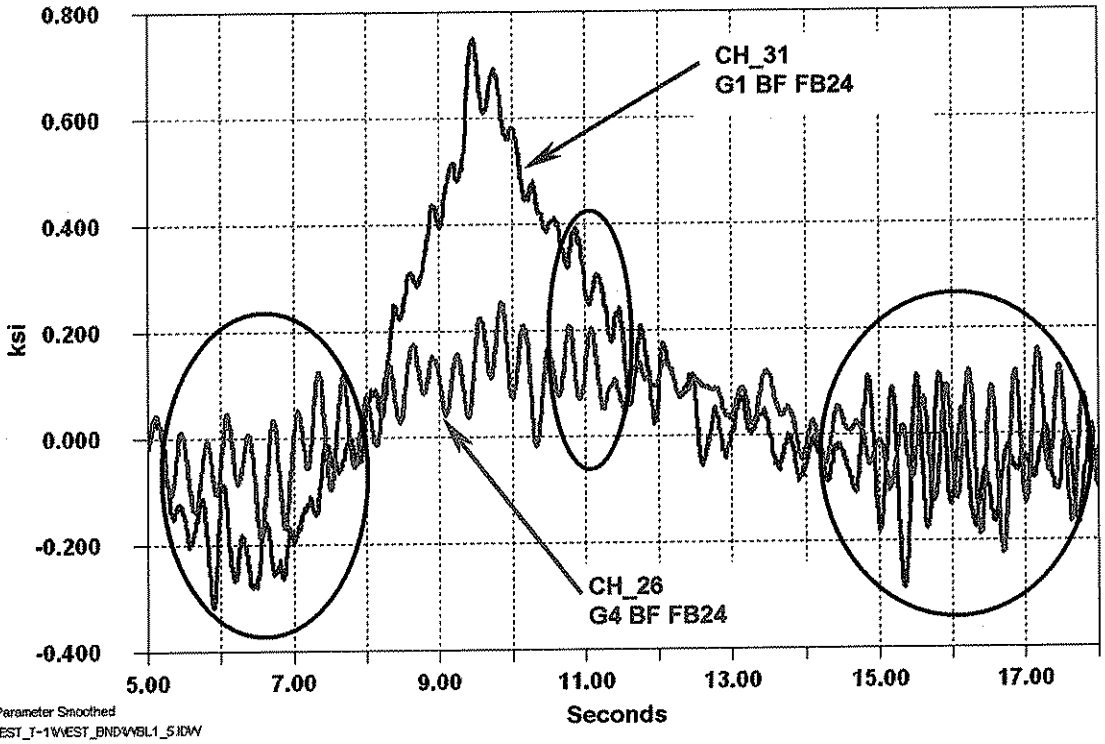

Figure 4.3 - Dynamic effects in girders G1 and G4 due to passage of test truck in lane 1

For girders not directly loaded during a particular test, the "static" stress range is small. However, the dynamic effects appear greater for these girders since the frequency response for all girders is approximately equal in the first mode. Figure 4.3 compares data from girders G1 and G4 at floorbeam FB24 for a test in which the test truck was traveling westbound in lane 1 near girder G1. As expected, the stress range is greatest in girder G1 and less in G4. However, the vibration response before, during and after the test truck passes is nearly equal for both girders at different times during the vehicle

passage. (*This is illustrated in the regions enclosed by the circles.*) Hence, while the magnitude of the first mode vibration of the bridge produces nearly equal vibration stress ranges in all girders, the stress range produced by the test truck does not. Since the dynamic amplification factor is the ratio of the dynamic response to the static response, the girders furthest from the test truck appear to have higher dynamic amplification factors. This is characteristic of lighter loaded trucks and the eccentricity of load on the cross-section. Obviously, the highest stress ranges are still produced by the girders nearest the passing vehicles.

4.1.2 Effect of Composite Action

The steel girders of the Kanawha River Bridge were not designed compositely with the concrete deck. Field measurements on non-composite highway bridges consistently demonstrate that some level of composite action always exists as a result of friction and bond between the top girder flanges and concrete slab. In order to investigate the level of composite action present on the Kanawha River Bridge, gages were installed on the top flanges of girders G1 and G2 in spans 10 and 11 at floorbeams 24 and 35, respectively. These gages were place directly above the gages installed on the bottom flanges.

Figure 4.4 illustrates the response of the test truck passing in lane one, headed westbound for gages installed in span 10. (this is the same test shown in Figures 4.1 and 4.2). Note the low compressive stress produced in the top flanges. Although the girders were designed as non-composite, the measurements verify that a significant degree of composite action is being developed.

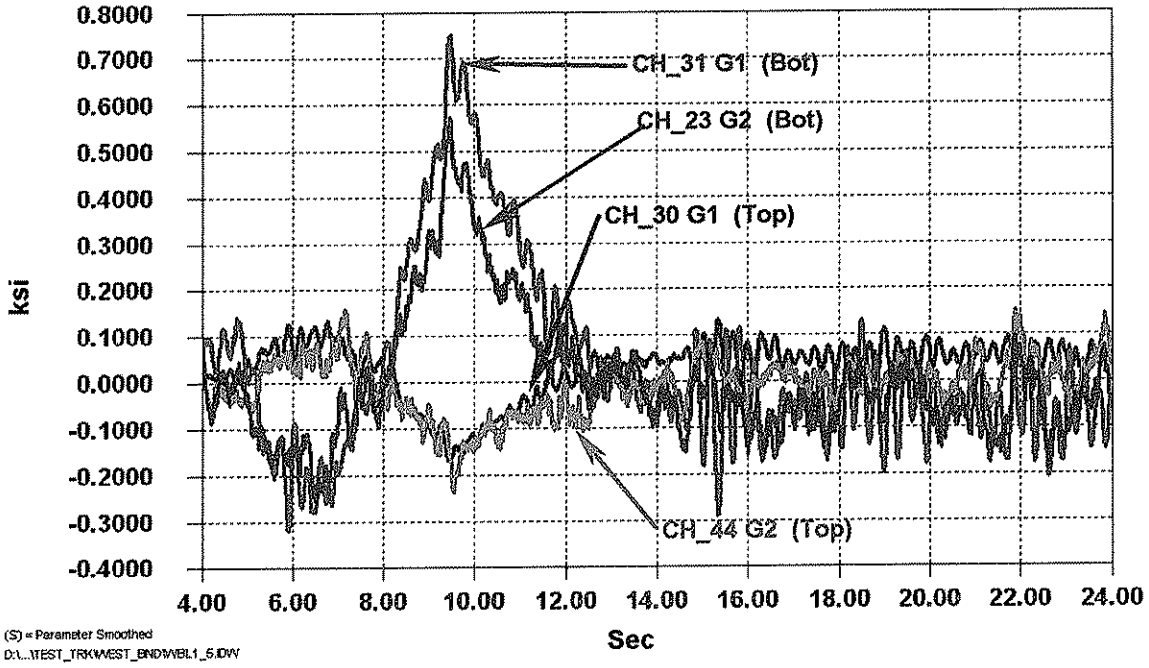

Figure 4.4 – Measured response as test truck passed in lane one, headed westbound
Note difference in stress range in top flange and bottom flange strain gages

A review of data collected during the controlled load tests and from on-site monitoring of traffic was made in order to estimate the location of the neutral axis. At floorbeam FB24, located in the center span (i.e., span 10), the depth of the web is 150 inches. Based on the measurements at this location, the neutral axis is between 30 and 35 inches below the bottom of the top flange. This places the neutral axis at roughly 80% of the depth of the web above the bottom flange. At floorbeam FB35, located in the end span (i.e., span 11), the girder begins to haunch "down" to the pier and the depth of the web is about 94 inches. At this location, the neutral axis was estimated from the measurements to be between 9 and 19 inches below the bottom of the top flange. Hence, at this floorbeam, the neutral axis is located at about 85% of the depth of the web above the bottom flange, similar to what was observed at floorbeam FB24.

The measurements indicate that a considerable level of composite action exists between the girders and the concrete deck, under all service loads. This results in lower stress ranges as compared to the non-composite design assumption. For a fatigue evaluation, analytical models should account for this composite action in order to avoid overly conservative estimates of remaining fatigue life. This is recognized in the AASHTO assessment procedure for fatigue damage [2]

4.2 Longitudinal Attachments

4.2.1 Longitudinal Stiffeners

Weld terminations on longitudinal stiffeners are classified as Category E details (CAFL of 4.5 ksi) with respect to longitudinal or in-plane stresses. Gages were installed at two locations where longitudinal stiffeners terminated at the transverse connection plates.

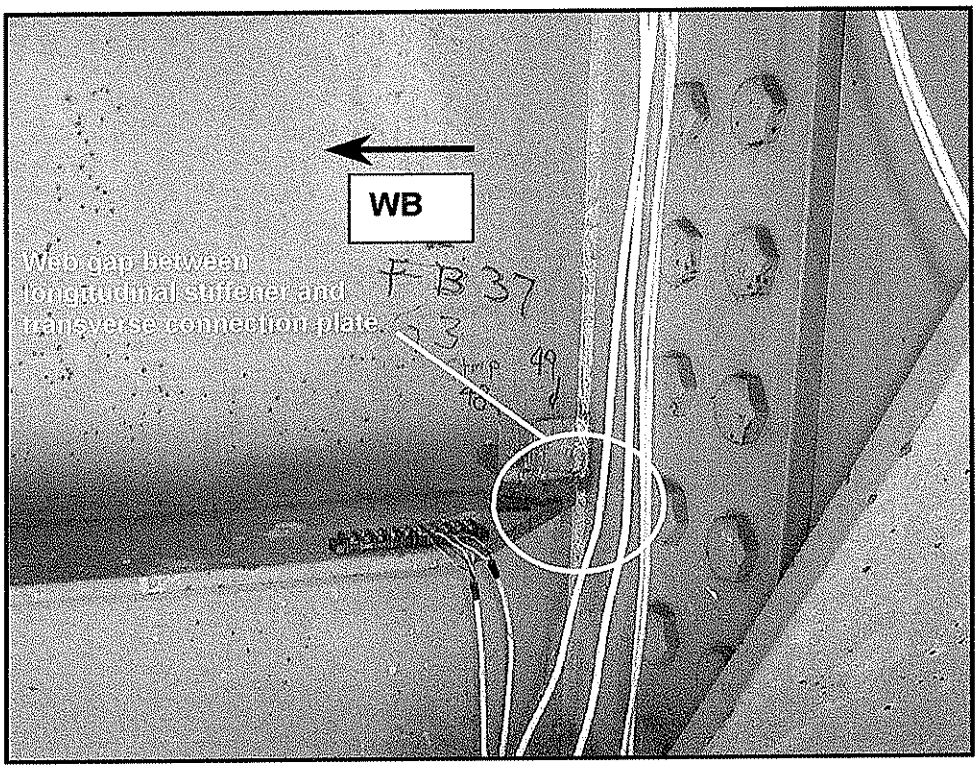

Figure 4.5 - Location of web gap between longitudinal stiffener termination and transverse connection plate

Out-of-plane displacement of the transverse connection plate may also occur within the small gap between the end of the longitudinal stiffener and the transverse connection plate (See Figure 4.5). Although the magnitude of the displacement is typically very small, it occurs over a short length of the web and subsequently can result in high stress ranges in the gap. The proportion of the stress range at the weld toe produced by out-of-plane displacements can be considerably higher than the nominal in-plane bending stress component. The in-plane and out-of-plane components are also additive.

In-plane stress ranges are also amplified at the end of the longitudinal stiffener due to the weld termination. The stress concentration at the end of the attachment is analogous to that of a welded cover plate. Although not designed to carry any significant stresses, the longitudinal stiffeners do comprise a part of the cross section effective in bending. Hence, the abrupt termination of the stiffener results in a stress concentration

and an eccentricity effect at the end of the longitudinal stiffener. The strain gage was placed above the gap and out of the stress concentration region.

The nominal in-plane stress range can be estimated using the bottom flange stress range and knowing the location of both the neutral axis and the longitudinal stiffener. According to the design drawings, the longitudinal stiffener at floorbeam FB35 is located 18 inches above the top of the bottom flange and the depth of the web is 94 inches. Because this floorbeam is near the contraflexure point, live-load stress reversals are expected.

Assuming the neutral axis is on average about 15inches below the top flange, the in-plane stress range at the stiffener can be estimated as:

$$\frac{94in-15in-18in}{94in-15in}\times S_r = 0.77\times S_r \qquad \text{Eq. 4.1}$$

Where S_r equals the stress range in the bottom flange

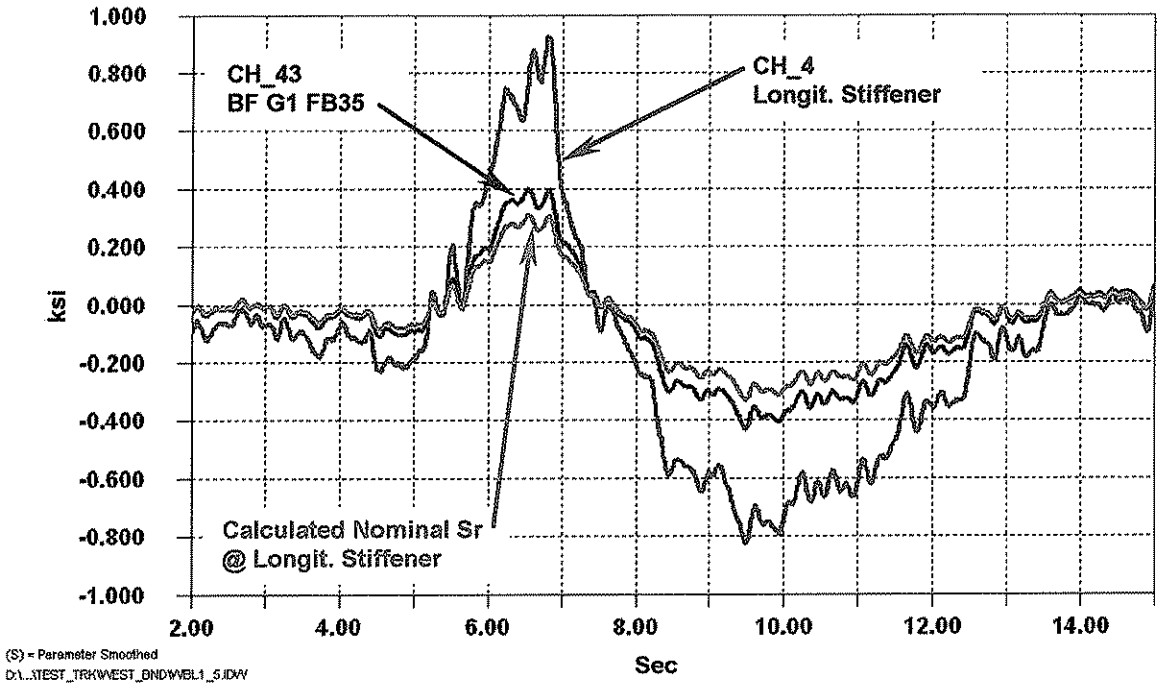

Figure 4.6 –Comparison of measured and calculated nominal in-plane stress range (S_r) at end of longitudinal stiffener at floorbeam 35 of girder G1

Data from channel CH_4, located at the end of the longitudinal stiffener at floorbeam FB35 and CH_43 located on the bottom flange of girder G1 at floorbeam FB35 are plotted in Figure 4.6. As can be seen, the stress range at the longitudinal stiffener (CH_4) is greater than at the bottom flange (CH_43). Also plotted in Figure 4.6 is the calculated in-plane nominal stress range in the web plate at the height of the stiffener, calculated using Eq. 4.1. The difference between the calculated and measured

stress is the result of out-of-plane stresses from distortion and eccentricity at the end of the longitudinal stiffener.

Comparing the measurements at CH_4 and CH_43 indicate that the measurements at each location are roughly proportional. For noteworthy values of stress, the ratio between CH_4 and CH_43 was observed to vary between 2.5 to 3.0, as would be expected if out-of-plane stresses dominate the response at channel CH_4. (*It should be noted that the increase in stress at CH_4 {i.e., greater than the calculated nominal stress range} is also the result of a disturbance in the stress field at the end of the longitudinal stiffener.*)

Table 4.2 summarizes stress ranges measured during the controlled load tests at longitudinal stiffeners. All stress ranges produced by the test truck are small and less than the CAFL of 4.5 ksi for category E.

Gage[1]	Location	Measured Stress Range (ksi)			
		Lane Position			
		1	2	3	4
CH_4	FB35 G1	1.8	1.2	1.0	0.7
CH_49	FB37 G3	1.7	2.1	3.1	2.0
CH_50	FB37 G3	1.2	0.7	1.6	2.3
CH_51	FB37 G3	1.3	0.8	1.6	2.3

Notes:
1. Channel CH_48 was not working during these tests

Table 4.2 - Stress ranges measured during controlled load tests at gages installed at the termination of longitudinal stiffeners

4.2.2 Gusset Plates

Several types of gusset plates are welded to the web using partial penetration groove welds and a closure fillet weld at each floorbeam. Because of the length of the gusset plates, they can all be considered category E details. Strain gages were not installed at the ends of the gusset plates. However, using the same procedure as used for the longitudinal stiffeners, the nominal stress range can be estimated. According to the design drawings, the gusset plates are a minimum of 4 inches above the bottom flange in spans 10 and 11.

Using data from floorbeam 35, and again assuming the neutral axis is on average about 15 inches below the top flange, the in-plane stress range at the gusset plates in the end span (span 11) equals:

$$\frac{94in-15in-4in}{94in-15in}\times S_r = 0.95\times S_r \qquad \text{Eq. 4.2}$$

Using data from floorbeam 24, and assuming the neutral axis is on average about 32.5 inches below the top flange, the in-plane stress range at the gusset plates in the main span (span 10) equals:

$$\frac{150in - 32.5in - 4in}{150in - 32.5in} \times S_r = 0.97 \times S_r \qquad \text{Eq. 4.3}$$

Where S_r equals the stress range in the bottom flange at floorbeam 35 and 24, respectively

According to Eq. 4.2 and 4.3, the stress range in the web at the gusset plate is nearly equal to the stress range at the top of the bottom flange. It will therefore be conservatively assumed that the stress range at the gusset plates is equal to the stress range measured at gages installed at the bottom flange. A review of Table 4.1 indicates that the test truck would not produce any fatigue cracking at the weld termination due to in-plane stresses at this detail. The effects of out-of-plane displacements at the "free" edges of the gusset plate (as shown in Figure 4.6a) are not expected to be as great as the stress measured at the web gaps at the transverse connection plates. Because the web is flexible at the ends of the gusset plate, high stresses, like those developed in small web gaps, will not occur.

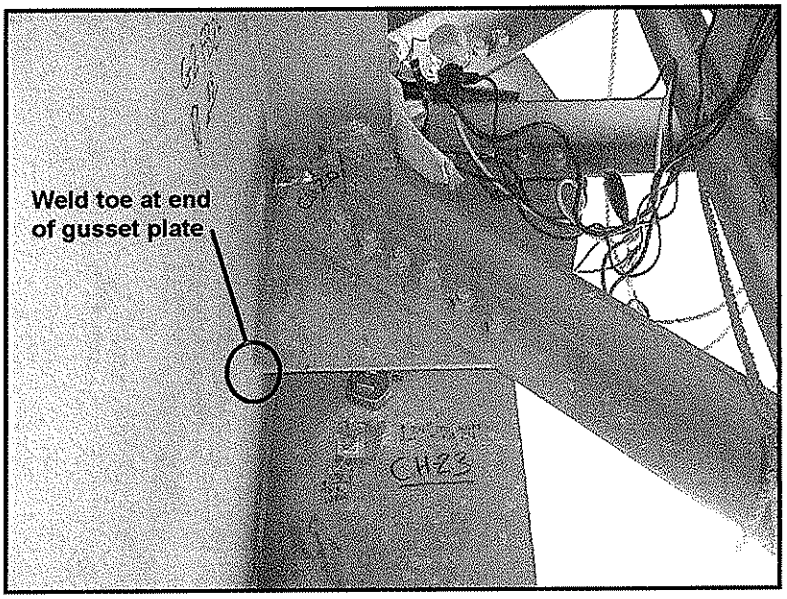

Figure 4.6a – Photograph of longitudinal weld termination at "free" end of gusset plate
Note the length of web that is available to accommodate out-of-plane displacement

4.3 Response at Web Gaps - General

Several gages were installed on the web adjacent to cope holes where stiffeners or connection plates were not rigidly attached to the flange plate as illustrated in Figure 2.2 and summarized in Table 4.3. Out-of-plane distortion was also assessed at lateral gusset plates that were slotted at the transverse floorbeam connection plates, as illustrated in Figure 2.3. Out-of-plane distortion has lead to web gap cracking on many bridges throughout the US [14, 9]. These cracks, if not properly retrofitted, can lead to crack extension into the girder web and flange and potentially fracture of the girder.

Gage[1]	Location	Measured Stress Range (ksi)			
		Lane Position			
		1	2	3	4
CH_5	G3 FB37 Horiz. strip gage between retrofit holes – Opposite CH_8 & CH_9	4.2	9.7	9.3	7.7
CH_6		1.3	<1.0	1.0	2.6
CH_7	G3 FB37 Vert. uniaxial gage @ bottom web gap - Opposite CH_10 & CH_11	<1	2.0	1.9	4.0
CH_8	G3 FB37 Horiz. strip gage between retrofit holes – Opposite CH_5 & CH_6	2.0	5.0	2.8	5.2
CH_9		1.0	<1.0	1.5	1.4
CH_10	G3 FB37 Vert. strip gage @ bottom web gap – Opposite CH_7	2.9	2.5	<1.0	4.3
CH_11		<1.0	1.3	1.0	3.0
CH_12	G3 FB37 Vert. strip gage @ top web gap – Opposite CH_7	<1.0	<1.0	<1.0	<1.0
CH_13		<1.0	<1.0	<1.0	1.1
CH_15	G4 FB37 Vert. strip gage @ bottom web gap –Opposite CH_17	<1.0	<1.0	<1.0	3.4
CH_17	G4 FB37 Vert. uniaxial gage @ bottom web gap - Opposite CH_15	<1.0	<1.0	<1.0	<1.0
CH_32	G2 FB24 Vert. weldable uniaxial gage @ bottom web gap	<1.0	<1.0	<1.0	<1.0
CH_38	G3 FB34 Vert. strip gage @ bottom web gap	<1.0	<1.0	<1.0	<1.0
CH_39		<1.0	<1.0	<1.0	<1.0
CH_40	G3 FB34 Vert. strip gage @ top web gap	<1.0	<1.0	<1.0	<1.0
CH_41		<1.0	<1.0	<1.0	1.9

Notes:
1. Channel CH_16 was not working properly during these tests

Table 4.3 - Summary of gages installed at web gaps and measured stress ranges due to passage of test truck

In order to assess the potential for web gap cracking on the Kanawha River Bridge and to evaluate the effectiveness of existing drilled holes and repair angles installed to minimize the web gap distortion, strain gages were installed at the following web-gap details: 1) the upper and lower ends of transverse connection plates; 2) at lateral gusset connections; and 3) at longitudinal stiffeners.

During the controlled load tests and on-site monitoring, measurements were made at these gages. In addition, out-of-plane displacements were measured at several locations (See Figure 3.3 and 4.1). The out-of-plane displacement measurements were used along with the strain gage data to assess the potential for fatigue cracking at these details. In addition, the effectiveness of existing retrofit details in preventing or decreasing out-of-plane displacements was evaluated. Details that are susceptible to fatigue cracking are discussed in the following sections.

4.3.1 Web Gaps at Top Flange

Table 4.3 reports measured stress ranges due to the passage of the test truck. Gages installed at top flange web gaps indicate that the existing retrofit angles appear to be providing sufficient restraint as evident by the response of gages CH_12 & CH_13 (G3 FB37 Top) and CH_40 & CH_41 (G3 FB34 Top). For channels CH_12 and CH_13, the test truck produced stress ranges less than 1.1 ksi for all lane positions. For channels CH_40 and CH_41, when the test truck was located in lane 4, a stress range of 1.9 ksi was measured at CH_41.

During the on-site monitoring, individual vehicles crossed the bridge which produced higher stress ranges in channels CH_13 (*up to 2.5 ksi*) and CH_41 (*up to 4.0 ksi*). Based on the response of gages installed on the main girders, the vehicles producing the larger stress ranges were headed eastbound and most likely located in lane 4. Although these stress ranges are still very low with respect to the fatigue resistance to out-of-plane distortion, due to the potential for random trucks to produce higher stress ranges, CH_13 and CH_41 were included in the remote long-term monitoring program. (*Higher stress ranges were measured at these gages during the remote long-term monitoring program. These data are discussed in Section 5.*)

Test Name	Girder – Flrbm - Flange	Corresponding Strain Gage(s)	Displacement Range (mils)[1,2]	Corresponding Stress (ksi)
FB35G1TD	G1 - FB35 - Top	-	0.5	-
FB35G2TD	G2 - FB35 - Top	-	0.8	-
FB37G3TD	G3 - FB37 - Top	CH_12, CH_13	0.3	1.2 (CH_13)
FB37G4TD	G4 - FB37 - Top	-	0.5	-
FB37G3BD	G3 - FB37 - Bottom	CH_7, CH_10, CH_11	0.7	6.3 (CH_7)
FB37G3GP	G3 - FB37 – Gusset	CH_5, CH_6, CH_8, CH_9	1.6	9.9 (CH_5)

Notes:
1. Displacement range is the largest measured displacement range observed that was produced by a single loading event. The loading event could be the result of multiple trucks.
2. 1.0 mil equals 0.001 inch.

Table 4.4 - Summary of gages installed at web gaps and measured stress ranges due to passage of test truck

Out-of-plane displacements were also measured at four transverse connection plates at the top flange, as shown in Table 4.4. Specifically, the relative displacement between the transverse connection plate and the top flange surface was measured. Data were also collected from all strain gages while displacements were measured. The largest displacement range and corresponding stress range measured are compared in Table 4.4.

4.3.2 Web Gaps at Bottom Flange

Gages were also installed at web gaps located near the bottom flange at several locations (See Table 4.3). Both uniaxial and strip gages were installed in order to assess the magnitude of out-of-plane stresses in the web. In addition, out-of-plane displacements were measured at four locations using an LVDT (See Table 4.4).

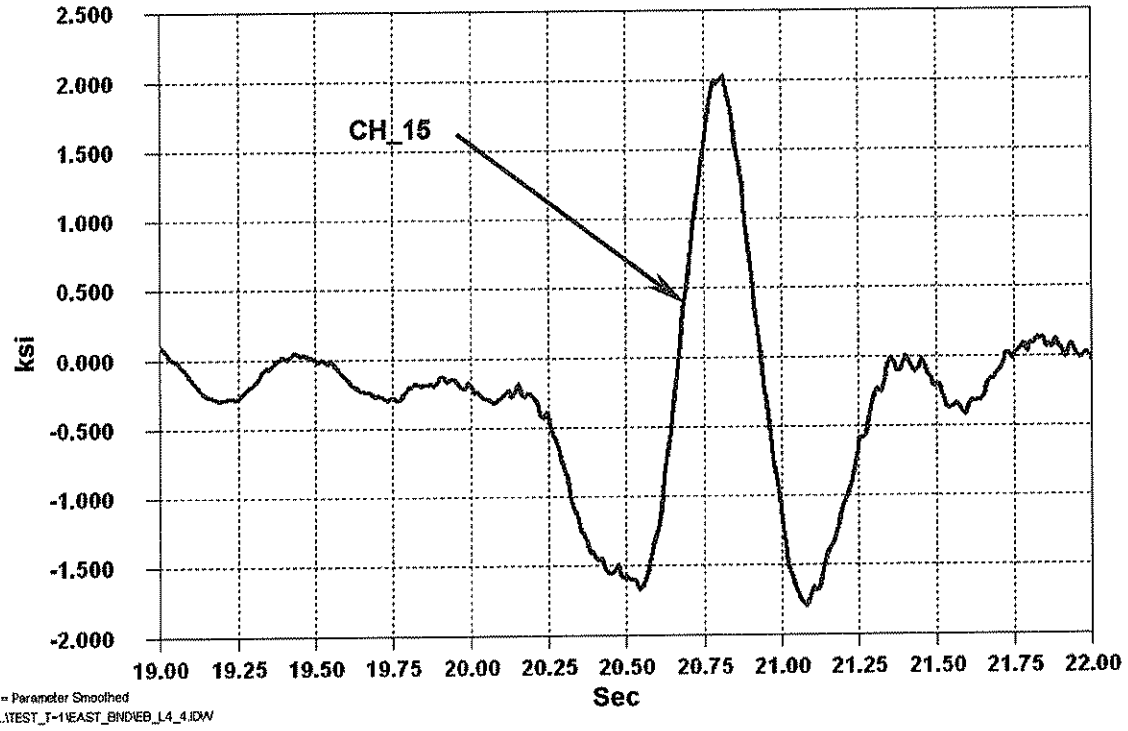

Figure 4.7 – Typical out-of-plane stress range at CH_15 located at bottom web gap on girder G4 FB 37 produced by test truck in lane four, Test #8. (Note stress reversal)

Figure 4.7 illustrates the response at channel CH_15 which was installed adjacent to the bottom web gap on G4 at FB37. This gage is oriented perpendicular to the longitudinal web/flange weld (i.e., vertically). The stress range produced by the test truck is about 3.9 ksi, with the test truck located in lane 4. A stress reversal occurs as the truck passes over the floorbeam. Larger stress reversals were observed at other gages as trucks passed in other lanes. For example, Figure 4.8 illustrates the response at channels CH_7 located at the bottom web gap on girder G3 at floorbeam 37. Note the stress reversal which occurs as random trucks cross the bridge during the on-site monitoring.

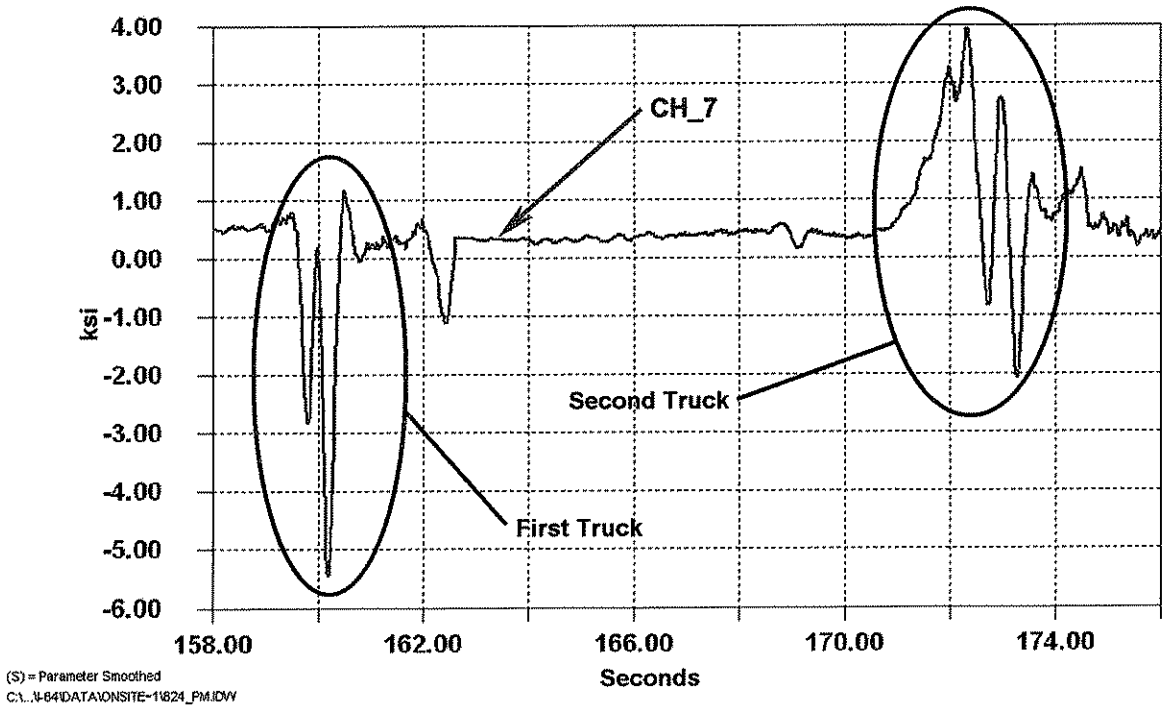

Figure 4.8 - Out-of-plane stress range at CH_7 and CH_13 located at bottom web gap on girder G3 FB 37 produced by random trucks – Note reversal in stress

The *individual* stress range for each of the events shown in Figure 4.8 is about 6.6 ksi and 6.0 ksi for the first and second trucks, respectively. Using the rainflow cycle counting method, the largest peak and valley of different stress ranges are combined to produce the maximum stress range of 9.4 ksi, (-5.4 ksi to 4.0 ksi) for these two events. Thus, the maximum stress range is not necessarily produced by an individual truck. The alternating effects of different trucks in different lanes will almost always produce the largest stress range at these types of details. *(For a full discussion describing the rainflow cycle counting method and its use related to the Kanawha River Bridge, see Section 6.)*

Measurements made at the bottom web gaps during the controlled load tests are also summarized in Table 4.3. As can be seen, out-of-plane stress ranges produced by the test truck are relatively low. However, similar to the observations at the upper web gaps, higher stress ranges were measured during the on-site monitoring program and the long-term monitoring program. These test results will be discussed in Section 5.

4.3.3 Web Gaps at Transversely Loaded Lateral Gusset Plates - General

At several locations, gusset plates are attached to the web of the girder but not to the transverse connection plate as shown in Figure 4.9. Cracking has been observed in the web gap between the gusset plate and the transverse connection plate at a few floorbeams, particularly in the end spans.

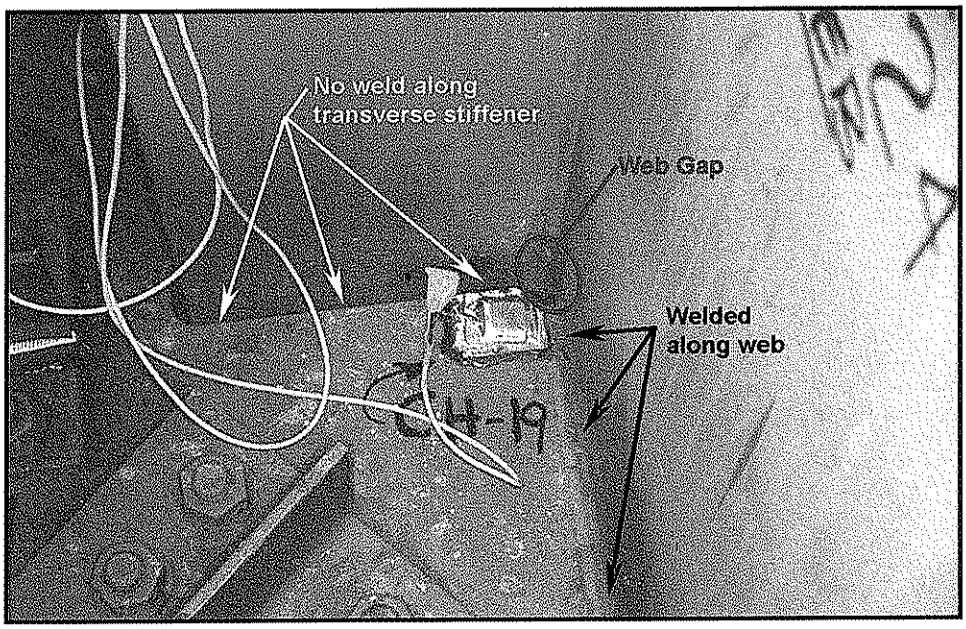

Figure 4.9 - Photographs showing a detail in which the gusset plate is attached to the web but not the gusset plate Note the location where web gap cracking typically occurs

At some gusset plates, an *indirect* connection is made to the transverse connection plate on the opposite side of the web for floorbeams FB16 to FB26 (See Appendix A). In these cases, out-of-plane displacements appear to be adequately minimized. As a result, out-of-plane stresses in the web gap are low enough (i.e., less than 10 ksi) to ensure cracking does not occur in the web gaps.

At details where there was no effective restraint provided, cracking is more likely to develop (i.e., floorbeams FB2 to FB6 and FB36 to FB40). In order to isolate the web gap region on each side of the transverse connection plates and arrest any potential cracks which may form, holes have been drilled as a retrofit at these locations as shown in Figure 4.10. If cracking does develop, it will grow into the holes and be arrested. Small segments of light angles have also been installed to provide a positive attachment between the gusset plate and transverse stiffener (See Figure 4.10). It is visually apparent from Figure 4.10 that only two bolts have been installed in the legs of the 3/8" angles.

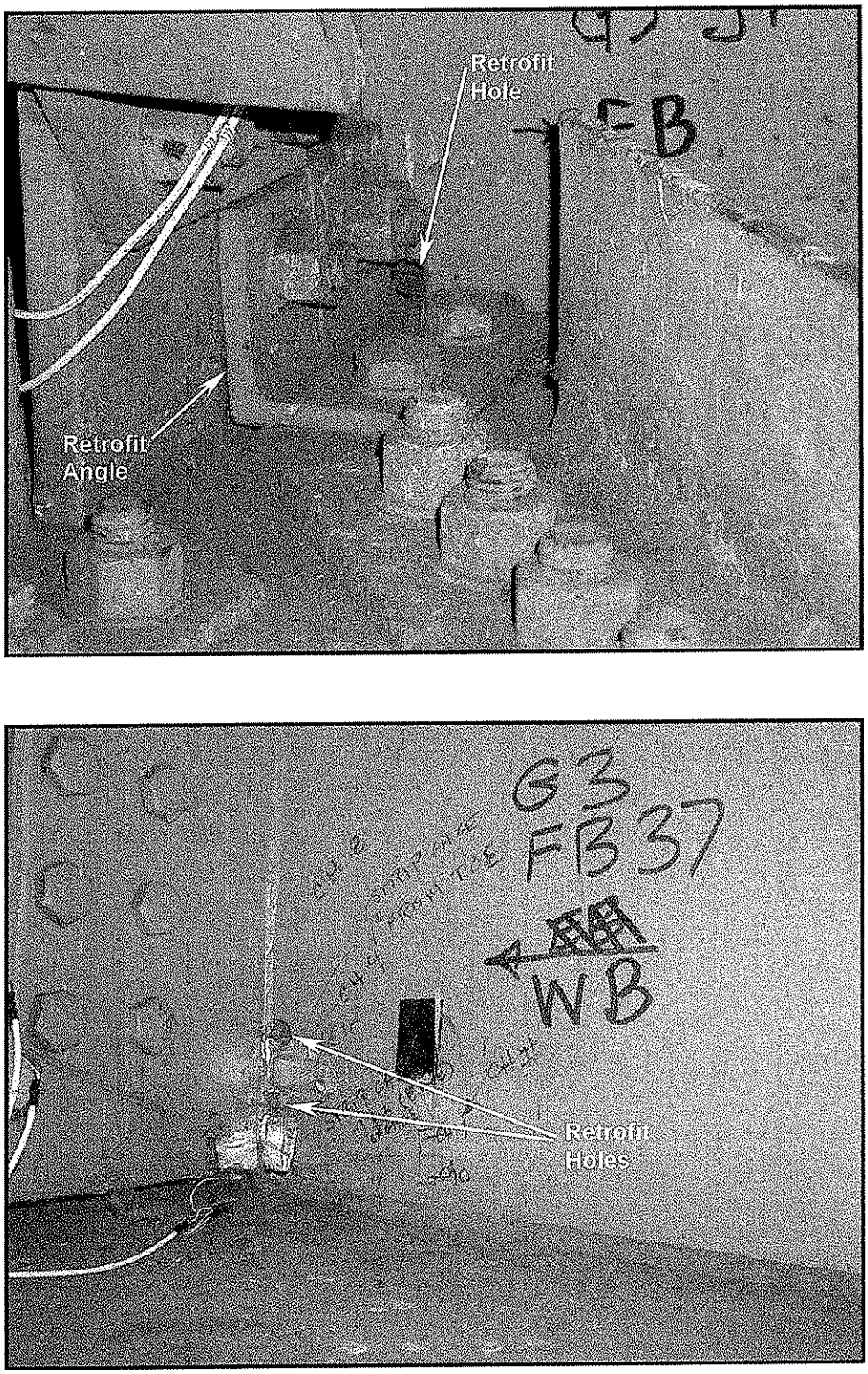

Figure 4.10 - Photographs of north and south faces of web at floorbeam 37 at girder G3. Note retrofit angles, drilled holes, and position of strain gages (the silver tape is installed to protect the gage from the environment)

4.3.3.1 Effectiveness of Existing Retrofits at Gusset Plates

The effectiveness of the retrofits used at the gusset plates was investigated by installing strain gages at selected locations. During the on-site monitoring, out-of-plane displacement was also monitored at one gusset plate during the passage of random traffic as described in Section 4.3.1, specifically at floorbeam 37 on G3 in bay 2. Figure 4.11 is a photograph of the displacement sensor (LVDT) used to measure relative movement between the gusset plate and the transverse stiffener.

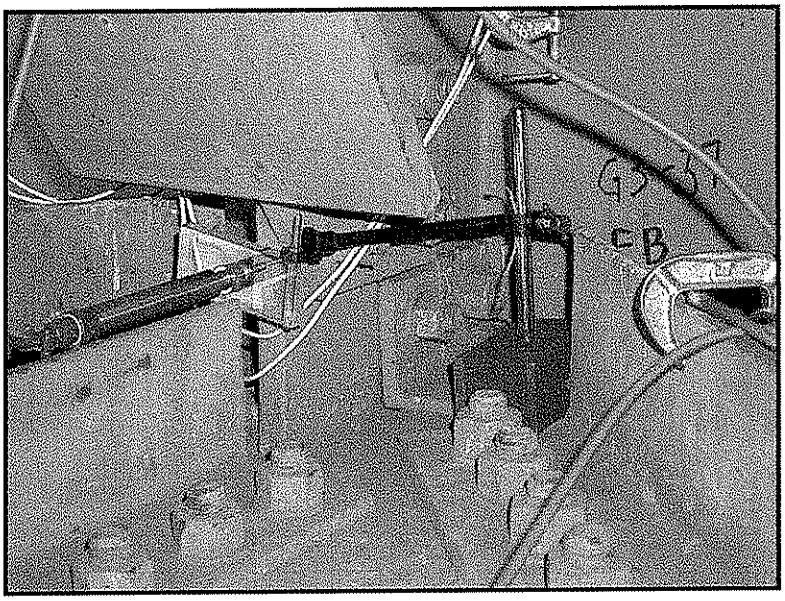

Figure 4.11 - Photograph of displacement sensor (LVDT) used to measure relative displacement between the gusset plate and the transverse connection plate at floorbeam FB37 on G3

Figure 4.12 compares the displacement response as a random truck crossed the bridge along with stresses measured at channel CH_5. For the data shown in Figure 4.12, the gusset plate moved away from the transverse connection plate as trucks passed. The response at channel CH_5, which is located on the opposite side of the web, is also plotted in Figure 4.12. As can be seen, tensile stresses develop at channel CH_5. Considering the location of channel CH_5, this affirms that the web plate is bending in the direction indicated by the LVDT. Other gages at this location (e.g., CH_6, CH_8, & CH_9), suggest that web is also subjected to a moderate "twisting" about the transverse connection plate. The twisting is the result of forces being applied by the lateral braces which frame into the connection at angles. Such behavior is typical in bridges with lateral bracing similar to the Kanawha River Bridge.

As shown in Table 4.4, the maximum out-of-plane displacement measured during the on-site monitoring was about 1.6 mils which corresponded to a stress range of 9.9 ksi at channel CH_5. This magnitude of displacement indicates that the retrofit angles are not fully effective in preventing relative movement between the two components. The retrofit used at this location is not as effective as the pairs of larger angles installed at the upper ends of the transverse connection plates.

During the remote long-term monitoring program, displacements were not measured. However, comparing data from channel CH_5 (which was included in the long-term program) suggests that relative displacements of up to 3 mils frequently occur.

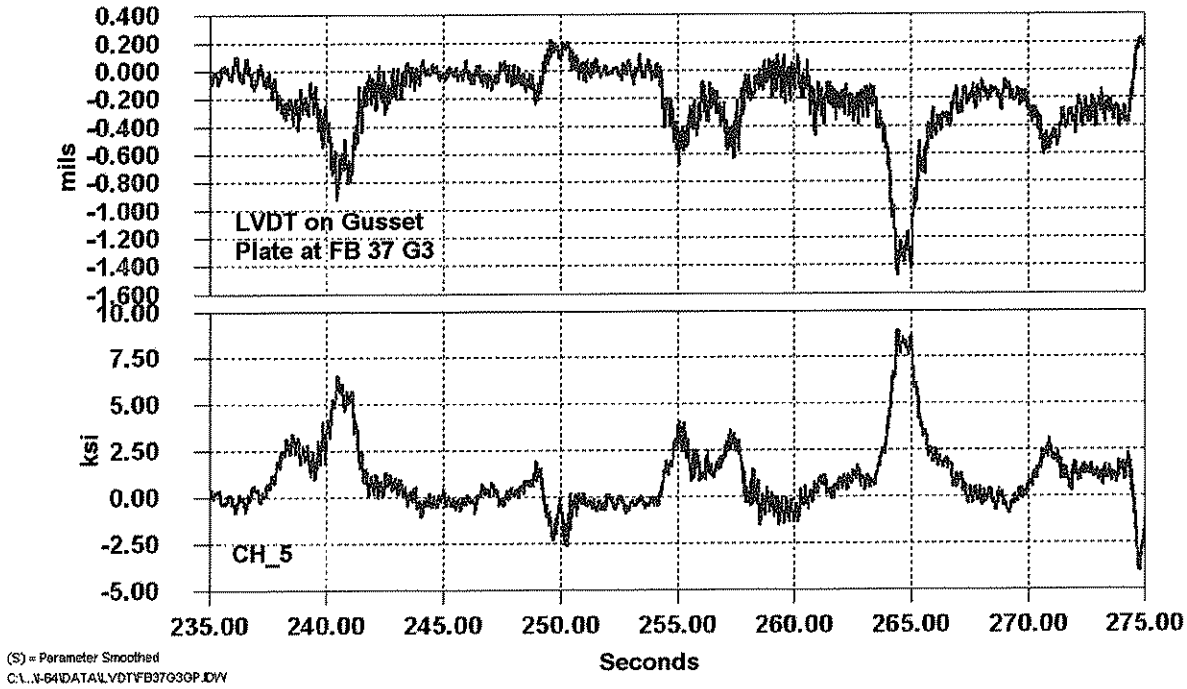

Figure 4.12 - Comparison of relative displacement measured between the gusset plate and the transverse connection plate at floorbeam FB37 on G3 and strain gage CH_5

Strain gages were installed on the opposite face of the web plate (CH_5, CH_6, CH_8, & CH_9) as this allowed complete access to the web gap region. Note that these gages are located between the two retrofit holes drilled above and below the gusset plate (see lower photograph in Figure 4.10 and Appendix A). Measurements made during the controlled load tests and the on-site monitoring indicated that the remaining "strip" of steel in the web will develop cracks in the future.

Table 4.3 summarizes the result of measurements made during the controlled load tests at channels CH_7, CH_10, and CH_11 which were oriented perpendicular to the web/flange weld (i.e., vertically) at the lower web gap (see Figure 4.10). As can be seen, the test truck produced relatively low stress ranges at these three gages. However, during the on-site monitoring, the greatest stresses were measured at channel CH_7 where individual trucks regularly produced stress ranges between 7.0 ksi and 8.0 ksi. The maximum stress range measured was about 11.0 ksi.

It must be noted that if the existing angles on the lateral gusset plate to transverse connection are replaced with a stiffer system, a more secure connection between the transverse connection plate and the gusset plate will be achieved. However, this will likely increase the stress range at the bottom web gap since most displacement will be

forced to occur between the flange and connection plate. This will be discussed in Section 6.

4.3.3.2 Lateral Struts with a Gusset Plate Attached to Web and Transverse Connection Plate

Strain gages were installed on each end of the lateral strut between girders G1 and G2 at floorbeam FB24 in bay 1. Gages CH_27 (shown in Figure 4.13) and CH_22 were installed on the flange of the WT near girders G1 and G2, respectively. In addition, gages CH_28 (shown in Figure 4.13) and CH_21 were located adjacent to the web of girder G1 and G2, respectively. Figure 4.13 is a photograph of the gages installed near girder G1.

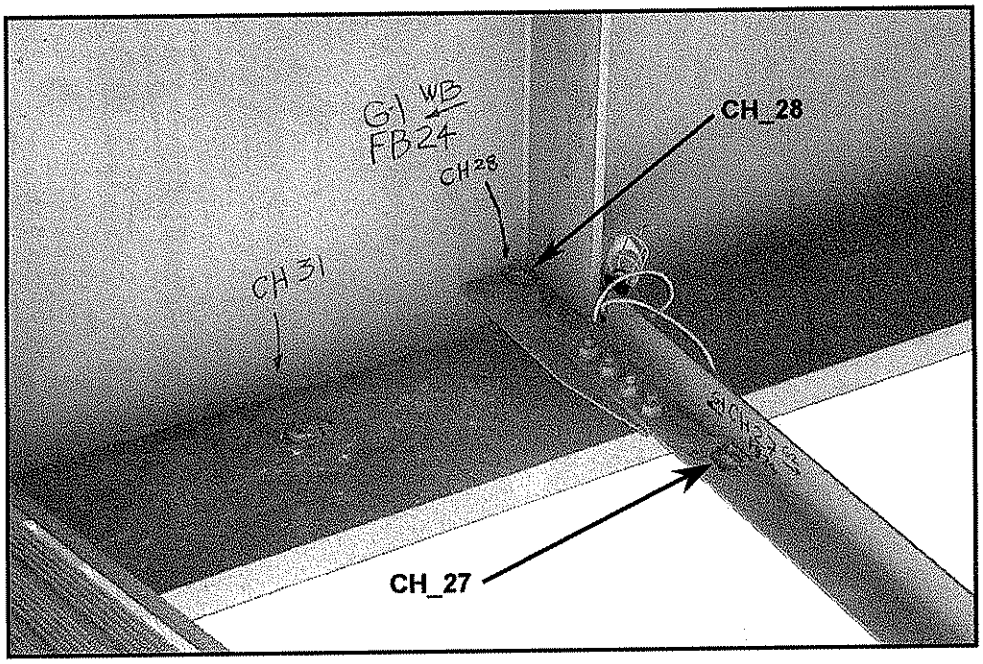

Figure 4.13 - Photograph of strain gages installed on lateral strut (CH_27) and on gusset plate connected to web and transverse connection plate (CH_28)

Channel CH_27 which was installed on the lateral strut near G1 was monitored during the controlled load tests and the on-site monitoring. The test truck produced stress ranges between 0.4 ksi to 0.6 ksi in CH_27 when the truck was headed west bound. Stress ranges of up to 0.8 ksi were measured during the on site monitoring of random traffic. Assuming that the stresses in the member are primarily the result of axial forces, estimates of the axial force "driven" into the transverse connection plate can be made.

4.3.3.3 Connections Subjected to Out-of-plane Forces with Lateral Gusset Plates on Each Side of the Web

In span 10 between floorbeams FB16 and FB26, the gusset plate attaching the lateral strut in bay 1 to the web of girders G1 and G2 is welded to both the transverse stiffener and the web. However, in bay 2, the lateral gusset is slotted and only welded to the web plate with no direct connection to the transverse connection plate as seen in Figure 4.9.

Because the gusset plate is only attached to the web in bay 2, out-of-plane forces imparted by the lateral system can produce large stresses in the web gap region between the transverse stiffener and the lateral strut gusset plate as was demonstrated in span 11 at floorbeam FB37. However, in span 10 at girder G2 in bay 1, the gusset plate is welded to both the web and the transverse connection plate and is directly opposite the gusset plate in bay 2. This connection provides a bridge across the gap on the opposite surface and should minimize the amount of out-of-plane distortion produced in the web gap. In order to determine the effectiveness of this restraint, strain gages were positioned on opposite sides of the web to assess the direct transfer of force through the web plate (i.e., channels CH_20 and CH_21).

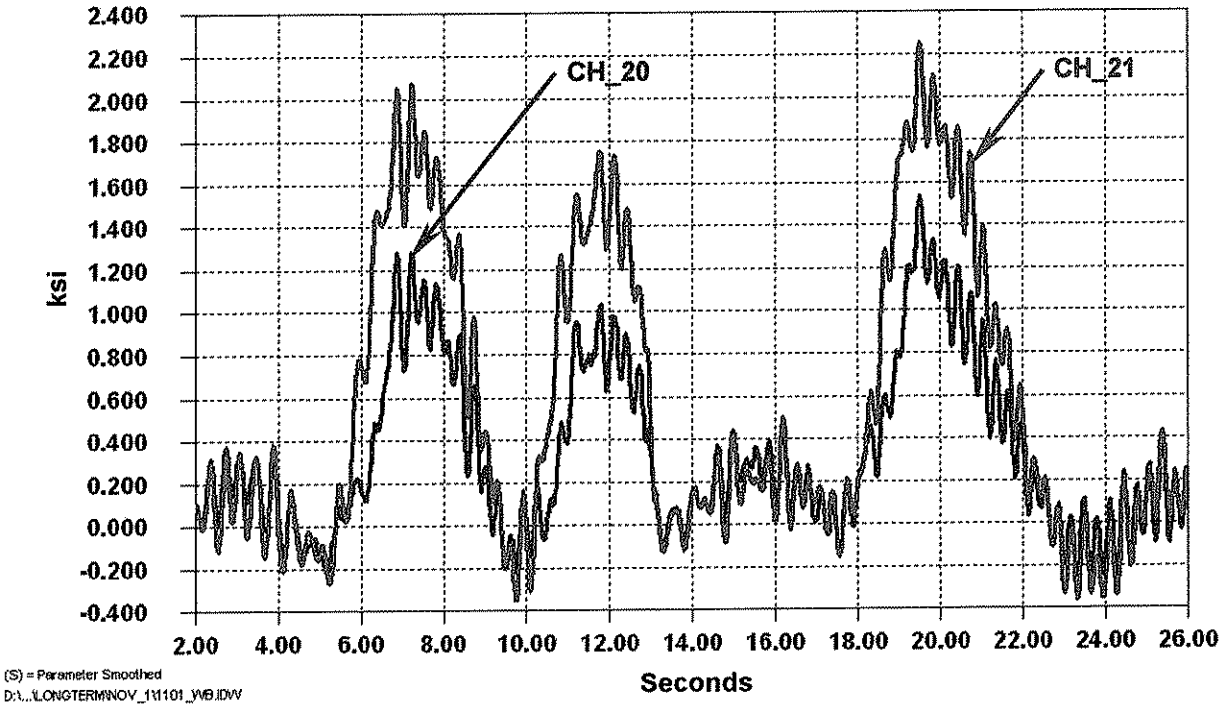

Figure 4.15 - Comparison of response from CH_21 and CH_20 during the passage of random trucks during the long-term monitoring program

Gages CH_21 and CH_20 were located on opposite sides of the web and directly in line with each other as shown in sheet 3 in Appendix A. Figure 4.15 presents the response from CH_21 and CH_20 during the passage of random trucks during the long-term monitoring program. Note that the response from each gage is nearly identical,

indicating continuity through the welded connections. The stress range at channel CH_20 (installed on the larger gusset plate) is less than at CH_21. This is expected since the lateral forces acting on the larger gusset plate that are normal to the girder web are being resisted by the smaller gusset plate in bay one which is both narrower and thinner, and would be expected to be subjected to a greater stress.

The continuity between the gusset plates indicated by the measurements confirms that the transverse connection plate in bay 1 is providing sufficient restraint and stiffness to bridge the web gaps of the connection in bay 2. Hence, web gap cracking from out-of-plane stresses will not develop at the slotted detail. Although only one of these details was instrumented, the observed continuity is representative of the other connections with similar geometry in span 10 and is consistent with the inspection observations that have shown no evidence of cracking.

4.3.3.4 Lateral Braces at Floorbeam 34 at G3

Uniaxial gages were installed on the lateral braces framing into the web and transverse connection plate at floorbeam 34 on girder G3 (CH_34 and CH_37) as shown in Figure 4.16. At this floorbeam, the lateral braces and lateral strut are in different horizontal planes. The lateral braces are about four inches above the bottom flange and about four inches below the lateral strut. Gages CH_35 and CH_36 were installed on the gusset plate perpendicular to the transverse connection plate (See Sheet 4 in Appendix A).

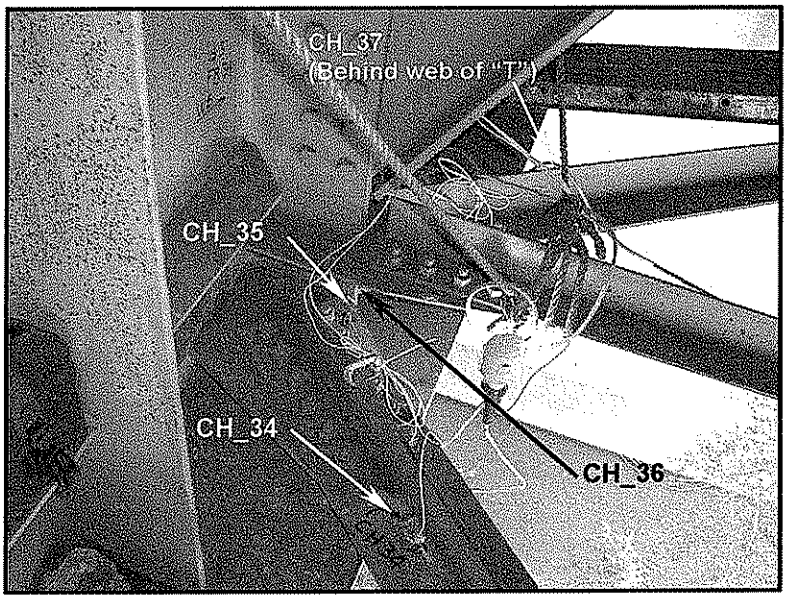

Figure 4.16 - Photograph of gages CH_34, CH_35, CH_36, and CH_37 installed at floorbeam 34 of G3 in bay 2

Small cracks were observed at the weld termination at the end of the of the gusset plate and the free edge of the transverse connection plate at floorbeams FB34 on girder G3 and FB8 of G3 [3]. A review of the inspection report [3] and photographs of the

detail, indicate that the cracks are most likely growing out of the lack of fusion zone on the lower side of the gusset plate. This cracking is shown in Figure 4.17. The single-bevel groove weld has a fillet weld placed at the root. A lack of fusion condition appears to exist at the plate edge. Depending on the size of the lack of fusion, cracks could be expected to grow at the plate edge into the welds at a lower stress range than from a weld toe. This appears to be the cause of the cracks observed at the gusset plates at floorbeams FB34 and FB 8.

Channels CH_35 and CH_36 were installed perpendicular to the weld toe of the gusset to transverse connection plate welds at floorbeam 34 of girder G3, as shown in Figure 4.16. These gages can be used to establish if additional weld toe cracking can be expected at these details.

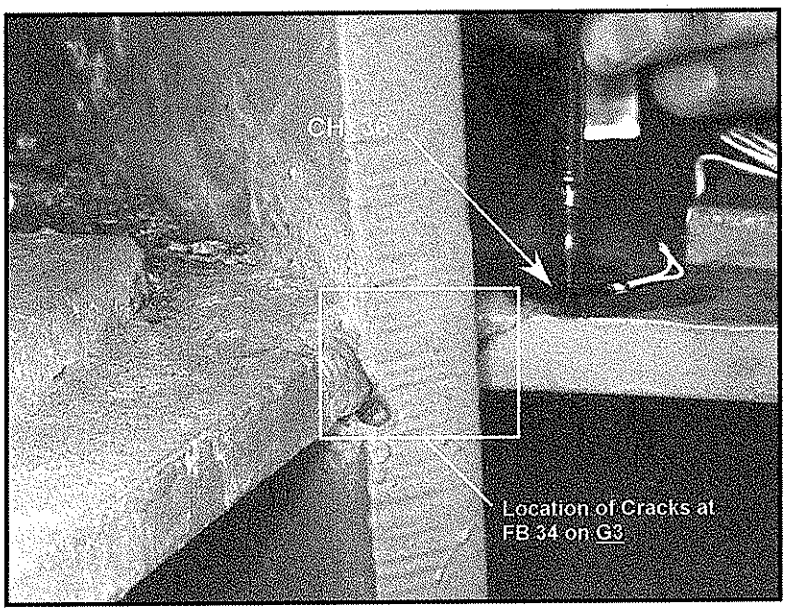

Figure 4.17 - Close-up photograph of gage CH_36 installed at floorbeam FB34 of G3 in bay 2.

During the controlled load tests and the on-site monitoring, the maximum stress range measured in channel CH_35 and CH_36 was 6.3 ksi and 4.0 ksi, respectively. A typical response from channels CH_35 and CH_36 are presented in Figure 4.18. The data were collected as a random truck crossed the bridge in lane four headed eastbound. Note that there is a sinusoidal vibration between 15Hz to 18Hz that occurs throughout the time history. It is apparent from Figure 4.18 that the vibration increases the maximum stress range due to the crossing vehicle by about 0.8 ksi. The larger "free" vibration induced stress is introduced after the vehicle crosses from span 10 into span 11. (*This was observed at several lateral members and gusset plates on the bridge. The maximum stress range associated with this vibration was about 1.5 ksi at FB34.*)

For weld toe cracking, the fatigue resistance of this detail can be categorized as category C for the cruciform type joint. The CAFL for category C is 10.0 ksi, which is

greater than the maximum stress range measured at this detail at floorbeam 34 on G2. It is unlikely that the other similar details in bay 2 (i.e., at floorbeams 27-30, 32, 33, and 35 near pier 10 and corresponding floorbeams near pier 9) are subjected to stresses much greater than measured at floorbeam FB34. Hence, weld toe cracking is not expected to occur at this type of detail during the remaining life of the structure.

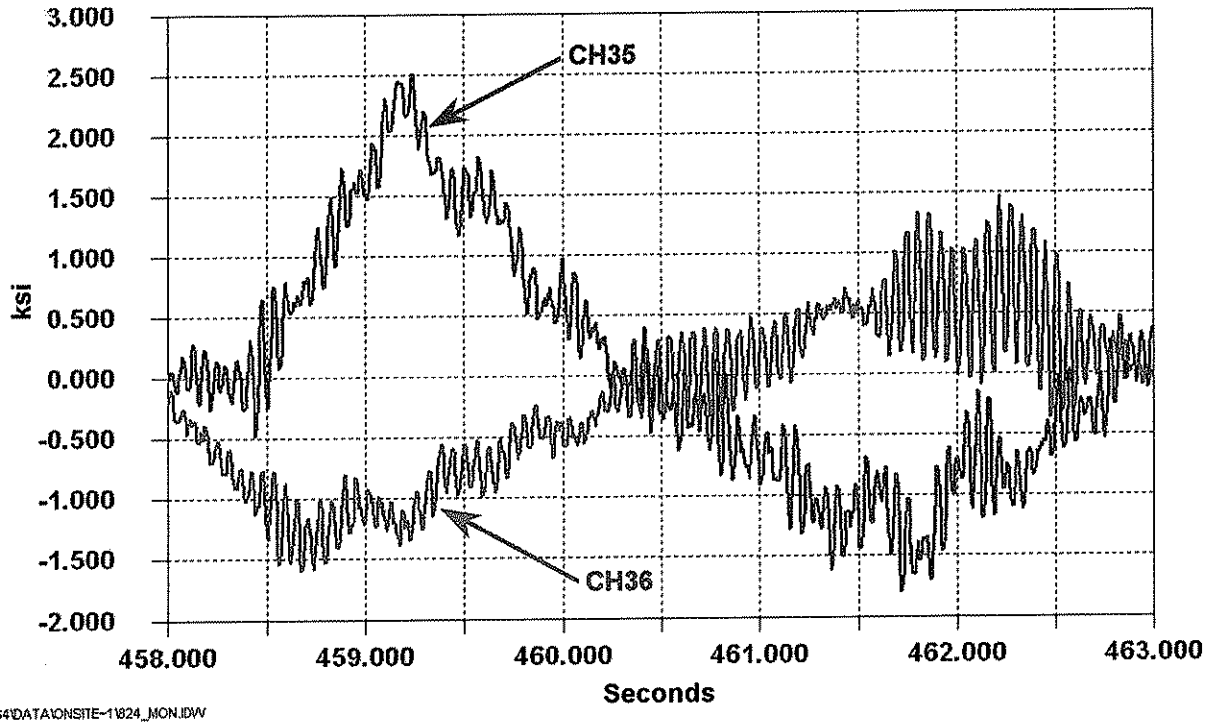

Figure 4.18 - Typical response from CH_35 and CH_36 at FB34 during the passage of a random truck headed eastbound during the on-site monitoring
Note vibration of 15Hz to 18Hz, particularly at channel CH_35

The test truck produced stress ranges less than 1.0 ksi for all lane positions. During the onsite monitoring, measured stress ranges were also small, less than 1.5 ksi. Considering the low magnitude of the stress range, this gage was not included in the remote long-term monitoring program. The main girder flanges in Span 10 were monitored at G1 and G4 near FB24. These test results provide an upper bound estimate of the web stresses during the monitoring period at the "defect" identified near FB18 on G3. Any embedded defect can be idealized as a circumscribed penny-shaped crack. For the defect in question:

$$\Delta K = \frac{2}{\pi} S_r \sqrt{a_r \pi} \sqrt{\sec \frac{a_r \pi}{2t}} \leq \Delta K_{th} = 3ksi\sqrt{in}$$

Even a 3/8 in circumscribed crack would be below the crack growth threshold at the maximum stress range of 4 ksi. No problems are expected at this apparent discontinuity.

4.4.2 Flange Splice

A single uniaxial strain gage was oriented longitudinally at an apparent weld discontinuity located in a bottom flange groove weld splice near FB33 on girder G2. This weld was made using the electroslag process. In previous inspection reports on the Kanawha River Bridge [4], this discontinuity is referred to as "discontinuity 2" or "R3" and is located about 178ft west of pier 11 (i.e., between floorbeams FB32 and FB33). Figure 4.20 is a photograph of this gage and location (channel CH_33). The acoustic emission monitoring had indicated that this site was active in AE.

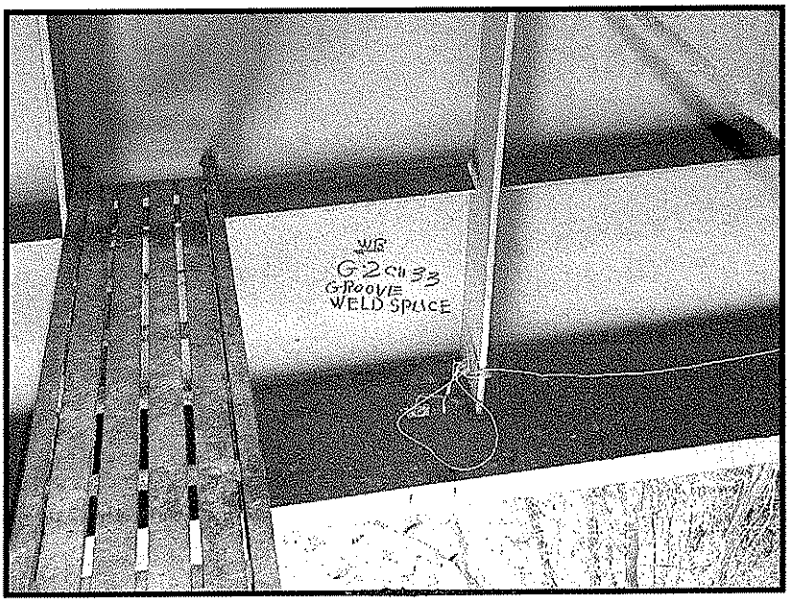

Figure 4.20 - Photograph of channel CH_33 installed at an apparent weld discontinuity in a groove weld splice on the bottom flange of girder G2 between floorbeams FB32 and FB33

The test truck and random traffic (measured during the onsite monitoring) produced stress ranges less than 1.0 ksi. Considering the low magnitude stress range, this gage was not included in the remote long-term monitoring program. The strain gage measurements further verified that crack extension at the electroslag groove weld was not likely as the stress range was well below the crack growth threshold and was in a region with primary compression stresses from dead load. The stress cycle was also dominantly in compression. This confirmed that any AE activity was more likely a result of web gap cracking at the transverse connection plate at floorbeam FB33 which was subsequently retrofitted in 1989.

5.0 Remote Long-Term Monitoring Program

The long-term remote monitoring program began on September 20, 2000 and was completed on November 21, 2000. However, data were only collected for a total of 55 days due to a problem with electromagnetic noise in the power supply. The review of the data indicate that daily truck traffic is consistent and trucks considerably heavier than the test truck regularly cross the bridge.

Table 5.1 summarizes the strain gages included in the monitoring program. These gages were selected after a review of the data collected during the controlled load tests and on-site monitoring. As can be seen in Table 5.1, several different types of details were included in the monitoring program. Triggered time history data and stress-range histograms were developed for all seventeen gages.

Ref #	Channel Name	LOCATION			S_r cutoff[1] (ksi)	Sheet #
		G#	FB#	Description		
1	CH_31	G1	FB24	Bottom Flange - 24in West of FB24	1.0	2
2	CH_26	G4	FB24	Bottom Flange - 24in West of FB24	1.0	2
3	CH_19	G2	FB24	S. East side of Bottom G.P. Perp. To Weld Toe	2.5	3
4	CH_21	G2	FB24	N. West side of Bot. Conn. Plate Gage is Perp. to Weld Toe (Opp. CH_20)	2.5	3
5	CH_34	G3	FB34	Gage on Bot. N. East Lateral Strut	1.0	4
6	CH_35	G3	FB34	N. East Conn. Plate for Lateral Strut – Gage is Perp. to Vert. Stiffener (Opp. CH_36)	2.5	4
7	CH_36	G3	FB34	N. West Conn. Plate for Lateral Strut – Gage is Perp. to Vert. Stiffener (Opp. CH_35)	2.5	4
8	CH_41	G3	FB34	S. East Top Web Gap – Retrofit Angle is Present	2.5	5
9	CH_43	G1	FB35	Bottom Flange - 24in West of FB35	1.0	2
11	CH_47	G4	FB35	Bottom Flange - 24in West of FB35	1.0	2
14	CH_20	G2	FB24	S. West side of Bot. G.P. Perp. To Weld Toe (Opp. CH_21)	2.5	3
15	CH_4	G1	FB35	Weld toe at @ S. West Longit. Stiffener	2.0	6
16	CH_5	G3	FB37	Adj. to Web/Stiffener Weld between Repair Holes (S. W. Repairs 5" above Bot. Flng., Opp. CH_8)	5.0	6
17	CH_7	G3	FB37	S. West Bottom Vertical Web Gap	3.0	6
18	CH_8	G3	FB37	Adj. to Web/Stiffener Weld between Repair Holes (S. E. Repairs 5" above Bot. Flng., Opp. CH_5)	5.0	6
19	CH_10	G3	FB37	S. East Bottom Vertical Web Gap	3.0	6
20	CH_11	G3	FB37	0.16 inches above CH_10	3.0	6

Notes:

1. S_r cutoff is the stress range below which cycles less than are ignored in the count.

Table 5.1 - Summary of strain gages included on remote long-term monitoring program which was conducted between September 21, 2000 and November 21, 2000

5.1 Main Girders

Gages installed on the bottom flanges of girders G1 and G4 were monitored at floorbeams 24 and 35. Specifically, channels CH_31 & CH_26 at floorbeam 24 and channels CH_43 & CH_47 at floorbeam FB35. As noted in Section 4.1, the measured stresses in girders G1 and G4 always exceeded stresses observed in girders G2 and G3.

The response of the main girders in these regions is primarily "global" in nature, (i.e., effects such as individual axles cannot be discerned). Hence, the response of the main girders in primarily influenced by the GVW of the truck(s) crossing the bridge.

During the remote long-term monitoring program, it became apparent that random trucks produced stress ranges significantly greater than the test truck. This observation was confirmed by the triggered time histories collected throughout the program.

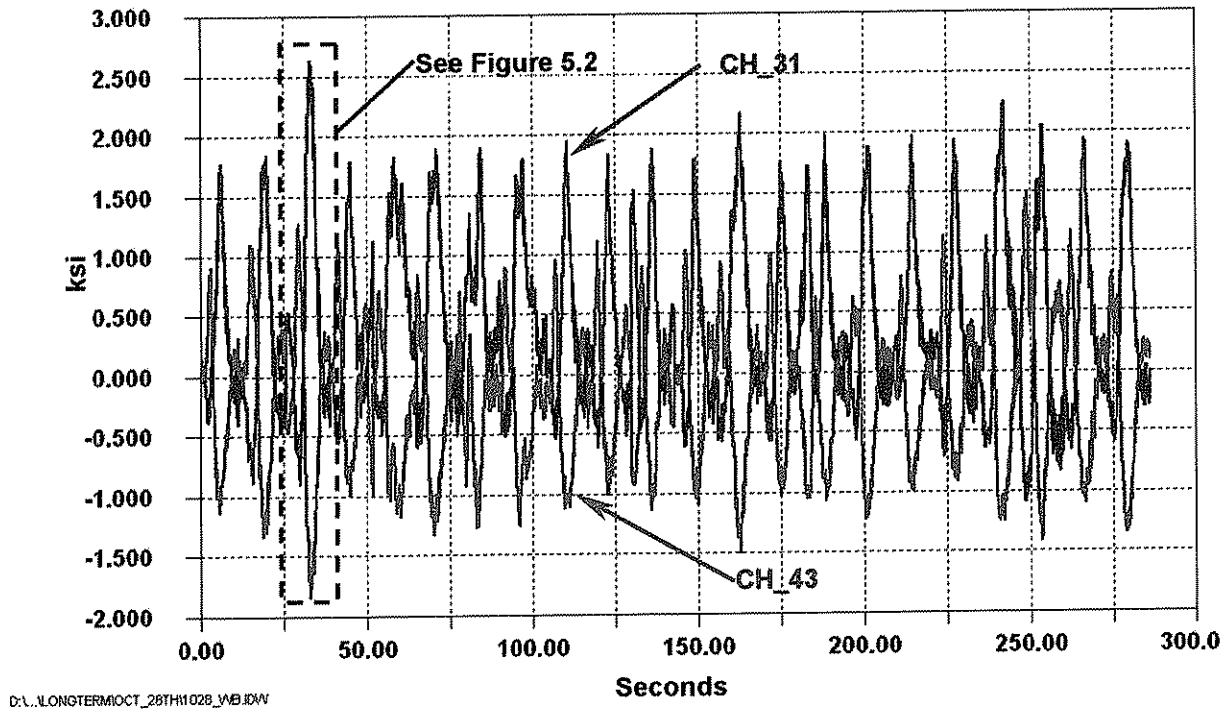

Figure 5.1 – Sample of triggered time history data for westbound traffic Data collected from channels CH_31 and CH_43 installed on bottom flange of G1 at FB 24 and FB35, respectively

Figure 5.1 is a sample of triggered time history data collected between 12:00AM on Monday October 23 and 12:00PM on Saturday October 28 of 2000. The data are from channels CH_31 and CH_43 located on the bottom flange of girder G1 at floorbeams FB24 and FB35, respectively. The stresses produced are for westbound traffic only. For these data, the trigger thresholds were set at +1.75 ksi for channel CH_31 and –0.75 for channel CH_43. Note that both of these conditions had to be met for the event to be recorded and that lighter trucks would not be included in the triggered time history data. However, all stress ranges cycles were accounted for in the rainflow cycle count.

Figure 5.2 is a detail of the event enclosed by the box in Figure 5.1. The stress range produced by this vehicle was about 3.5 ksi and 3.1 ksi for gages CH_31 and CH_43, respectively. This is considerably greater than 1.1 ksi and 0.8 ksi measured at these locations during test conducted using the controlled loads (see Table 4.1). A review of the data suggests that there were no other trucks on the bridge when this event was recorded. Table 5.2 summarizes the results of the remote long-term monitoring program for the gages installed on the bottom flanges of the girders. Only stress cycles exceeding 1 ksi were counted. As can be seen from Table 5.2, the effective stress range (Sreff) and the maximum stress range (Srmax) are consistent for all four gages. A greater number of cycles are produced in girder G1 than in girder G4 due to more frequent trucks and their heavier GVW headed westbound.

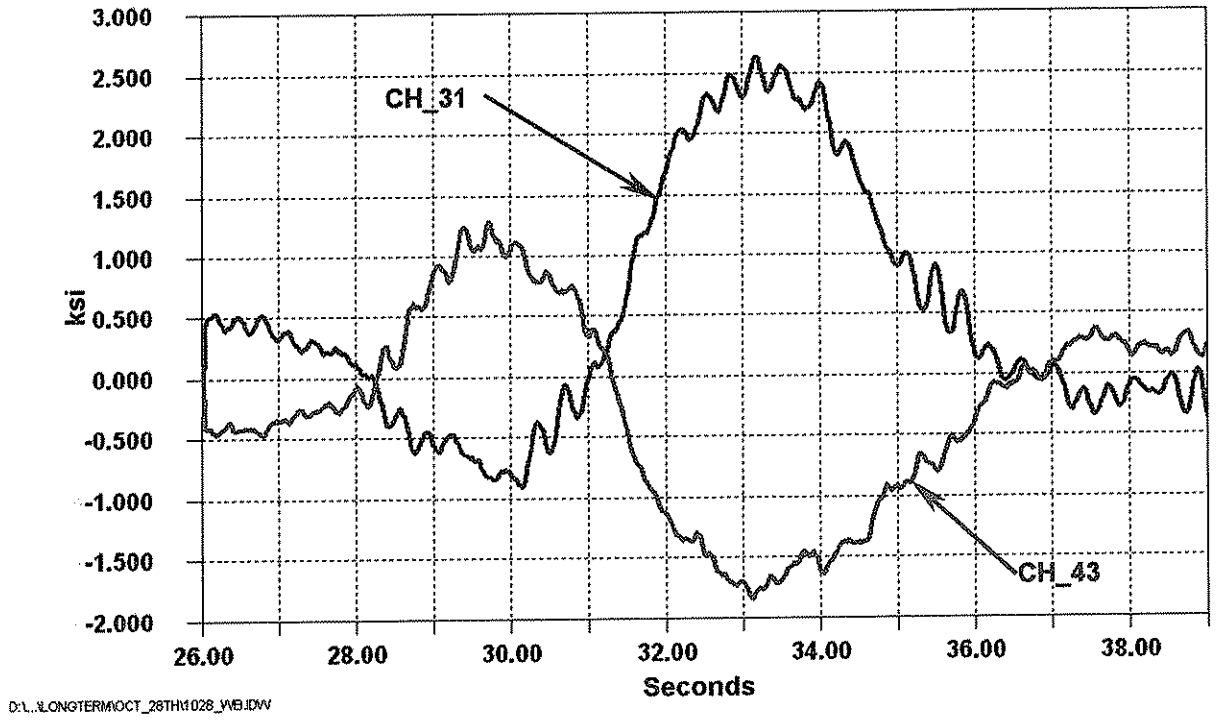

Figure 5.2 – Detail of event shown in Figure 5.1

Channel / Location	S_{rmax} (ksi)	# Cycles > CAFL[2]		S_{reff} (ksi)	Total # Cycles[1]	Cycles/ Day[3]
		#	%			
CH_31 G1/FB24	3.5	0	0.0	1.3	103,094	1,874
CH_26 G4/FB24	4.0	0	0.0	1.3	89,126	1,620
CH_43 G1/FB35	4.0	0	0.0	1.3	54,355	988
CH_47 G4/FB35	3.0	0	0.0	1.3	22,533	410

Notes
1. The monitoring program covered the period between September 21, 2000 to November 20, 2000.
2. Assumes Category C.
3. Total number of cycles divided by 55 days.

Table 5.2 – Maximum and effective stress ranges for gages installed on the top of the bottom flanges of girders G1 and G4

Many vehicles were observed to produce stress ranges greater than the test truck. The gross vehicle weight (GVW) of the test truck was 58.6 kips. West Virginia Department of Transportation, indicated that a significant number of "permit" vehicles regularly cross the Kanawha bridge. In order to gain some insight into the types of trucks crossing the bridge, a sample of permits issued during the monitoring program were obtained from the Department. The permit data will be discussed in Section 6.0 and compared with the data collected during the controlled load tests and long-term monitoring program.

5.2 Top Web Gap Retrofits

As shown in Table 5.1,channel CH_41, installed at the top web gap at floorbeam FB34 on girder G3 was included in the monitoring program as the test truck results showed it to be higher stressed than the gap at FB37. Retrofit angles were installed at both locations. Table 5.3 summarizes the results of the monitoring program at gage 41 on FB34.

Channel / Location	S_{rmax} (ksi)	# Cycles > CAFL[2]		S_{reff} (ksi)	Total # Cycles[1]	Cycles/ Day[3]
		#	%			
CH_41 G3/FB34	6.0	0	0.0	3.0	17,522	319

Notes
1. The monitoring program covered the period between September 21, 2000 to November 20, 2000.
2. Assumes C.
3. Total number of cycles divided by 55 days.

Table 5.3 – Maximum and effective stress ranges for gages installed on the top of the bottom flanges of girders G1 and G4

The magnitude of the measured effective and the maximum stress ranges indicate that the upper flange retrofit angles are providing sufficient restraint to out-of-plane forces. None of the stress cycles exceeded the CAFL for the web gap weld toes. This was also confirmed by the controlled load tests and out-of-plane displacement measurements, as discussed in Section 4.3.

5.3 Bottom Web Gap

Three gages installed at the FB37 web gap near the bottom flange were monitoring during the remote long-term monitoring program. Specifically, channels CH_7, CH_10, and CH_11 as seen on Sheet 6 of Appendix A. The axis of each gage was oriented perpendicular to the web/flange weld. These measurements are summarized in Table 5.4.

Channel / Location	S_{rmax} (ksi)	# Cycles > CAFL[2]		S_{reff} (ksi)	Total # Cycles[1]	Cycles/ Day[3]
		#	%			
CH_7 G3/FB37	15.0	646	0.2	4.7	399,095	7,256
CH_10 G3/FB37	10.0	0	0.0	3.8	165,518	3,009
CH_11 G3/FB37	11.0	2	0.0	3.8	203,716	3,704

Notes
1. The monitoring program covered the period between September 21, 2000 to November 20, 2000.
2. Assumes Category C.
3. Total number of cycles divided by 55 days.

Table 5.4 – Maximum and effective stress ranges for gages installed at the bottom web gap of girder G3 at FB37

It is clear from Table 5.4 that the effective stress range at all three gages is reasonably consistent. However, the number of cycles is considerably higher at channel CH_7 that at CH_10 and CH_11. Channels CH_10 and CH_11 are located on the opposite side of the transverse connection plate as channel CH_7 (See Sheet 6 in Appendix A). A similar observation was noted for channels CH_5 and CH_8 (see Section 5.5) at the level of the gusset plate. Channel CH_5, located on the same side of the gusset plate as channel CH_7, is also subjected to a greater number of cycles and greater peak stress range compared to channel CH_8. All data collected at this detail suggests that the stress range on the west side of the transverse connection plate (i.e., the side that channels CH_5 and CH_7 are on) is subjected to a greater stress. This difference is likely the result asymmetric out-of-plane web distortion and forces in the diagonal lateral member.

5.4 Web Gaps at Longitudinal Stiffeners

Channel CH_4, on girder G1 at floorbeam FB35 was included in the long-term monitoring program. Channel CH_4 was installed on girder G1 at floorbeam FB35 (See Sheet 8 in Appendix A) adjacent to the longitudinal stiffener weld toe as shown in Figure 5.3. Table 5.5 summarizes the results of the measurements made during the long-term monitoring program. The fatigue resistance of this detail to in-plane stresses can be categorized as a category E detail. The constant amplitude fatigue limit (CAFL) for category E is 4.5 ksi.

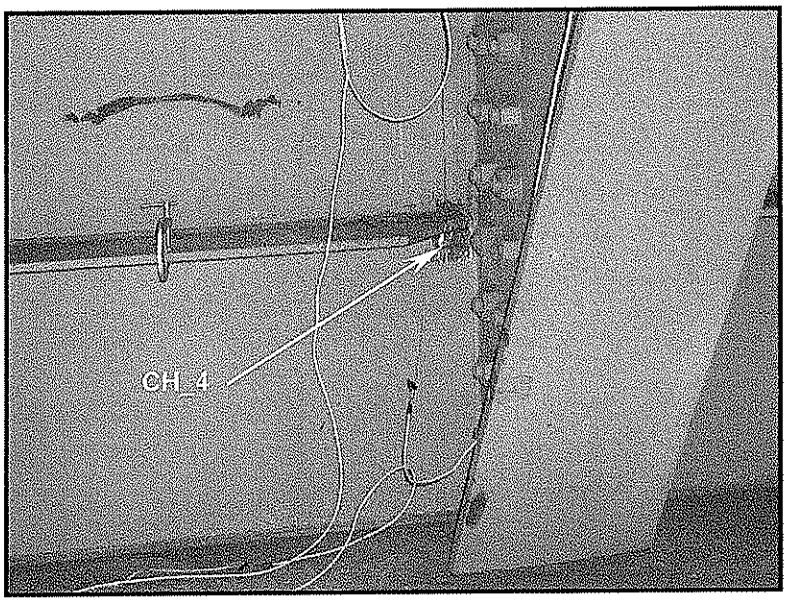

Figure 5.3 – Photograph of strain gage CH_4 installed at the web gap of a longitudinal stiffener at floorbeam FB35 at girder G1

Channel / Location	S_{rmax} (ksi)	# Cycles > CAFL[2]		S_{reff} (ksi)	Total # Cycles[1]	Cycles/ Day[3]
		#	%			
CH_4 G1/FB35	6.5	234	0.3	2.5	80,513	1,464

Notes
1. The monitoring program covered the period between September 21, 2000 to November 20, 2000.
2. Assumes Category E.
3. Total number of cycles divided by 55 days.

Table 5.5 – Maximum and effective stress ranges for gage CH_4 installed at the web gap of a longitudinal stiffener at floorbeam FB35 at girder G1

5.5 Web Gaps at Transversely Loaded Gusset Plate

Channels CH_5 and CH_8 were installed on the web of girder G1 at floorbeam FB37 opposite the longitudinal web gap created by the gusset plate and transverse connection plate (see Figure 4.10 and Sheet 6 in Appendix A). The axis of these gages were oriented perpendicular to the vertical weld for the transverse connection plate.

During the controlled load testing and on-site monitoring, high stress ranges were also measured at these locations. As expected, larger stress ranges were observed during the remote long-term monitoring program. Figure 5.4 presents a typical triggered time history for channels CH_5 and CH_8 recorded in late October, 2000. The two events presented (outlined in dashed boxes) were produced by different trucks and occurred about one hour and twenty minutes apart. As can be seen, a considerable stress reversal occurs.

The test results demonstrate that the two small retrofit angles installed in 1989 do not provide enough rigidity between the gusset and transverse connection plate to prevent high web gap cyclic stresses.

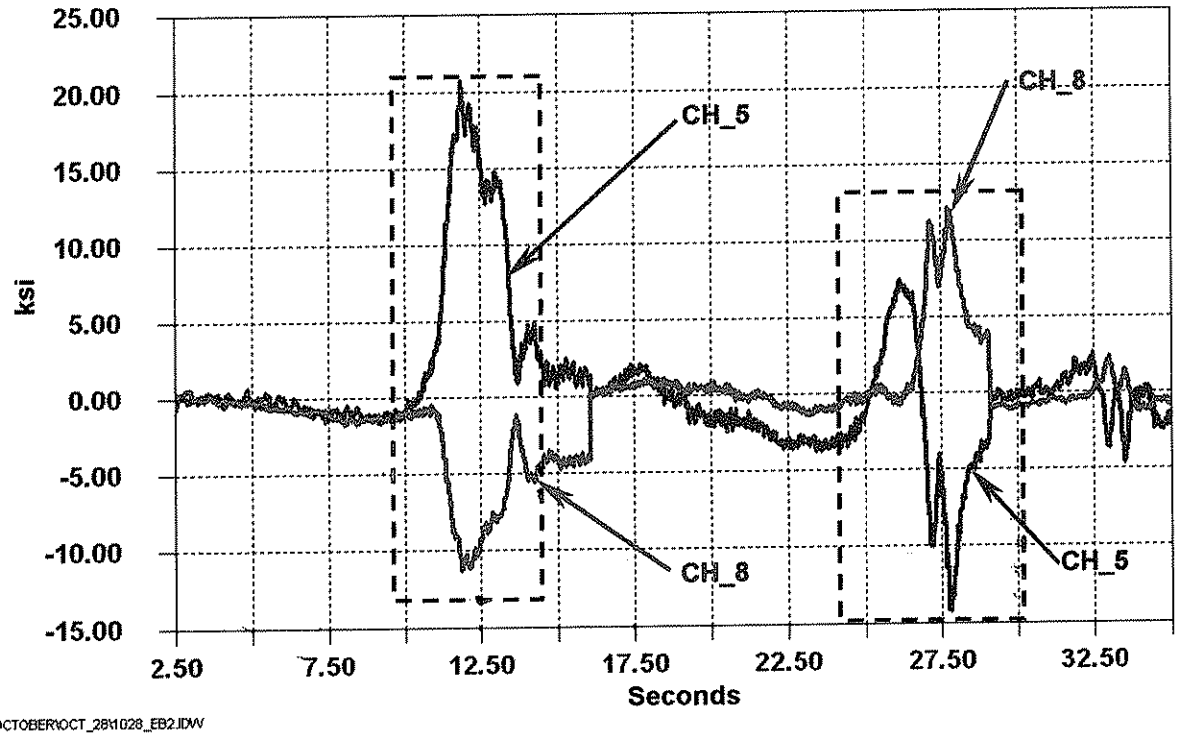

Figure 5.4 - Measured response at channel CH_5 and CH_8 installed on opposite side of gusset plate web gap at floorbeam FB37, girder G3 Note reversal in stress

Using the rainflow cycle counting method, the maximum peak and minimum valley of different cycles are added to calculate the peak stress range. For the data shown in Figure 5.4, this results in a stress range of about 34.8 ksi and 23.4 ksi for channels CH_5 and CH_8, respectively.

Table 5.6 summarizes the results of the web gap measurements made at channels CH_5 and CH_8. As can be seen, the maximum stress ranges are quite high. This is the result of the addition of peaks and valleys from different cycles, a described in Figure 5.4.

Channel / Location	S_{rmax} (ksi)	# Cycles > CAFL[2]		S_{reff} (ksi)	Total # Cycles[1]	Cycles/ Day[3]
		#	%			
CH_5 G3/FB37	38.0	53,624	22.9	9.7	234,383	4,262
CH_8 G3/FB37	28.5	6,678	11.2	8.1	59,393	1,080

Notes
1. The monitoring program covered the period between September 21, 2000 to November 20, 2000.
2. Assumes Category C.
3. Total number of cycles divided by 55 days.

Table 5.6 – Maximum and effective stress ranges for gage CH_5 and CH_8 installed on the opposite side of the web gap at a gusset plate at floorbeam FB37 at girder G3

The test results indicate the fatigue cracks will develop in the web gaps that are isolated by the four retrofit holes in the girder web at the gusset plate intersection with the floorbeam connection plate.

5.6 Gusset Plates and Lateral Bracing Members

Strain gages installed on the gusset plate at floorbeam FB24 of girder G2 were included in the long-term monitoring program. Specifically, channels CH_19, CH_20, and CH_21. These gages were positioned perpendicular to the web plate and adjacent to the weld toe attaching the gusset plate to the web (see Figure 5.5 and Sheet 3 of 8 in Appendix). Channels CH_19 and CH_20 were located on the south side of the girder (i.e., bay 2), while channel CH_21 was located on the north side of the girder (i.e., bay 1).

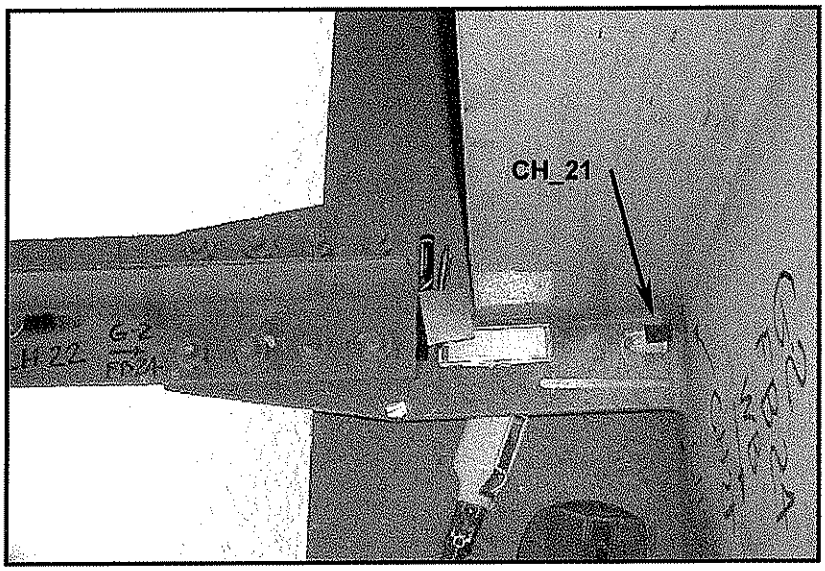

Figure 5.5 - Photographs showing orientation of channels CH_21 located on gusset plate at floorbeam 24 at girder G2
Gages CH_19 and CH_20 located in similar positions on opposite side of web

Table 5.7 summarizes the results of the measurements made at channels CH_19, CH_20 and CH_21 during the monitoring program.

Channel / Location	S_{rmax} (ksi)	# Cycles > CAFL[2]		S_{reff} (ksi)	Total # Cycles[1]	Cycles/ Day[3]
		#	%			
CH_19 G2/FB24	5.5	0	0.0	2.9	10,010	182
CH_20 G2/FB24	6.5	0	0.0	3.0	17,970	327
CH_21 G2/FB24	5.5	0	0.0	3.0	11,611	211

Notes
1. The monitoring program covered the period between September 21, 2000 to November 20, 2000.
2. Assumes Category C.
3. Total number of cycles divided by 55 days.

Table 5.7 – Maximum and effective stress ranges for gage CH_19, CH_20, and CH_21 installed on gusset plates at floorbeam FB24 at girder G2

Figures 5.6 and 5.7 compare the response at channels CH_19, CH_20, and CH_21 for eastbound and westbound truck traffic. These data were collected as heavy trucks passed in the eastbound (Figure 5.6) or westbound (Figure 5.7) lanes. Note that the response at each gage is opposite for eastbound and westbound traffic. This behavior is consistent with that observed during the controlled load tests (see Figure 4.8) and other bridges with similar details.

These reversals in stress result from the eccentricity of the loading which causes the lateral bracing system to push or pull on the gusset plate. As can be seen in Figures 5.6 and 5.7, east bound traffic results in compression in channels CH_20 and CH_21, whereas west bound traffic produces tension stresses. At CH_19 the opposite stress cycles occur, indicating that the lateral gusset plate is rotated out of plane as vehicles traverse the structure.

Reversals in stress range are expected due to differences in differential deflections between girders as trucks pass in different lanes. As mentioned earlier, the maximum stress range from sequential vehicles is the summation of the peak and valley for each channel. It must be noted that these stress reversals increase the stress range at the lower web gap (i.e., between the connection plate and the flange). *Although no strip gages could be installed at the lower web gap in span 10, estimates of the stress range at lower web gaps have been made and are discussed in Section 6.0.*

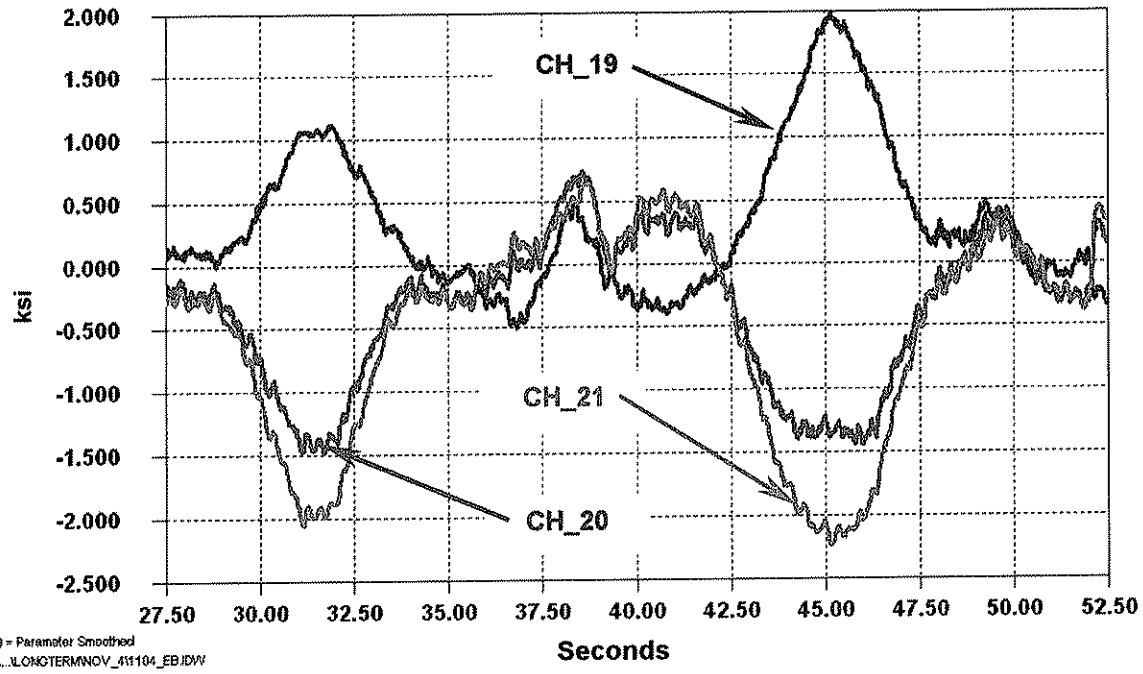

Figure 5.6 - Response of channels CH_19, CH_20, and CH_21 to random eastbound traffic

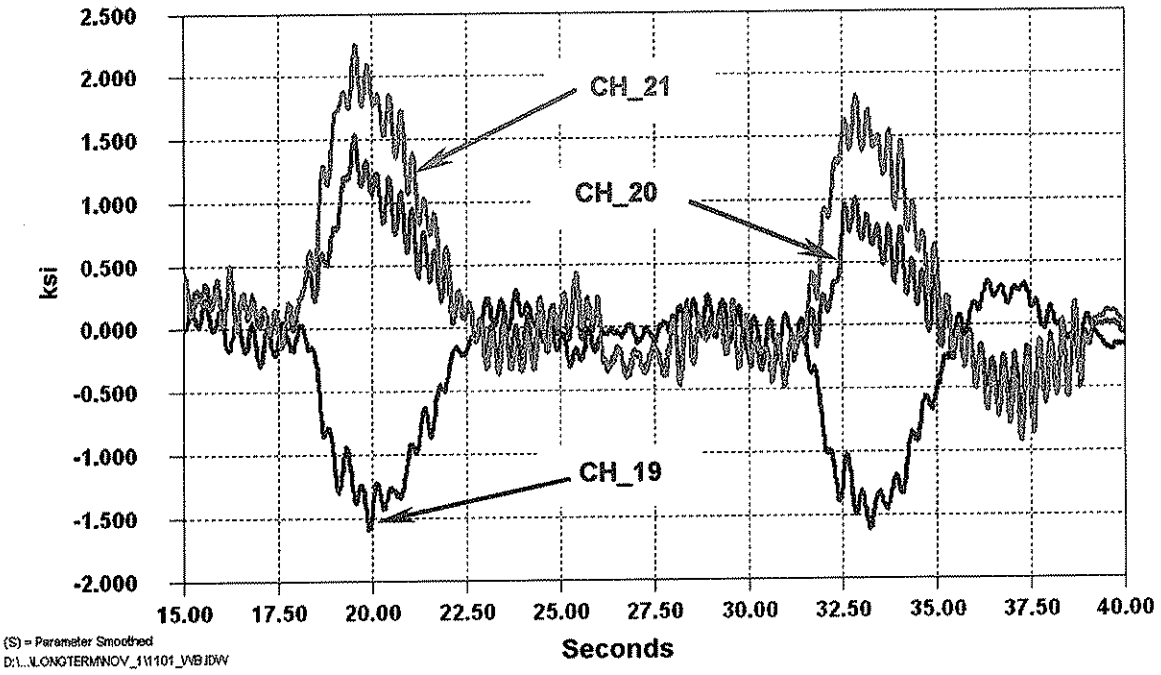

Figure 5.7 - Response of channels CH_19, CH_20, and CH_21 to random westbound traffic

Uniaxial strain gages were also installed at floorbeam FB 34 of Girder G3 on the gusset plate and lateral braces (See Sheet 4 in Appendix A). Three gages, CH_34, CH_35, and CH_36 were included in the long-term monitoring program (See Figures 5.8 and Figure 4.17). Cracks have been reported at the ends of the gusset plate near the free edge of the transverse connection plate (i.e., near channels CH_35 and CH_36) [3]. These measurements are summarized in Table 5.8.

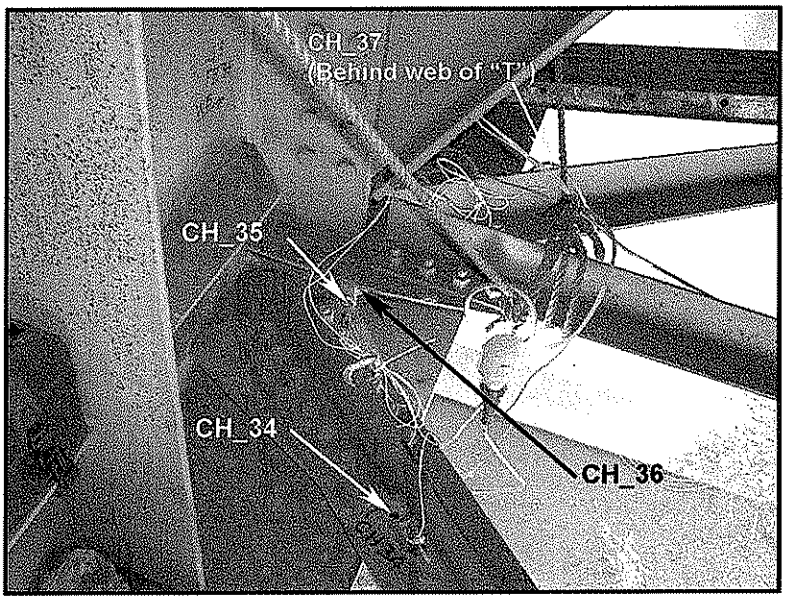

Figure 5.8 – Photograph of gages installed on gusset plate and lateral members at floorbeam FB 34 of Girder G3

Channel / Location	S_{rmax} (ksi)	# Cycles > CAFL[2]		S_{reff} (ksi)	Total # Cycles[1]	Cycles/ Day[3]
		#	%			
CH_34 G3/FB34	2.5	0	0.0	1.3	64,894	1,180
CH_35 G3/FB34	8.0	0	0.0	3.4	183,073	3,329
CH_36 G3/FB34	6.0	0	0.0	3.0	37,072	674

Notes
1. The monitoring program covered the period between September 21, 2000 to November 20, 2000.
2. Assumes Category C.
3. Total number of cycles divided by 55 days.

Table 5.8 – Maximum and effective stress ranges for gage CH_34, CH_35, and CH_36 installed on gusset plates and lateral brace at floorbeam FB_34 at girder G3

The strain gages installed on the gusset plate, CH_35 and CH_36, indicate that the effectives stress range and maximum stress range are in reasonably good agreement. During the long-term monitoring program, the maximum stress range measured was 8.0 ksi and 6.0 ksi in channel CH_35 and CH_36, respectively. However, the number of cycles measured at channel CH_35 are considerably higher than at channel CH_36. A review of the on-site monitoring data and triggered time history indicated that considerably more cycles are produced by vibrations on the west side of the connection. This was also observed while on site.

The measurements indicate that the lateral brace between floorbeams FB34 and FB35 is bending the gusset plate as it vibrates as well as pulling or pushing on it. The stress-range cycles in the gusset plate (CH_35) are about three times greater in magnitude than the lateral brace (CH_34). The large difference in cycles is due to the truncation levels, which was 1.0 ksi at CH_34 and 2.5 ksi at CH_35.

6.0 Interpretation of Results

Controlled load testing, on-site monitoring, and remote long-term monitoring were conducted in order to assess the fatigue life of the main spans of the Kanawha River Bridge at Dunbar. The results of the testing and monitoring program indicate that the overall global behavior of the bridge is consistent for a bridge of this type. The measurements also revealed that significant composite action is being developed even though these spans were designed as non-composite. The remote long-term monitoring program, which was conducted from September 21, 2000 to November 20th, 2000, revealed that very heavy vehicles regularly cross the bridge. This observation will be discussed further in Section 6.2.1.

This section of the report interprets and discusses the results of the testing program. In addition, the need for retrofits and potential retrofit concepts are also presented. Prior to this discussion, background information pertaining to strain gage measurements and the development of the stress range histograms is presented.

It should also be noted that some variability in test data, especially that collected during field testing, occurs because of the variation in vehicle weight, geometry and the randomness of the live loads. Other variables contributing to these deviations include variations in vehicle position as well as variations in fabrication and material tolerances. After reviewing the data collected at the I-64 Bridge, these factors were determined to be small. The controlled load tests also demonstrated that the data were consistent and repeatable.

6.1 Stress-Range Histograms

The stress-range histogram data collected during the uncontrolled monitoring permitted the development of a random variable-amplitude stress-range spectrum for seventeen strain gages. It has been shown that a variable-amplitude stress-range spectrum can be represented by an equivalent constant-amplitude stress range equal to the cube root of the mean cube (rmc) of all stress ranges (i.e., Miner's rule) [5] (i.e., $S_{reff} = [\Sigma\alpha_i S_{ri}^3]^{1/3}$).

During the long-term monitoring program, stress-range histograms were developed using the rainflow cycle counting method [6]. Several other methods have been developed to convert a random-amplitude stress-range response into a stress-range histogram. The rainflow cycle counting method is widely used and accepted for use in most structures. During the long-term monitoring program, the rainflow analysis algorithm was programmed to ignore any stress range less than 0.25ksi (9με). The of validity of stress range cycles less than this are questionable due to electromechanical noise.

The effective stress ranges presented for each channel in Section 5 were calculated by ignoring all stress-range cycles less than predetermined limits. For all welded steel details, a cut-off or threshold is appropriate and necessary, as will be discussed below. The limits were typically about ¼ the constant amplitude fatigue limit for the respective detail. For example, for strain gages installed at details that are characterized as category C, with a CAFL of 10.0ksi, the cutoff was set at 2.5ksi. Hence, stress range cycles less than 2.5 ksi were ignored in the preparation of the stress-range histograms. The threshold was selected for two reasons.

Previous research has demonstrated that stress ranges less than about ¼ the CAFL have little effect on the cumulative damage at the detail [7]. It has also been demonstrated that as the number of random variable cycles of lower stress range levels are considered, the predicted cumulative damage provided by the calculated effective stress range becomes asymptotic to the applicable S-N curve. A similar approach of truncating cycles of low stress range is accepted by researchers and specifications throughout the world [8].

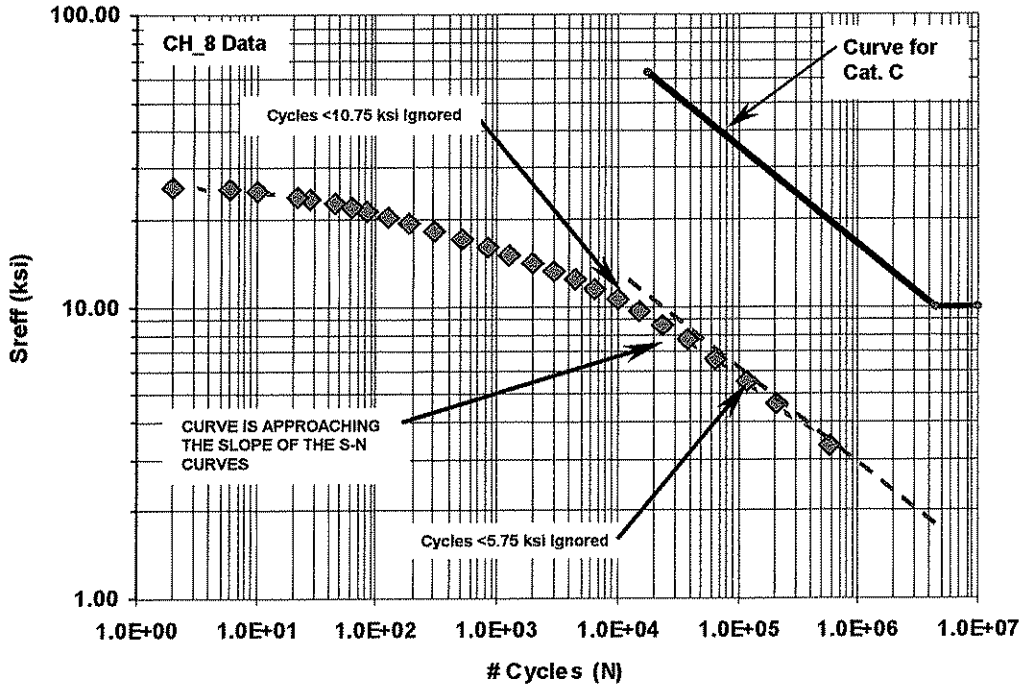

Figure 6.1 – Effect of truncating cycles at different stress range cut off levels
Data from October 2000 for channel CH_8

Figure 6.1, shows the effect on the calculated effective stress range for several levels of truncation using test data collected from channel CH_8 during the second monitoring period. Although only data from the month of October 2000 are considered, it is sufficient to illustrate the concept. The data presented in Figure 6.1 are also listed in Table 6.1 showing the selected truncation level and its impact on the effective stress range.

As demonstrated by Figure 6.1, as the truncation level decreases, the effective stress range and corresponding number of cycles approaches the slope of the S-N curve for Category C, which is also plotted in Figure 6.1 (i.e., a slope of –3 on a log-log plot). As long as the cut off level selected is consistent with the slope of the fatigue resistance curve, considering additional stress cycles at lower truncation levels does not improve the damage assessment and can therefore be ignored. As can be seen, using a truncation level as high as 10 ksi, the curve is nearly asymptotic to the slope of the S-N curves. Hence, an accurate prediction of fatigue life results.

The load spectrum assumed in the AASHTO LRFD specifications for design was developed by only considering vehicles greater than about 20kips [12]. Thus the AASHTO LRFD design also implicitly truncates and ignores stress cycles generated by lighter vehicles and vibration [11]. The observed frequency of stress cycles obtained from traffic counts is also consistent with the frequency of vehicles measured.

Cut Off (ksi)	Number Cycles > Cut Off Value	S_{reff} (ksi)
0.75	575,867	3.3
2.75	117,869	5.5
4.75	37,842	7.6
6.75	15,112	9.6
8.75	6,547	11.5
10.75	2,938	13.3
12.75	1,284	15.1
14.75	509	17.0
16.75	191	19.3
18.75	85	21.3
20.75	45	22.6
22.75	22	23.9
24.75	6	25.1
25.75	2	25.7

Table 6.1 – Calculated effective stress ranges using different stress range cut off levels
Only every other data shown in Figure 6.1 is shown for brevity
Data are for channel CH_8

The maximum stress ranges listed in the tables developed in Section 5 were determined from the rainflow count. According to rainflow cycle counting procedures, the peak and valley that comprise the maximum stress range may not be the result of a single loading event and may in fact occur hours apart. In other words, an individual truck did not *necessarily* generate the maximum stress range shown in the tables. This is particularly true of distortion induced stresses that are subjected to reversals in stress due to eccentricity of the loading. In many cases, it was possible to identify this maximum stress range with a specific vehicle passage, but in other cases, the maximum rainflow stress range exceeded the maximum stress range from any individual vehicle. During the remote long-term monitoring program, the stress range histograms were updated every ten minutes. Hence, the longest interval between nonconsecutive peaks and valleys is ten minutes.

6.2 Stress-Range Histograms – Main Girders

Stress range histograms were developed at four locations on the main girders as described in Table 5.2. The largest stress range measured during the remote long-term monitoring program was 4.0 ksi. (*As previously stated, the strain gages were placed on the top of the bottom flange. Hence stress ranges on the bottom surface will be slightly higher.*) The fatigue resistance of the welded transverse connection plates and transverse stiffeners, although not directly welded to the flanges, can be characterized as category C. The constant amplitude fatigue limit (CAFL) for category C is 10.0ksi. Strain gages were not placed on the web at the end of vertical fillet weld for the transverse connection plate. However, it is reasonable and conservative to assume that the stress range measured at the bottom flange is equal to the in-plane bending stress in the web at the end of the transverse connection plate. Considering the low stress ranges measured in the girders, fatigue is not expected to be a problem in the flanges or at the welded transverse stiffeners and connection plates for in-plane bending stresses. *(Out-of-plane effects at web gaps at transverse connection plates are considered in Section 6.3)*

The remote long-term monitoring program revealed that heavy trucks regularly cross the structure. The maximum stress ranges produced by the test truck were observed in girders G1 and G4 when the test truck positioned in lane one or four, respectively (1.1 ksi in girder G1 and 1.0 ksi in girder G4). However, during the monitoring program, larger stress ranges were measured. Figure 5.1 presented a typical of triggered time histories recorded in October of 2000. A review of the data confirm that these events were produced by individual trucks crossing the bridge. Heavy trucks commonly produced stress ranges of about 2.0 ksi, or about twice that produced by the test truck. If it is assumed that the gross vehicle weight (GVW) of these heavy trucks is roughly proportional to the increase in stress range, an estimate of the GVW of these trucks can be made. Hence, the GVW of the heavy trucks crossing the bridge can be estimated as $(S_{rrandom}/S_{rtest\ truck}) \times GVW_{\ test\ truck}$. This suggests that the GVW of typical heavy trucks crossing the bridge is about 117 kips (the GVW of the test truck was 58.6 kips). Obviously, 117 kips seems very high compared to the GVW of the test truck. However, a short five axle truck having rear axles that weigh the same as the test truck would weigh about 100 kips. During the on-site monitoring, individual trucks were observed to produce stress ranges as high as 2.3 ksi.

6.2.1 Review of Permits for Heavy Trucks

In order to verify that heavy vehicles are crossing the bridge, permits for heavy trucks issued by the West Virginia DOT were requested and data are summarized in Appendix B. A review of the permits indicated that many heavy vehicles regularly cross the bridge. These permits were issued between September 21, 2000 and November, 17, 2000. Each permit is valid for two weeks, so the permits cover the period between September 21, 2000 and December 1, 2000. On average all permitted vehicles (i.e., eastbound and westbound) were 95ft long, weighed 165 kips and had 9 axles. The heaviest truck weighed 298kips and was 164 ft long with 18 axles.

A histogram of the permit data is presented in Figure 6.2 and summarized in Table 6.2.

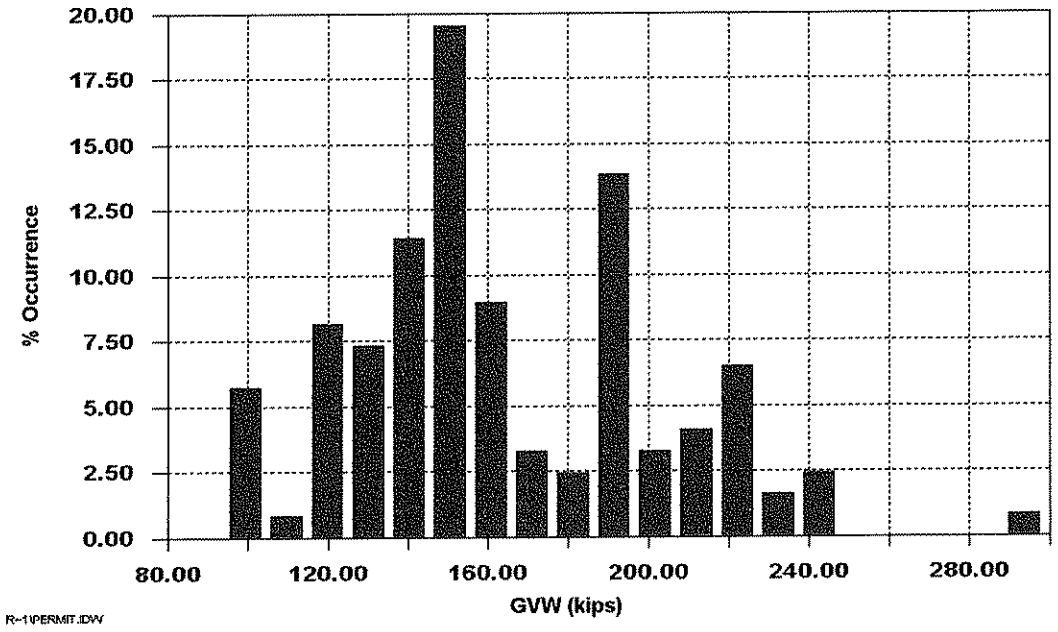

Figure 6.2 - Histogram of permit vehicles for eastbound and westbound traffic
Permits issued between September 18, 2000 and November 17, 2000

Bin #	Lower Limit of Bin (kips)	Upper Limit of Bin (kips)	Average of Bin (kips)	Percent Occurrence	# of Trucks
1	75.0	85.2	80.1	0	0
2	85.2	95.5	90.3	0	0
3	95.5	105.7	100.6	5.69	7
4	105.7	115.9	110.8	0.81	1
5	115.9	126.1	121.0	8.13	10
6	126.1	136.4	131.3	7.32	9
7	**136.4**	**146.6**	**141.5**	**11.38**	**14**
8	**146.6**	**156.8**	**151.7**	**19.51**	**24**
9	**156.8**	**167.0**	**161.9**	**8.94**	**11**
10	167.1	177.3	172.2	3.25	4
11	177.3	187.5	182.4	2.44	3
12	187.5	197.7	192.6	13.82	17
13	197.7	208.0	202.8	3.25	4
14	208.0	218.2	213.1	4.07	5
15	218.2	228.4	223.3	6.5	8
16	228.4	238.6	233.5	1.63	2
17	238.6	248.9	243.8	2.44	3
18	248.9	259.1	254.0	0	0
19	259.1	269.3	264.2	0	0
20	269.3	279.5	274.4	0	0
21	279.6	289.8	284.7	0	0
22	289.8	300.0	294.9	0.81	1

Table 6.2 - Summary of permit data used to make histogram in Figure 6.2

6.2.2 Use of Permit Data

In order to establish if the larger stress ranges were the result of permit vehicles, several factors which influence the load effects (i.e., stress range) from a given truck must be considered. These factors are discussed hereafter.

6.2.2.1 Geometry of Vehicle

Gross vehicle weight is not the only parameter that influences the response in the girders. The length of the vehicle and number of axles can greatly affect the measured stress range. Permits typically require that heavier vehicles spread the total load out over a greater length and to more axles. The permits received from the West Virginia DOT appeared to require such longitudinal load spreading or distribution.

6.2.2.2 Speed of Vehicle

The permits often placed a restriction on the speed of the vehicle in order to minimize dynamic amplification as well as for other safety concerns. Where restrictions were recorded on the permit, the maximum speed was always less than 30mph. Knowing that the speed of the vehicle is considerably slower than normal traffic and that the test truck is useful information. Because the permitted vehicles are very long and slow moving, the time history data should appear considerably different in the time domain than that produced by the test truck. (i.e., it should take longer for the permit vehicles to complete a stress range cycle.)

6.2.2.3 Number of Permits Issued

Finally, the number of permits issued during the 60 day period was 123. Of these, 50 were for eastbound travel and 64 were for westbound travel. The remaining 9 were described as either two-way trips or not identified. These numbers can be compared to the number of cycles counted during the monitoring program.

6.2.3 Comparison of Permit Data and Stress Range Histograms

The triggered time history data were reviewed to establish if permitted vehicles were responsible for some or all of the high stress ranges observed in the stress-range histograms. The average length of the permit vehicle was 95 ft and had 9 axles. This is about five times longer than the 18.9 ft test truck. The ratio of the GVW to total length of the vehicle can be thought of as a measure of load intensity. For the test truck, this was calculated as 58.6 kips/18.9 ft=3.1 kip/ft. However, for the permit vehicles this ratio was much less, on average only about 1.72kip/ft with a maximum of only 2.36kip/ft. This indicates that the weight of the permitted vehicles is more distributed, both in terms of physical length (95ft vs. 18.9ft) and load intensity. By dividing the load intensity factor by the number of rear axles (i.e., those carrying significant load) also gives some insight to how the load is distributed. For the test truck, this ratio is 3.1kip/ft/2axles=1.55. For the permitted vehicles, this ratio never exceeds 0.45 and averages only about 0.22. The test truck, although lighter than the permit vehicles produces a much more concentrated load. *(This discussion does not consider the effect of span length. It is intended to just compare how the loads of different trucks are distributed.)*

The data in Appendix B indicates that the permit vehicles are considerably heavier than the estimated GVW of the trucks causing higher stresses (i.e., 117 kips vs.

165 kips). However, because the load is much more distributed, the stress ranges produced by permitted vehicles would tend to be reduced. As a result, a direct relationship between the test truck and very long permit vehicles does not exist. Nevertheless, although the permit vehicles are long they are very heavy and could produce stress ranges in the main girders similar to those observed during the monitoring program.

A review of the triggered time history data reveals that the response of the main girders to random heavy trucks was similar to that of the test truck in the time domain. In other words, the stress range cycle produced by most of the random trucks took about the same time interval as the test truck. The permit vehicles were on average five times longer than the test truck and traveled at about half the speed. Hence, the time to complete a stress range cycle should be at least twice as great as the test truck. The stress range cycle produced by the test truck at channel CH_31 took between eight to ten seconds to complete. For a typical permit vehicle, the cycle should have taken between 16 and 20 seconds to complete. Only a very small number of vehicles produced stress cycles that approached these values. This suggests that the vehicles recorded during the triggered time histories were primarily the result of relatively short, fast moving trucks and not permit vehicles traveling at restricted speed.

Further, the number of permits issued is much less than the number of large stress range cycles observed in the triggered time history data. It is likely that the permit vehicles comprise a relatively small portion of the larger cycles counted. This implies that large numbers of high stress range cycles are the result of very heavy random vehicles that are not permit related.

6.3 Estimated Stress Range at Bottom Web Gaps – Spans 10 and 11

At some locations, one of the gusset plates is welded to both the web and the transverse connection plate. However, the transverse connection plate is not attached to the flange. As a result, cracking can occur due to out-of-plane displacements within the bottom web gap region as shown in Figure 6.3. *(Although Figure 6.3 illustrates this condition at a top flange, the behavior is similar at the bottom flange.)* Laboratory and field testing programs have demonstrated that cracking typically occurs at the toe of the fillet weld connecting the web to the flange or at the web to the transverse connection plate [9,10,13]. The fatigue resistance of this detail, subjected to an out-of-plane stress range, can be characterized using the S-N curve for category C [10]. Category C has a constant amplitude fatigue limit (CAFL) of 10ksi

Due to limited access, bondable strip (strain) gages could not be installed in the web gap at the bottom portion of the transverse connection plate. However, at one location (FB24 on G2), a weldable strain gage, channel CH_32, was installed (see sheet 3 in Appendix A). The response at the interior and exterior girders will be discussed separately below.

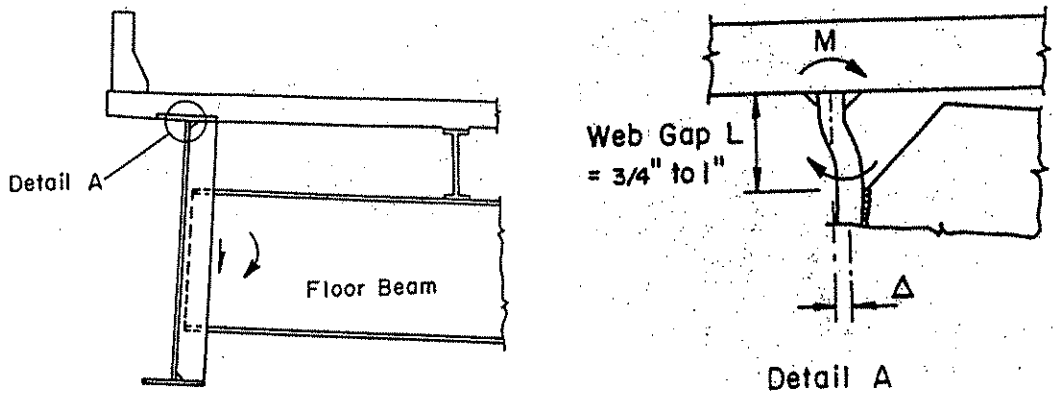

Figure 6.3 - Web gap distortion due to out-of-plane displacements
At top flange (bottom flange similar)

6.3.1 Bottom Web Gap – Exterior Girder

In order to better understand the behavior at this cross frame, concurrent time history data from channels CH_28 & CH_27, at girder G1 and channels CH_22 & CH_21 at girder G2 were reviewed. Figure 6.4 presents the typical response at these gages during the passage of a random truck. It is clear that the greatest stresses occur in gages installed adjacent to girder G2. At first glance, this appears inconsistent, especially for channels CH_22 and CH_27 which are located on different ends of the same member. However, further review of the structural system and force path shed some light on the measured behavior. Figure 6.5 illustrates the force distribution for a given load condition assuming simple statics and truss theory. According to basic truss theory, the portion of the lower strut enclosed in the dashed box must be a zero force member. Forces can only be carried through the deck and through the connection of girder G2 to girder G3 through the lateral system and cross frame in bay 2. However, due to some inherent stiffness

provided by the girder web, a small force can be carried through this end of the angle, as evidenced by the small stresses measured in channel CH_27 and CH_28.

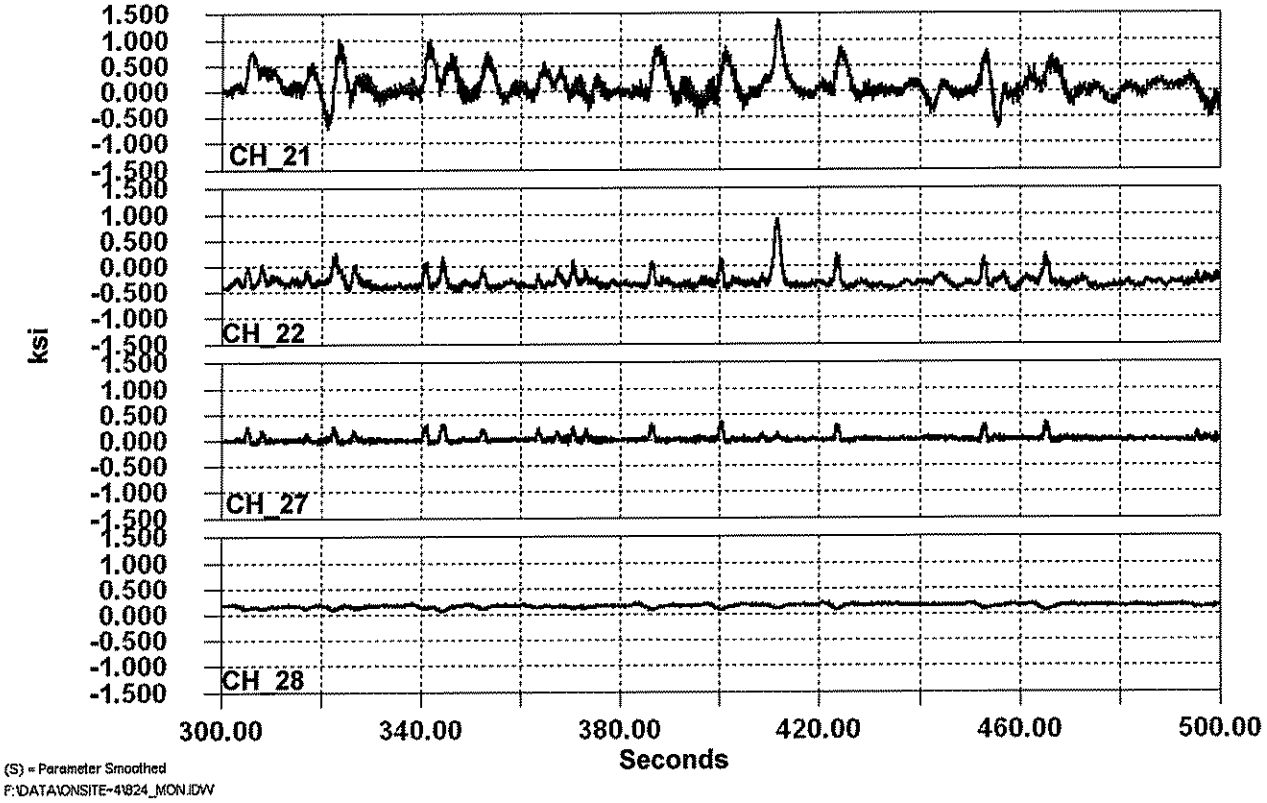

Figure 6.4 - Comparison of response e at channels CH_21, CH_22, CH_27 and CH_28

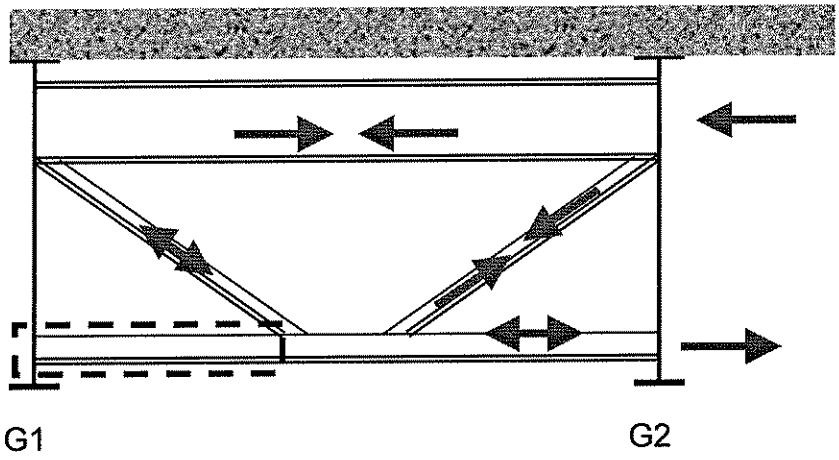

Figure 6.5 - Force transfer in cross frames in bay one or three
(Bay one shown, bay three opposite hand)

The lateral strut is a WT 5 x 16.5 and has an area of 4.85 in^2. The stress at channel CH_27 was between 0.5 and 0.75 ksi during the on-site monitoring. Although the magnitude of stress is relatively low, the force in the member (assuming axial stress) could be as high as 3.6 kips. Recall that web gap cracking is the result of out-of-plane displacements. Since there are no members on the outside of girder G1, all restraint is provided by the out-of-plane stiffness of the web. Hence, the connection is very flexible when subjected to even small out-of-plane forces.

In order to assess the possibility of cracking at the exterior girder, a simplified model was developed using the finite element method. Figure 6.6 is a general view of the model and contains a detailed view at the stiffener and web connection. Although it can not be clearly discerned in Figure 6.6, a very fine mesh was used in the web gap region. All components were modeled using three dimensional plate elements. Hence, the effect of additional constraint provided by the fillet welds is not considered. Nevertheless, the model does provide a reasonable estimate of the magnitude of stresses that could be expected at this detail.

Using the measurements made during the on-site monitoring of random traffic (a portion of which is shown in Figure 4.4), an estimate of the force applied to the connection was made. This force was then applied to the connection as shown in Figure 6.6. Based on the finite element analysis, stress ranges of 10 ksi to 14 ksi could be expected in the web gap at this detail when subjected to the 3.6 kip force in the lateral strut. The calculated out-of-plane displacement is only 0.0018 inches. Note the displacement measured at FB37 (see Table 4.4) showed that a movement of 0.0007 in resulted in a stress range of 6.3 ksi during passage of the test truck.

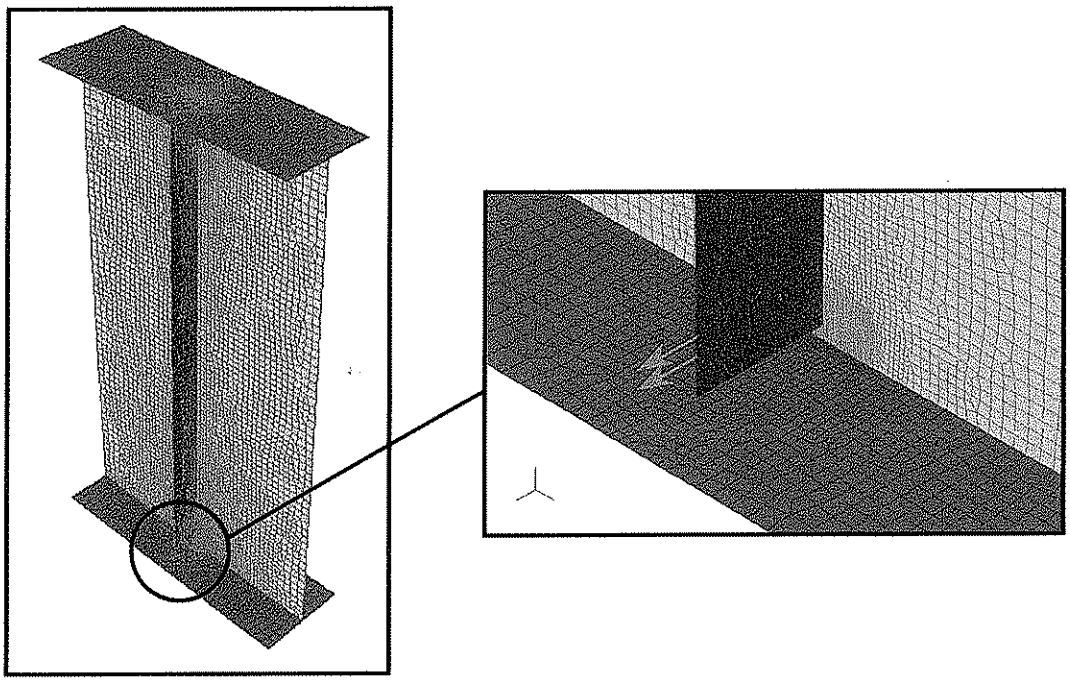

Figure 6.6 – Finite element models used to estimate stress range at bottom web gap at floorbeam FB24 on girder G1

Channel CH_27 was not included in the long-term monitoring program. Hence, a stress range histogram must be estimated using data from channel CH_21. Channel CH_21, mounted on the gusset plate near G2 (See Drawing 3 in Appendix A) was included in the long-term monitoring program. The data from this channel can be used to make reasonable estimates of the variable amplitude stress range spectrum at CH_27 and CH_22. Based on a comparison of the data collected during the controlled load tests and the on-site monitoring, the maximum stress range that could be expected at channel CH_27 is about 1/4 to 1/3 of the measured stress range at channel CH_21(see Figure 6.4). The long-term monitoring program indicated that the peak stress range at channel CH_21 was about 5.25ksi. This corresponds to a stress range at channel CH_27 of about 1.75ksi and estimated force of 8.5 kips in the WT 5 x 16.5. This is about 2.2 times greater than measured during the on-site monitoring program. These upper bound values result in out-of-plane stresses of 22ksi to 30ksi in the web gap. An estimate of the number of cycles greater than the CAFL based on the cycle frequency provided in Table 5.7 indicates that cracking resulting from out-of-plane forces could be expected at this type of detail.

Cracks have been observed at similar details in span 10 (e.g., G4 FB22, G1, FB16) [3]. These cracks have been observed to grow through the weld throat and not at the weld toe, which is characteristic of smaller web gaps. The measurements and the finite element model reasonably predict the potential for cracking at this type of detail.

6.3.2 Bottom Web Gap – Interior Girder

At the interior girder, forces applied by the lateral system in bay 1 are resisted by the lateral system in bay 2. Hence, a path of direct force transfer exists at girders G2 and G3. As discussed above, channel CH_32 was installed at the bottom web gap at floorbeam FB24 on girder G2 in bay 1. The gage used at this location was a weldable strain gage that has a 0.25 in. gage length compared with the individual gages contained in the strip gages 0.031 in. used in span 11. As a result, channel CH_32 measures the average strain over a longer length in the gap. In regions of a "steep" strain gradient, the peak strain may not be accurately measured with a longer gage. However, as was illustrated in Sections 4 and 5, single gage CH_7 at FB37 provided comparable stress range values to strip gages CH_10 and CH_11.

The stress ranges measured at channel CH_32 were relatively low during the on-site monitoring, between 1.2 and 1.5 ksi. The primary reason that the measured stress is low is due to the restraint provided by the members on the other side of the web in bay 2. As illustrated in Figure 4.15, the similarity in the response of channels CH_20 & CH_21 indicates that continuity is provided through the connection. Since the forces are mainly resisted by the lateral system and not the web of the interior girder, the stress range in the web gap is lower at the interior girders.

Only limited test data were obtained at FB24 for the bottom connection plate web gap at girder G2 at channel CH_32 and on the lateral strut in bay 1 at channel CH_22. No long-term data were collected at channel CH_32 as the test truck and on-site monitoring resulted in very low stresses at this location. Extensive test data were acquired at CH_19, CH_20 and CH_21 which were located on the gusset plates. Figure 6.7 compares data from channels CH_20 and CH_32 that were collected during of the on-site monitoring. Considering the random data collected on-site, it was found the stress

range at channel CH_32 is typically only 50% to 75% of the stress range at channel CH_22. Conservatively using the upper limit of 75%, the data for channel CH_20 found in Table 5.7, an estimate of the maximum and effective stress range was made for channel CH_32. The results are provided in Table 6.3.

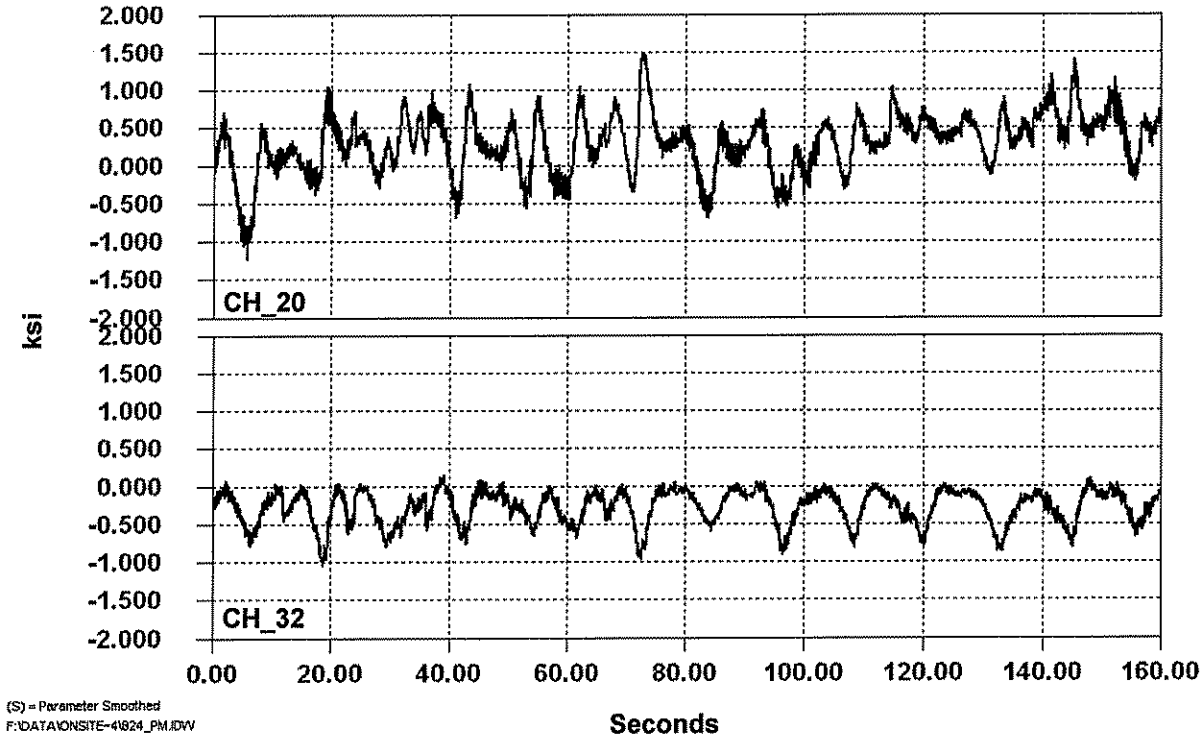

Figure 6.7 – Comparison of response at channels CH_20 and CH_32

Channel / Location	S_{rmax} (ksi)	# Cycles > CAFL[2]		S_{reff} (ksi)	Total # Cycles[1]	Cycles/ Day[3]
		#	%			
CH_20 G2/FB24	6.5	0	0.0	3.0	17,970	327
CH_32 G2/FB24[4]	*4.9*	*0*	*0.0*	*2.3*	*17,970*	*327*

Notes
1. The monitoring program covered the period between September 21, 2000 to November 20, 2000.
2. Assumes Category C.
3. Total number of cycles divided by 55 days.
4. S_{rmax} and S_{reff} calculated using 75% of the measured data for channel CH_20.

Table 6.3 – Estimated maximum and effective stress range at channel CH_32

The results listed in Table 6.3 indicate that web gap cracking at the interior girders would not be expected. Even if the maximum stress is doubled, the maximum stress range is only 9.8 ksi, which is less than the CAFL of the detail. This is compatible with the behavior as no cracking has been observed in Span 10 at any of the bottom web gaps at the interior girders.

A potential retrofit for the two outside girders in span 10 would be to bolt a WT section to the transverse connection plate and the bottom flange, similar to the double angles installed at the top flange. A WT section is suggested as they provide greater stiffness and minimize out-of-plane distortion. These elements can be easily installed on the outside surfaces of Girders G1 and G4 in span 10 between FB10 and FB32 as there are no gusset plates and floorbeam haunches to interfere with the installation. This will permit the installation of at least four bolts in the flange and transverse connection plate connections. More recent retrofits on the I-79 bridge in western Pennsylvania have used a WT 13.5x89 section. The Hoan bridge is using a WT 12x55 section. Both structures used four 7/8 inch A325 bolts in the web and flange connections.

6.3.3 Bottom Web Gaps in Spans 11 (and 9)

As discussed in Sections 4.3.2 and 6.6, the out-of-plane stress ranges experienced from random variable traffic during the long-term monitoring program resulted in stress-range levels that will eventually produce cracking in the bottom web gaps at floorbeams FB2 through FB6 and FB36 through FB40. At these locations it appears desirable to install WT section in both bays one and three. Since no lateral gusset plates exist in bays one and three, the WT sections can be installed on all four girders without a great deal of difficulty. A segment of the transverse connection plate can be removed by cutting a 1-1/2 inch hole in the connection plate centered about 1-1/2 inches above the bottom flange surface and cutting off the end of the stiffener to accommodate the flange of the WT section. The stiffener should be cut using a plasma cutter since it produces a high quality cut surface. This will allow the WT section to be connected to the transverse connection plates with existing bolts from the floorbeam haunch end connections.

6.4 Gusset plate at Floorbeam 34 Girder G3

As previously stated, cracks have been reported at this type of detail at two locations (see Figure 4.17 for a photographs of this detail) 3]. Using the results of the long-term monitoring program, an estimate of the fatigue limit for this detail was made using a conservative fracture mechanics model.

At the free edge of the gusset plate, an estimate of the fatigue resistance can be made from the relationship

$$\Delta K = S_r\sqrt{\pi a} \le \Delta K_{th} \qquad \text{Eq. 6-1}$$

Where "a" is the half width of the lack of fusion (LOF) at the root of the partial penetration groove weld and the reinforcing fillet and ΔK (*delta K*) is the cyclic stress intensity factor at the crack with units of ksi√in. The entire crack is 2a, which is equal to the lack of fusion zone at the detail. Field observations suggest that 2a is approximately equal to 0.25 inches. Knowing ΔK_{th} (*delta K threshold*), an estimate of the maximum allowable ΔK can be calculated. For structural steels with good toughness, a reasonable lower bound estimate for ΔK_{th} is 3.0ksi.√in. Equation 6-1 yields:

$$\Delta K = S_r\sqrt{\pi(0.125)} \ge 3.0ksi\sqrt{in} \qquad \text{Eq. 6-2}$$

$$= 0.63S_r \ge 3.0\text{ksi}\sqrt{\text{in}}$$

Based on the long-term monitoring, the maximum stress range is 7.8ksi which results in a ΔK of:

$$\Delta K = 7.8x0.63 = 4.9ksi\sqrt{in} > \Delta K_{th} \qquad \text{Eq. 6-3}$$

Equation 6-3 indicates that ΔK applied (i.e., 4.9 ksi√in) is greater than the threshold limit of 3.0 ksi√in, and therefore cracking will occur when the threshold is exceeded. At this location, the effective stress range is 3.4ksi (CH_35) and averages about 3,329 cycles/day. At that stress range level, the number of cycles to extend the crack 2a from 0.25 in to 0.75 in can be estimated using the following:

$$N = \frac{1}{A}\int_{0.125}^{.0375}\frac{da}{(S_r\sqrt{\pi a})^3} \qquad \text{Eq. 6-4}$$

$$N = \frac{2}{A(S_{re}^3)\pi^{3/2}}\left[\frac{1}{\sqrt{a_i}} - \frac{1}{\sqrt{a_f}}\right] \qquad \text{Eq. 6-5}$$

$$N = \frac{2}{3.6x10^{-10}(S_{re}^3)\pi^{3/2}}\left[\frac{1}{\sqrt{.125_i}} - \frac{1}{\sqrt{.375_f}}\right]$$

$$N = \frac{9.98x10^{-8}}{3.6x10^{-10}(S_{re}^3)\pi^{3/2}}[2.8284 - 1.633]$$

Hence,

$$N = \frac{11.93x10^{8}}{S_{reff}^3} \qquad \text{Eq. 6-6}$$

Using Equation 6-6 and the measured effective stress range of 3.4 ksi yields a value for "N" of about $30.35x10^6$ cycles. Assuming 3,329 cycles/day (from the long-term monitoring), an estimated life of about 25 years was calculated to extend the existing defects at the gusset edge through its thickness.

Although other cracks may develop, they pose no threat to the integrity of the structure unless the entire weld between the transverse connection plate and the gusset fails. *(If the weld between the transverse connection plate and the gusset plate were to fail, very high out-of-plane stresses would be generated in the web gap since the gusset would only be attached to the web.)* At this time it does not appear necessary to retrofit these limited type of gusset plate connections. Only eight of these type of gusset plates exists. Routine and scheduled inspections should be adequate to assess whether or not cracks will propagate at the gusset plate edge.

6.5 Longitudinal Stiffener Terminations

Strain gages installed at the ends of longitudinal stiffeners were monitored during the controlled load tests and on-site monitoring as discussed in Section 4 (See Table 4..2). One gage, channel CH_4 installed at floorbeam FB35 of girder G1 was included in the long-term monitoring program.

The maximum (S_{rmax}) and effective stress range (S_{reff}) for channel CH_4 was 6.5 ksi and 2.5 ksi, respectively. The fatigue resistance of this detail can be classified as category E with a CAFL of 4.5 ksi. Since the CAFL is exceeded, fatigue crack growth could be expected to occur. At channel CH_4, the estimated remaining fatigue life was calculated to be 106 years, as summarized in Table 6.3. Hence no problems are expected at this specific location.

During the controlled load tests, strain gages installed at the weld termination of the longitudinal stiffener at floorbeam FB37 of girder G3 revealed that the stress ranges produced by the test truck were from 1.3 (CH_51) times greater than at channel CH_4. In order to estimate the fatigue life at these details, the stress-range histogram data collected at channel CH_4 were used to develop approximate effective stress-range values for the other gages installed at the end of the longitudinal stiffeners at G3 FB37. From the long-term monitoring program, it was found that the effective stress range at channel CH_4 is about 1.4 times greater than the stress range produced by the test truck. Assuming that this ratio is similar for all locations, an estimated effective stress range was calculated for the other three strain gages at FB37 Girder G3 (i.e., CH_51). Assuming that the same number of cycles occurs at each location, permits an estimate of the remaining fatigue life at FB37. These results are summarized in Table 6.4.

Channel / Location	S_r Test Truck[1]	S_{reff} (ksi)	1.4xS_r Test Truck	Cycles/ Day[3]	Total Life[2] (Yrs)	Remaining Life[3] (Yrs)
CH_4 G1/FB35	1.8	2.5	2.5	1,464	132	106
CH_51G3/FB37	2.3	-	*3.2*	*1,464*	63	*37*

Notes:
1. Maximum stress range produced by the test truck for all lane positions.
2. Calculated total fatigue life using strain line extension of S-N curve for Category E and the following relationship: $N=(A/S^3_{reff})$ where $A=11x10^8$.
3. Remaining fatigue life was calculated assuming bridge was open for 26 years at time of this report (1974 to 2000).

Table 6.4 - Estimated remaining fatigue life at channels CH_4 and CH_51 located at the termination of the longitudinal stiffener at floorbeam FB37 of girder G3

The predicted lives shown in Table 6.4 indicate that there is little likelihood that fatigue cracks will develop at the ends of the longitudinal stiffeners. Previous experience has demonstrated that cracking at longitudinal stiffener terminations is most likely to occur in the contra-flexure regions of the girder. In these locations, the girders are subjected to the greatest stress reversals due to live load. An effective and relatively simple retrofit is to drill holes at the ends of the stiffener, as shown in Figure 6.8. Considering the life of the bridge and the fact that no cracks have been observed at these details to date, it is sufficient to

inspect these details as any other welded detail and take corrective action if and when required.

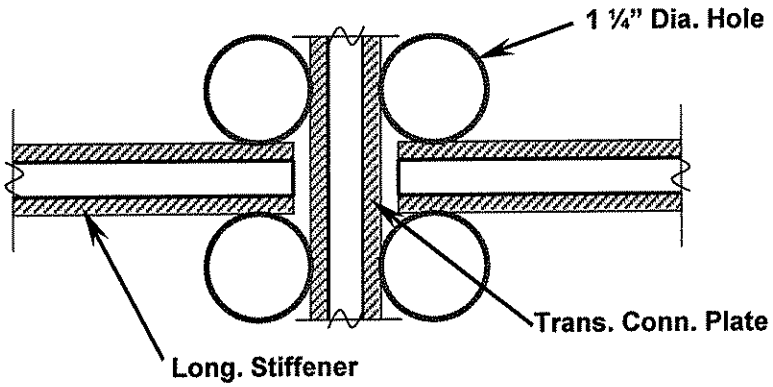

Figure 6.8 - Potential retrofit at longitudinal stiffener weld termination at intersection with transverse connection plates

It should also be noted that the strip gages at the transverse connection plate weld to provided higher values of stress range during passage of the test truck. However, the fatigue resistance of the transverse stiffener is Category C whose fatigue limit is 10 ksi. The test results suggest that the fatigue cracking is not likely to develop at the transverse connection plate weld toes in the web gap.

6.6 Gusset Plates not Attached to the Transverse Connection Plate

Measurements have revealed that at side span locations where the gusset plate is welded to the web but not directly attached to the transverse connection plates on either side of the web are the most critical details on the Kanawha River Bridge. Out-of-plane distortion in the web gap region occurs between the transverse connection plate and gusset plate as shown exaggerated in Figure 6.6. Although the displacement is very small, it is concentrated over a very short web gap length, as shown in Figure 6.9.

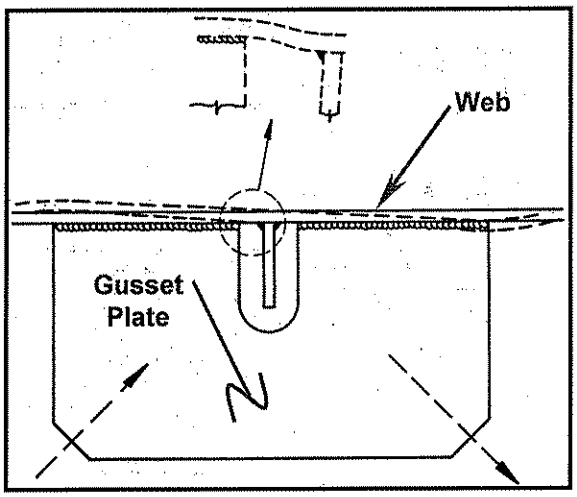

Figure 6.9 - Out of plane displacements at web gaps
between transverse connection plates and gusset plates

This type of connection detail has received considerable attention in the last few months due to the failure of the Hoan Bridge in Milwaukee, Wisconsin on December 13th, 2000. The Hoan Bridge, which carries I-794 over the Milwaukee River, was opened to traffic in 1974. The bridge is supported by three girders, two of which fractured full depth, leaving only one girder remaining. Although the detail used on the Kanawha River Bridge and the Hoan Bridge are similar, there are differences which drastically affect the potential for a similar occurrence on the Kanawha River Bridge. These difference will be discussed later in this section.

The strain gage measurements made both on-site and during the long term monitoring program indicated that high stress cycles are being produced in the web gap region from distortion. Although retrofit angles have been added in the past (see Figure 4.10) they are too light to provide a stiff enough connection between the transverse connection plate and the gusset plate. The most important function of the retrofit is to ensure that the gusset plate, transverse connection plate, and web act together in resisting out-of-plane forces. Hence, stiffness, and not strength must govern the design of any future retrofit.

In order to provide sufficient restraint, it is suggested that the existing angles be removed and replaced with heavier angles or a 1 inch thick plate. The thickness of the angles should be a minimum of ¾". If the angles are limited to the two bolt connections between the outstanding angle legs and the transverse connection plate and the gusset plate,

supplemental welds should be added to the exposed edges of the angle legs and the transverse connection plate and the lateral gusset plates. Alternatively, 1 inch thick plates could be used to replace the 3/8 inch angle segments. A ¾ inch bevel could be fabricated on one edge that would be fitted against the transverse connection plate. This would allow a partial penetration groove weld to be installed between the 1 inch plates and the transverse connection plate. The plates could be held in place with bolts installed in the gusset plate while the weld was made. Then, ½ inch fillet welds could be placed along two edges of the 1 inch plate and the gusset plate surface. All welding would be down hand which should improve the quality. There will be no adverse affects of field welding to the transverse connection plate and gusset plate as the cyclic stress in those elements are low. Appropriate surface preparation and welding techniques should be employed. The lower end of the knee brace and the ends of the diagonals framing into the gusset plate can be trimmed as required. This would allow four bolt connections in the angle legs.

Retrofitting this portion of the connection is only half the solution however. Once the gusset plate and transverse connection plate are firmly connected, an increased out-of-plane displacement will occur in the lower web gap between the transverse connection plate and bottom flange (see Figure 6.10).

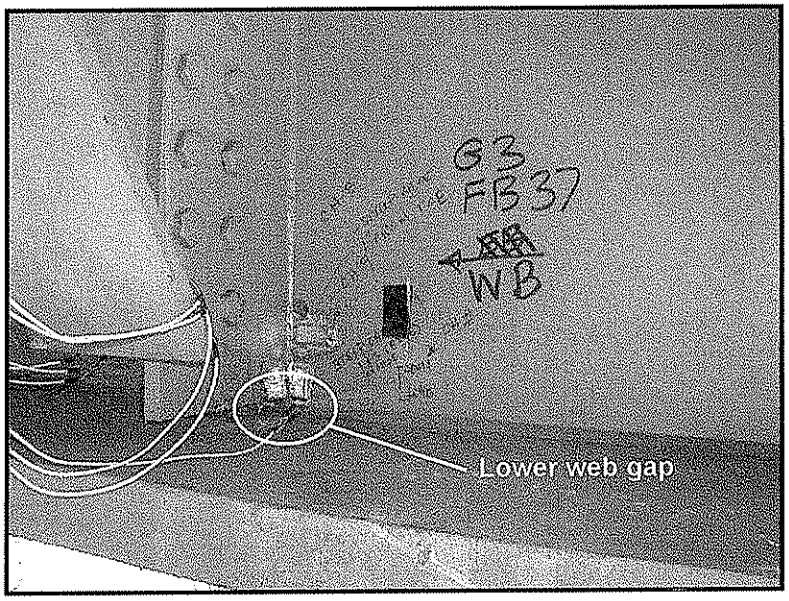

Figure 6.10 - Area susceptible to fatigue cracking after retrofit of connection between the gusset plate and transverse connection plate (opposite side of web shown for clarity)

Out-of-plane distortion can be minimized by attaching the transverse connection plate to the bottom flange. This procedure has been used with success on many bridges throughout the US [9,14]. The connection can be made using a WT section bolted to the transverse connection plate and the bottom flange. Four bolts should be used to connect the web of the WT to the transverse connection plate. The connection between the bottom flange and the WT can also be made with four bolts as well, thereby reducing the holes in the flange. This retrofit may require trimming the end of the transverse connection plate in

some locations to permit clearance for the WT. Adequate stiffness should be provided by a heavy WT section. Considering the low magnitude of measured stresses in the bottom flange, the placement of holes will not be significant. Although this retrofit is needed on every girder at selected floorbeams, it is only needed in bays one and three of the side spans. A WT installed on one side of the girder webs is adequate and will provide sufficient stiffness. The center span A514 steel section would also benefit from the installation of structural tees on the exterior sides of girders G1 and G4. The interior girders G2 and G3 appear to provide reduced levels of distortion with the back-to-back gussets and floorbeam knee-braces that frame into each side of the girders.

6.6.1 Comparison to Hoan Bridge

The connection detail between the gusset plate, transverse connection plate, and web plate of the Kanawha River Bridge is similar in some aspects to that utilized in the Hoan Bridge in Milwaukee Wisconsin. Field inspection and ongoing failure analysis has revealed that there are considerable differences between the two details with respect to detailing and constraint. Figure 6.11 illustrates the "as designed" detail at an interior girder of the Hoan Bridge. The gusset plates on each side of the interior girder web were slotted with a 1 ½ in wide slot. They in turn were welded only to the girder web with a ½ in partial penetration weld in a ¾ in gusset plate. Most often the slotted gusset was pushed against the ¾ in transverse connection plate so that the longitudinal welds overlapped the connection plate fillet welds. This created a condition of high triaxiality in the girder web at the small gap. The high constraint and initial crack-like condition eventually resulted in brittle fracture without significant fatigue crack extension. The high triaxiality resulted in stresses in the girder web that were at least 36% greater than the yield point of the A36 steel web plate.

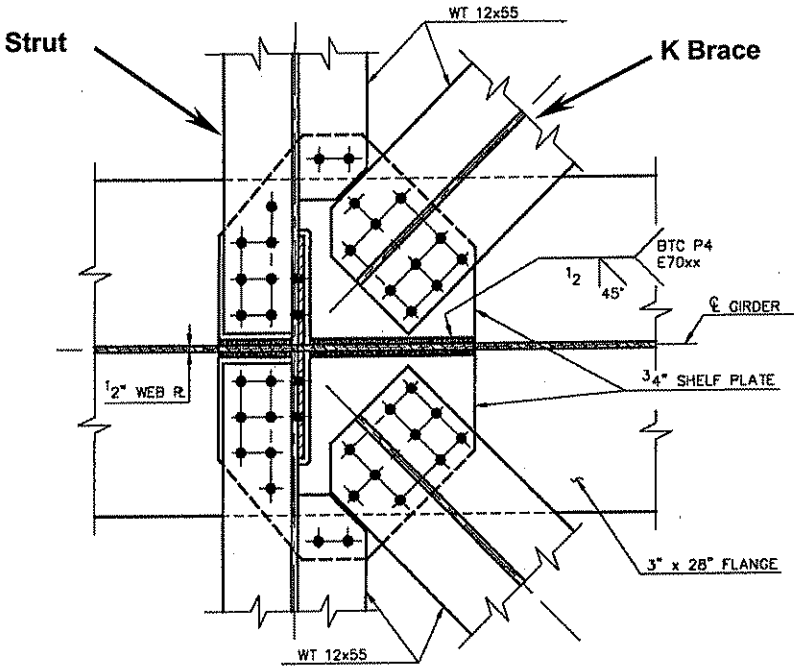

Figure 6.11 Gusset plate detail for interior girder used on failed span of Hoan Bridge in Milwaukee Wisconsin

The fabrication procedures used on the Hoan Bridge, (i.e., placing the gusset plate in contact with the transverse connection plate) were not observed on any of the Kanawha River Bridge slotted gusset details. As a result, the web gap is larger and nearly equal on both sides of the transverse connection plate. In addition, there was only a small "snipe" at the end of the gusset plate slot in the details utilized in the Hoan Bridge. This further reduced the web gap and resulted in overlapping welds increasing the stress and constraint in this region. The details used in the Kanawha River Bridge have a significantly larger web gap, (1 to 1.5 inches). Snipes were observed at all locations inspected in the Kanawha River Bridge, one of which is shown in Figure 6.12. The cutout in the gusset plate was also centered about the transverse connection plate ensuring larger gaps on both sides of the connection plate. This results in a significant reduction in the triaxiality in the web gap so that normal stress conditions are developed. Although susceptible to fatigue cracking from web gap distortion, they are not as susceptible to fracture as the Hoan Bridge.

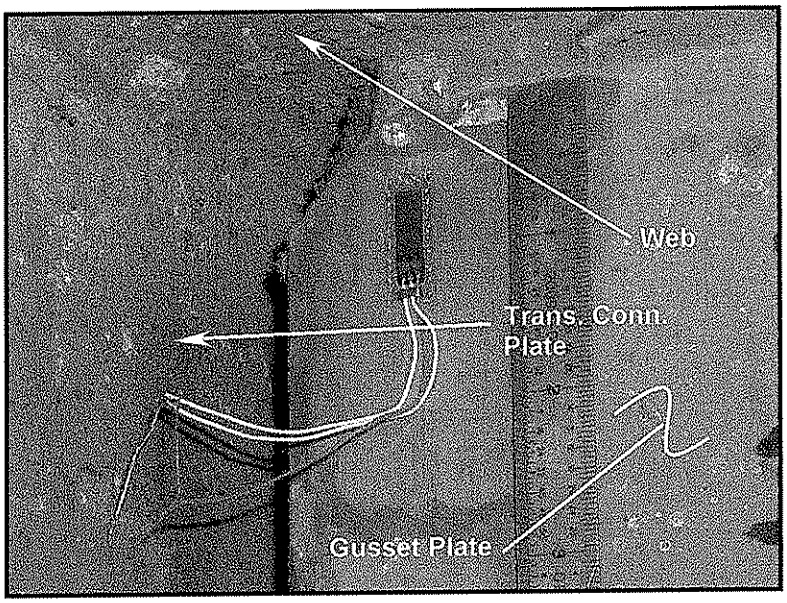

Figure 6.12 - Photograph showing gap between transverse connection plate and gusset plate as built on the Kanawha River Bridge
(Note snipe in gusset plate which increases web gap thereby decreasing stress in the gap)

Although fatigue cracks may grow in the absence of a retrofit, sudden brittle fracture from a macro-scopic fatigue crack is unlikely in the Kanawha River Bridge. Furthermore, the retrofit holes that were installed in 1989 insure that fatigue cracks will be arrested should web gap cracks develop.

7.0 Summary and Recommendations

The measurements carried out on the Kanawha River Bridge assisted in the assessment of the fatigue resistance of various welded details, the adequacy of existing retrofit measures, and the potential for further cracking. Following is a summary of the findings of this study and the recommendations for corrective measures that will further enhance the service life of the bridge structure.

1. The discontinuities identified in the groove welds that were monitored for acoustic emission and indicated to have AE activity are not susceptible to fatigue crack extension. The stress range at those locations assuming a crack-like defect are well below the fatigue crack growth threshold even for the largest stress event.

2. The main girder measurements indicated that although designed as non-composite members, they are acting compositely with the slab for the live loads on the structure. This is beneficial to the structural system and reduces the stress cycle.

3. Each truck was observed to produce one dominant stress cycle in the main girders at the two cross-sections that were instrumented in Spans 10 and 11.

4. Random trucks during the long-term monitoring period produced stress ranges in the main girders that were up to 4 times greater than the stress range (1 ksi) produced by the 58.6 kips test truck. A review of the triggered time history data indicated that these stress range events were the result of heavy trucks similar to the test truck configuration. Permit vehicles were identified by their longer length and slower speed and only a small number of vehicles crossing the bridge exhibited characteristics compatible with the overload vehicle characteristics.

5. At the bottom web gaps at the end of the floorbeam transverse connection plates, out-of-plane stresses were observed to have maximum stress range levels that exceeded the fatigue limit in all girders of side span 11 and the exterior girders of center span 10. The cycle frequency and effective stress range levels as well as reported isolated cracking in the inspection reports confirm that fatigue cracking is expected and occurring. Recommendations for retrofitting these locations are provided in Sections 6.3 and 6.6.

6. The floorbeam transverse connection plate web gap adjacent to the top flange which was retrofitted and bridged with a pair of connection angles in 1989 was found to adequately minimize distortion and will prevent further cracking at those locations throughout the bridge.

7. Most lateral gusset plates in bay 2 are notched and not directly attached to the transverse connection plates in regions of the center and side spans. In side spans 9 and 11 this had resulted in cracking in the past which was retrofitted by the installation of small 3/8 in. angle segments. These were connected to the gusset and the transverse connection plate with two bolts. The retrofit was found to be ineffective allowing continued out-of-plane distortion. The four holes that were also installed will prevent an undesirable fracture but will not prevent crack growth in the web gaps between the vertical holes and the potential for further cracking beyond the holes.

8. It is recommended that the small angles be replaced with heavier angles so a stiffer connection can be provided between the angle legs and the gusset and transverse connection plate. One option is to provide a combination of two bolts with welded joints or alternative a four bolt joint should be provided in both angle legs. A second option is to replace the smaller angles with 1 inch thick plates that are beveled on one edge so that a ¾ inch partial penetration weld could be made between the plate and the 7/8 inch transverse connection plate. Fillet welds could be used on two edges of this plate to connect it to the lateral gusset plate (See Section 6.6).

9. The lateral gusset plates in Span 10 are also slotted and not attached to the transverse connection plate. However, the total connection differs from the side spans as the transverse struts under the floorbeams in bays 1 and 3 are attached to shorter gusset plates that lie in the same plane. These gussets are welded to the web and transverse connection plates in bays 1 and 3 and prevent web gap distortion. This mode of behavior was verified by the experimental measurements. No other positive attachment is needed in bay 2.

10. The lateral gusset plates at several bay 2 floorbeams (i.e. FB34) in the side span are welded to the web and to the transverse connection plate. These transverse weld joints are partial penetration groove weld with a root reinforcing fillet weld. They provide an embedded lack of fusion condition that has been identified as a crack at the edge of the gusset plate. An assessment based on the long-term measurements indicates that it will require about 25 years to extend the existing defects through the gusset plate thickness. Only 8 of these details exist. It is recommended that no corrective action be taken and the details be monitored during routine scheduled inspections. That will permit an assessment of whether or not these are truly a crack-like condition susceptible to crack growth.

11. The longitudinal stiffeners are cut short at the transverse stiffeners and floorbeam connection plates. This provides a Category E detail at the end of the longitudinal stiffener weld and Category C at the transverse connection plate welds in the web gap. No cracking has been detected to date and none appears to be likely in the next three decades. These locations are also recommended for routine scheduled inspections particularly near inflection points where stress reversal is occurring. Should cracking ever develop it can be easily retrofitted by installing holes above and below the web gap as illustrated in Section 6.5.

12. Another alternative that should be explored is to evaluate the feasibility of removing the lateral gusset plates and laterals in bay two of the floorbeams in side spans 9 and 11. This would include floorbeams FB2 through FB6 and FB36 through FB40. This will require sufficient analysis to ascertain if the structural system can resist the lateral forces that would be transmitted to Piers 8 and 11 through the composite acting structure. This type of retrofit is being used to remove all of the bottom lateral system of the Hoan bridge in Milwaukee.

References:

1. American Association of State Highway and Transportation Officials, *AASHTO LRFD Bridge Design Specifications 2nd Edition & 2000 Interims*, Washington, D.C.
2. AASHTO fatigue assessment
3. Bridge Inspection Report for South Charleston-Dunbar Bridge, Bridge #20-64-53.27 (2550), Prepared by Burgess and Niple, Prepared for the West Virginia Department of Transportation, Division of Highways, November 12, 1999.
4. Acoustic Emission Monitoring of Electroslag and Butt Welds on the Dunbar Bridge, Publication No. FHWA/WV-85-002, West Virginia Department of Transportation and Federal Highway Administration, 1985.
5. Miner, M.A., *Cumulative Damage in Fatigue*, Journal of Applied Mechanics, Vol. 1, No.1, Sept., 1945.
6. Downing S.D., Socie D.F., *Simple Rainflow Counting Algorithms*, International Journal of Fatigue, January 1982.
7. Fisher, J.W., Nussbaumer, A., Keating, P.B., and Yen, B.T., *Resistance of Welded Details Under Variable Amplitude Long-Life Fatigue Loading, NCHRP Report 354*, National Cooperative Highway Research Program, Washington, DC, 1993.
8. *Steel Structures – Material and Design*, Draft International Standard, International Organization for Standardization, 1994.
9. Fisher, J.W., *Bridge Fatigue Guide – Design and Details*, American Institute of Steel Construction, 1977.
10. Fisher J.W., Jin J., Wagner, D.C., Yen, B.T., *Distortion-Induced Fatigue Cracking in Steel Bridges NCHRP Report 236*, National Cooperative Highway Research Program, Washington, DC, December, 1990.
11. Moses, F., Schilling, C.G., Raju, K.S., *Fatigue Evaluation Procedures for Steel Bridges, NCHRP Report 299*, National Cooperative Highway Research Program, Washington, DC, 1987.
12. Schilling, C.G., *Variable Amplitude Load Fatigue, Task A - Literature Review: Volume I - Traffic Loading And Bridge Response*, Publication No. FHWA-RD-87-059, Federal Highway Administration, Washington, DC, July 1990.
13. Fisher, J.W., Menzemer, C.A., Lee, J.J., Yen, B.T., Kostem. C.N., *Distortion Induced Stresses in a Floorbeam-Girder Bridge: Canoe Creek*, Fritz Laboratory Report, 500-2(86); April, 1986.
14. Cornelia, D.E., Fisher, J.W., Fatigue Cracking of Steel Bridge Structures Vol-1, A Survey of Localized Cracking in Steel Bridges, 1981 to 1988, Publication No. FHWA-RD-89-166, Federal Highway Administration, Washington, DC, March 1990.

ACKNOWLEDGMENTS

This work was conducted for TY Lin International and funded by the West Virginia Department of Transportation. Thanks are also due to the West Virginia Department of Transportation for their support during the field testing and providing the test truck.

The authors would like to recognize Mr. Russ Longenbach, Mr. Zuo-Zhang Ma, and Mr. Brian Metrovich for their efforts during the field investigations of this project. In addition, Mr. Duncan Paterson greatly assisted in the preparation of the as-built gage plans.

Appendix A

Gage Plans

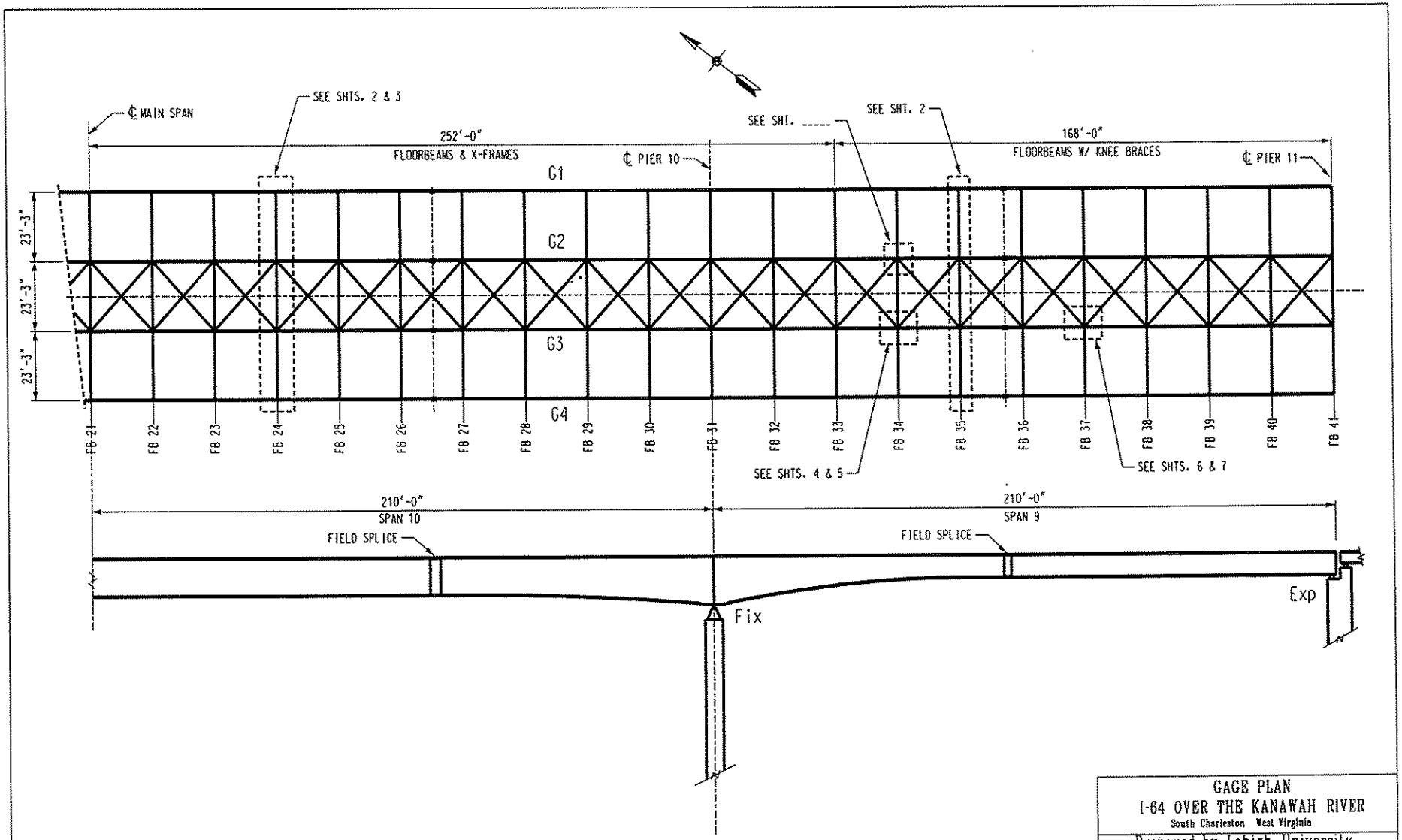

GAGE PLAN
I-64 OVER THE KANAWAH RIVER
South Charleston West Virginia

Prepared by Lehigh University
Bethlehem PA

Date - 4/25/00	Rev - 1/22/01	
Des- JWF/RJC	Drawn - RJC	1 OF 8

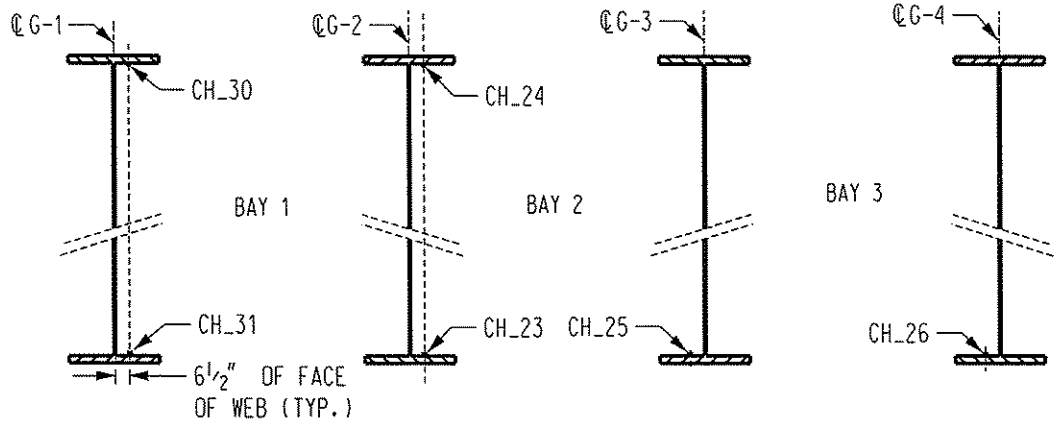

CROSS SECTION AT 24" WEST OF FB 24
GAGES MOUNTED ON MAIN GIRDERS
LOOKING EASTBOUND

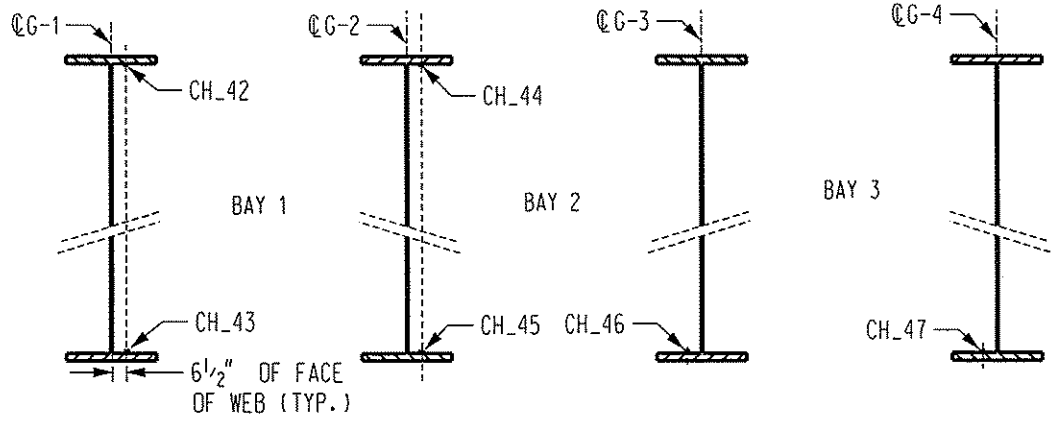

CROSS SECTION AT 24" WEST OF FB 35
GAGES MOUNTED ON MAIN GIRDERS
LOOKING EASTBOUND

FB24 & FB35 - MIAN GIRDER GAGE PLAN I-64 OVER THE KANAWAH RIVER South Charleston West Virginia		
Prepared by Lehigh University Bethlehem PA		
Date - 4/25/00	Rev - 1/22/01	
Des- JWF/RJC	Drawn - RJC	2 OF 8

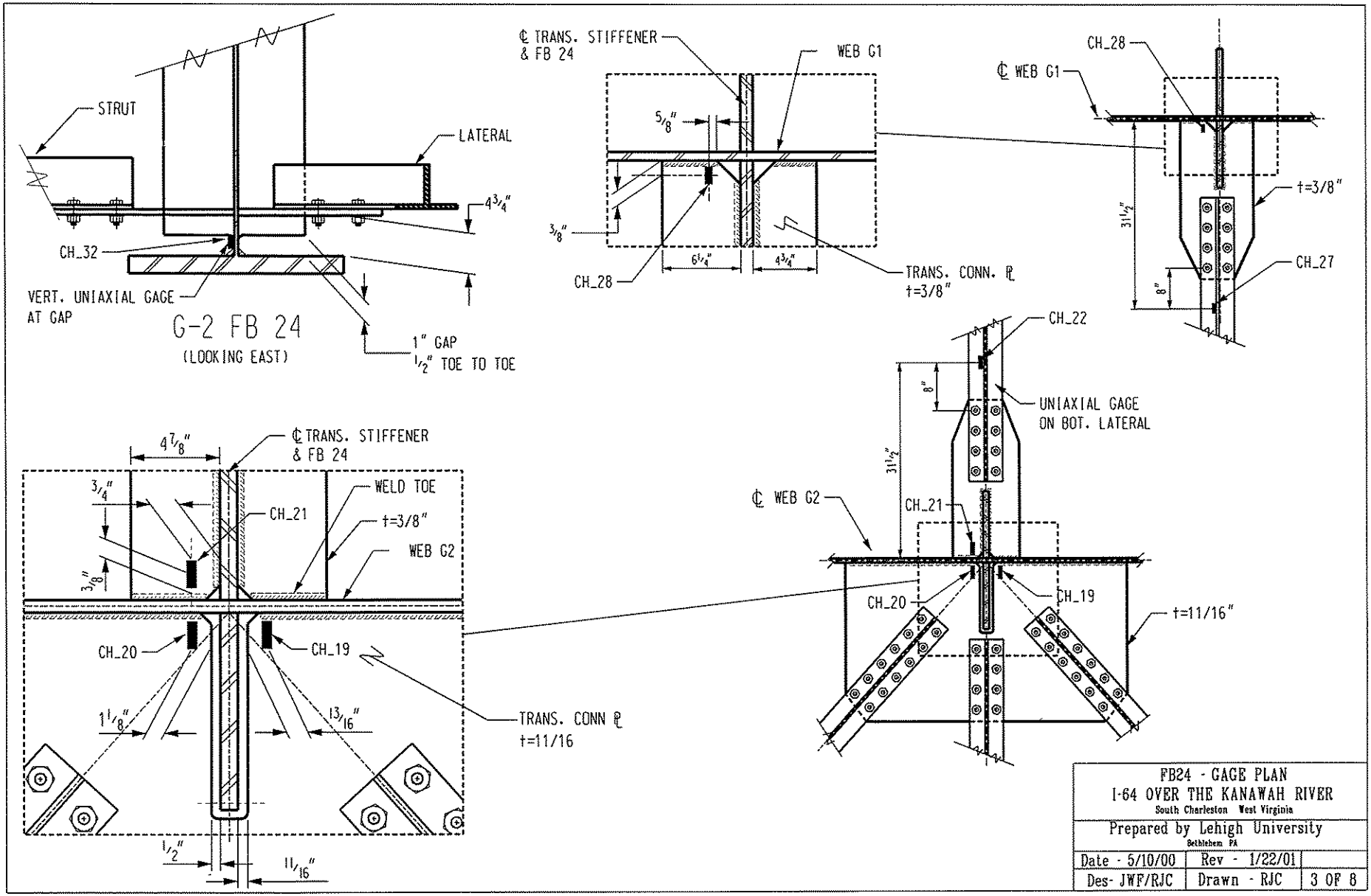

FB24 - GAGE PLAN
I-64 OVER THE KANAWAH RIVER
South Charleston West Virginia

Prepared by Lehigh University
Bethlehem PA

Date - 5/10/00	Rev - 1/22/01	
Des- JWF/RJC	Drawn - RJC	3 OF 8

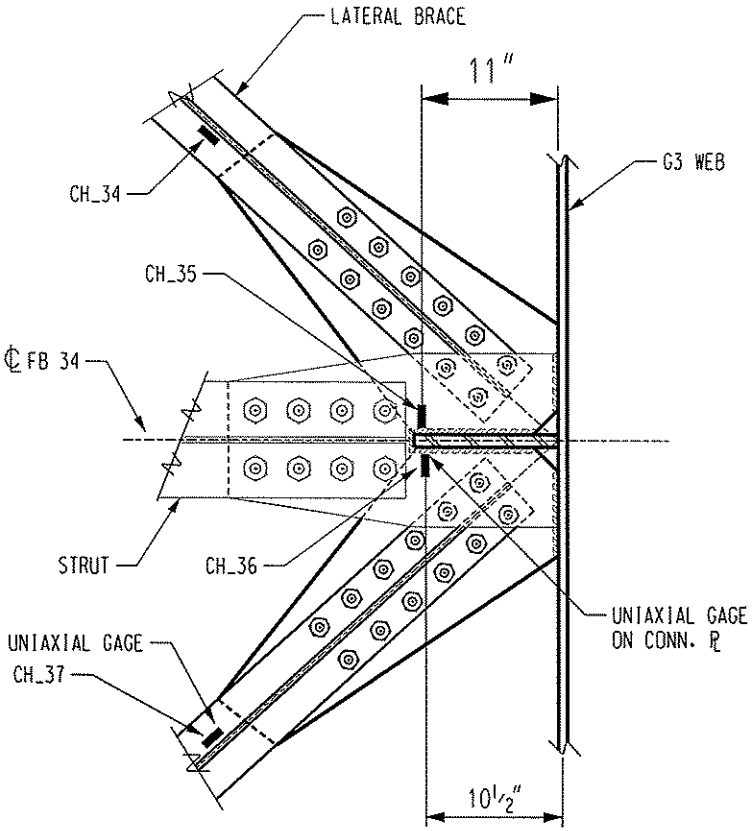

VIEW C-C

(FB KNEE BRACE NOT SHOWN FOR CLARITY)

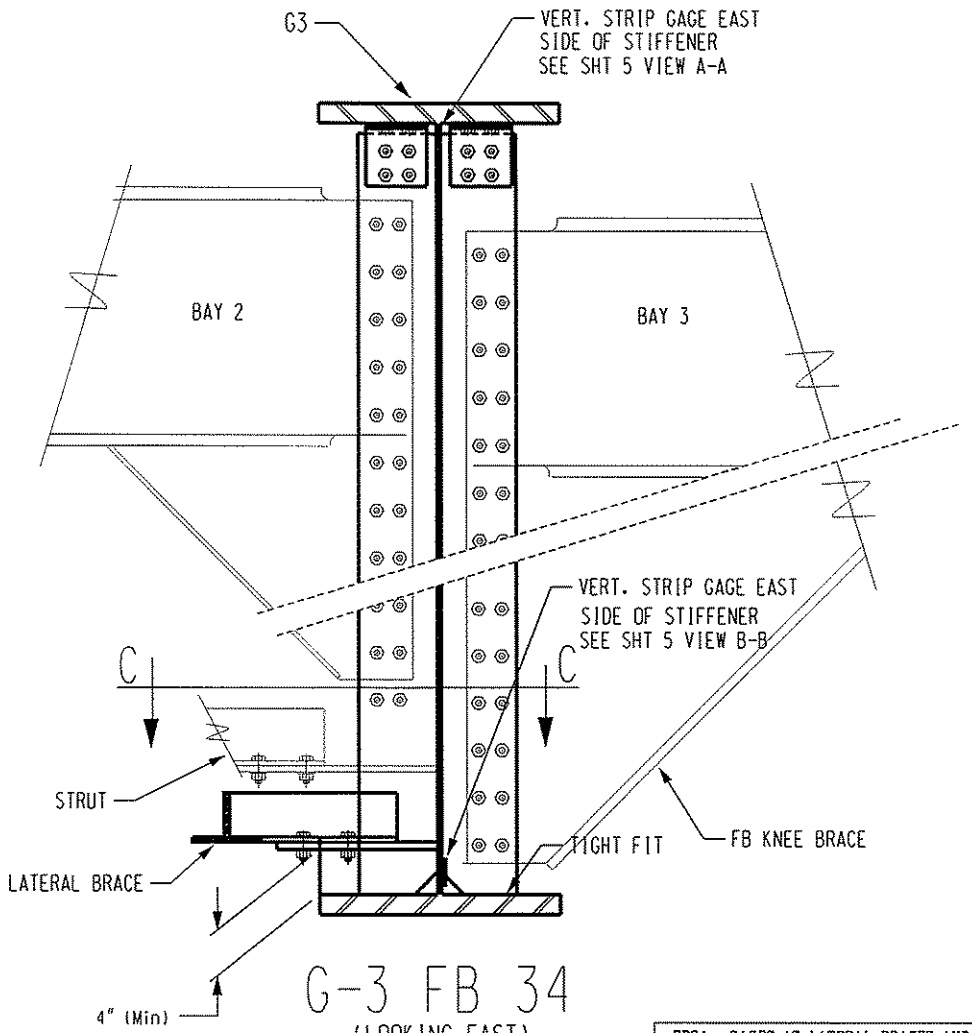

G-3 FB 34

(LOOKING EAST)

FB34 - GAGES AT LATERAL BRACES AND STRUTS I-64 OVER THE KANAWAH RIVER South Charleston West Virginia		
Prepared by Lehigh University Bethlehem PA		
Date - 4/10/00	Rev - 1/10/01	
Des- JWF/RJC	Drawn - RJC	4 OF 8

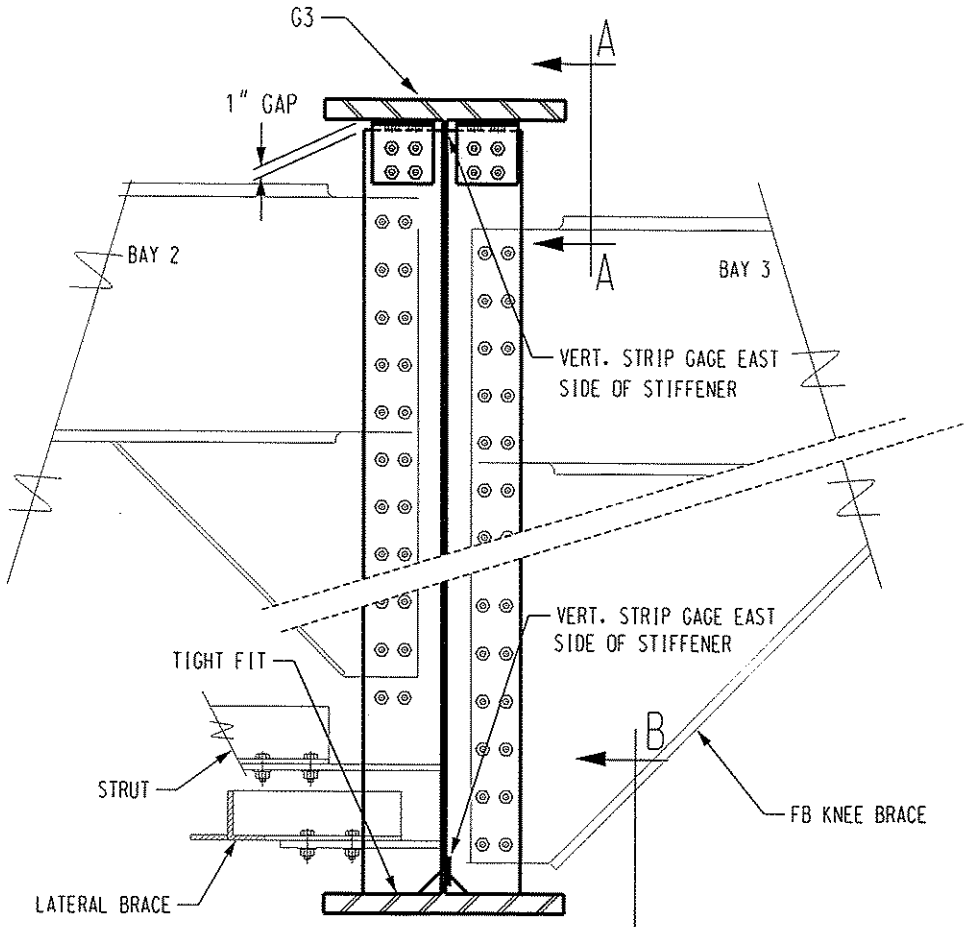

G-3 FB 34
(LOOKING EAST)

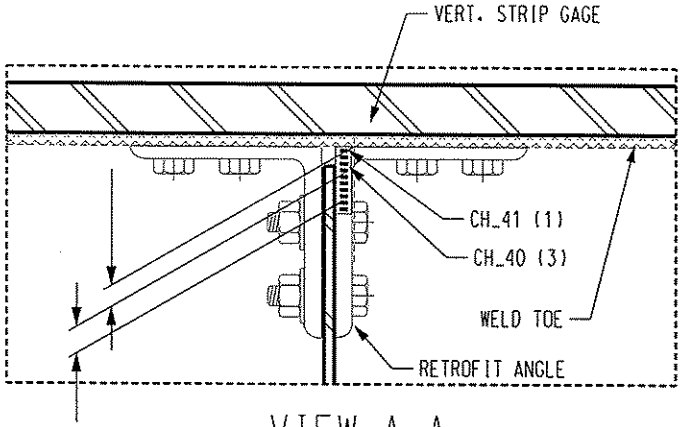

VIEW A-A
(LOOKING NORTH)

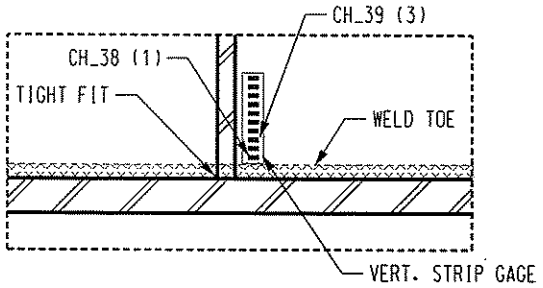

VIEW B-B
(LOOKING NORTH)

FB34 - GAGES AT TOP & BOT WEB GAP I-64 OVER THE KANAWAH RIVER South Charleston West Virginia		
Prepared by Lehigh University Bethlehem PA		
Date - 4/10/00	Rev - 1/23/01	
Des- JWF/RJC	Drawn - RJC	5 OF 8

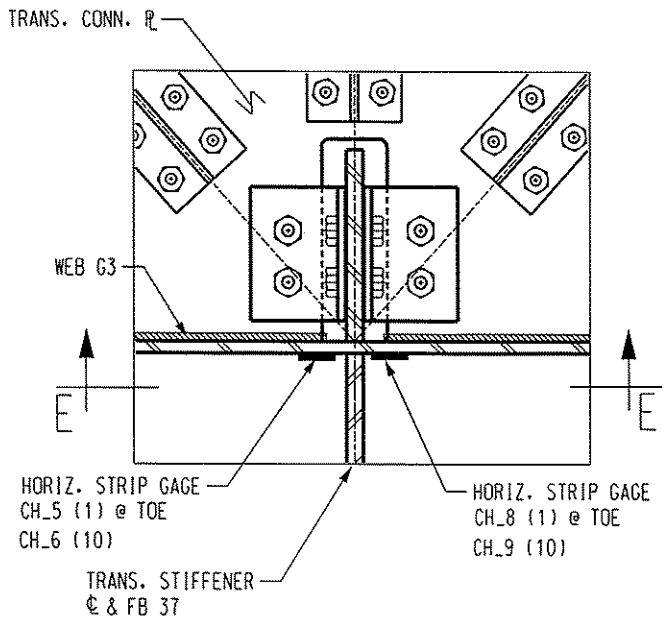

PLAN VIEW @ BF G3 - FB 37

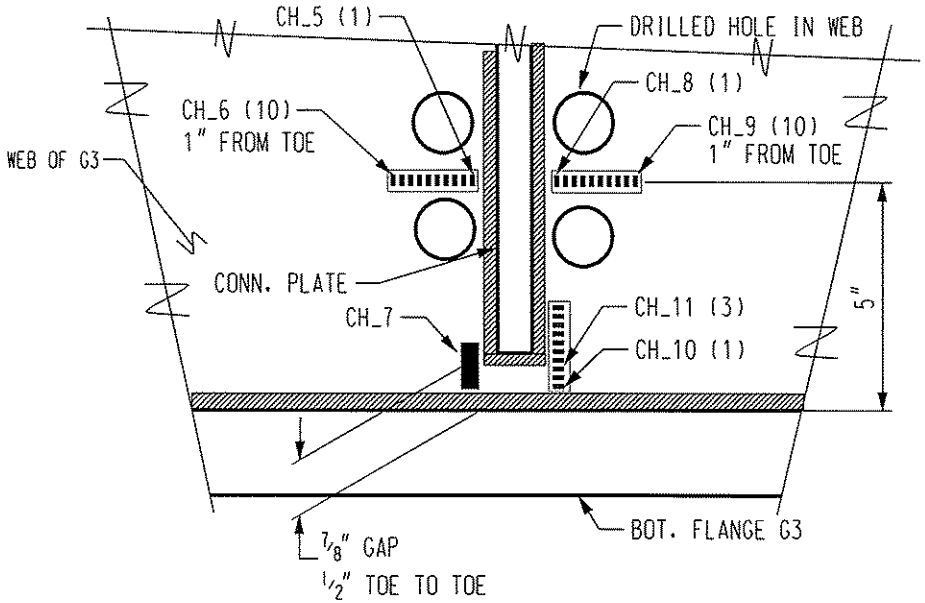

VIEW E-E
LOOKING NORTH @ G3 - FB 37

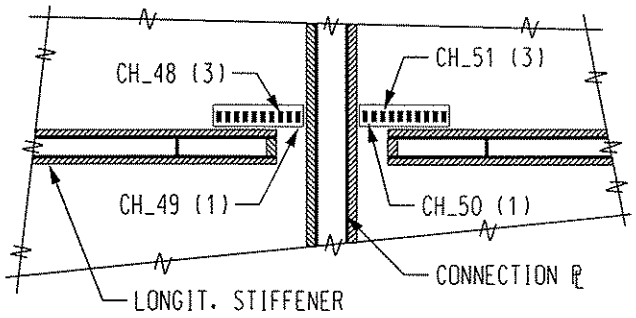

ELEV. VIEW @ LONGIT. STIFENNER
G3 - FB 37

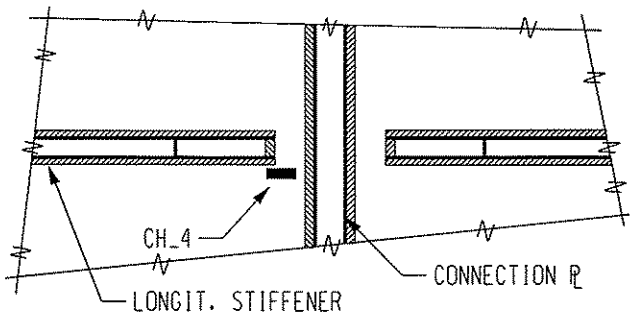

ELEV. VIEW @ LONGIT. STIFENNER
G1 - FB 35

G3 FB37 GAGE PLAN I-64 OVER THE KANAWAH RIVER South Charleston West Virginia		
Prepared by Lehigh University Bethlehem PA		
Date - 5/10/00	Rev - 1/23/01	
Des- JWF/RJC	Drawn - RJC	6 OF 8

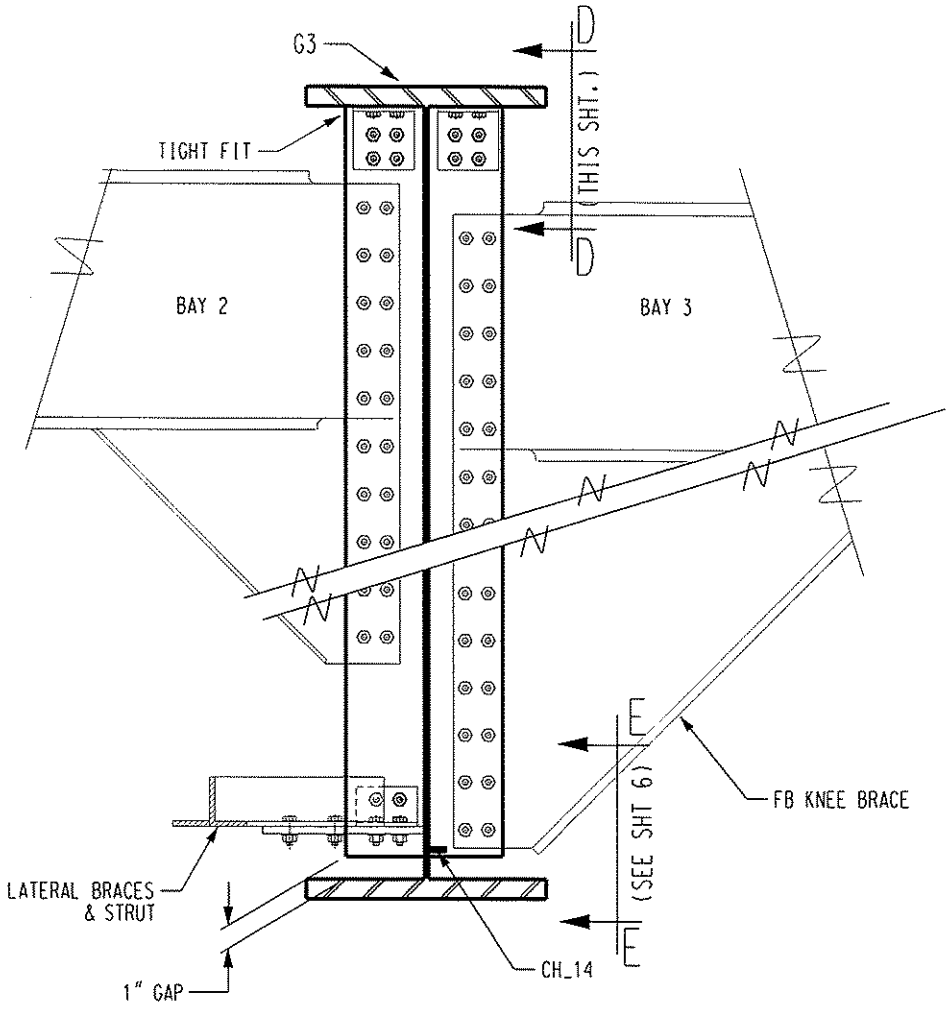

G-3 FB 37

(LOOKING EAST)

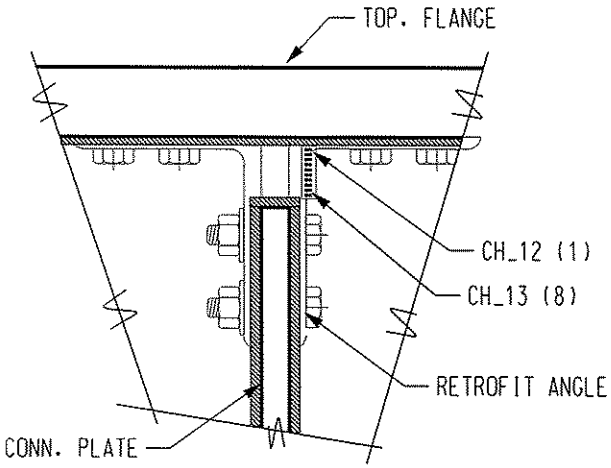

VIEW D-D

LOOKING NORTH @ WEB OF G3 - FB 37

PROPOSED GAGE PLAN FB 37 I-64 OVER THE KANAWAH RIVER South Charleston West Virginia		
Prepared by Lehigh University Bethlehem PA		
Date - 5/10/00	Rev - 1/23/01	
Des- JWF/RJC	Drawn - RJC	7 OF 8

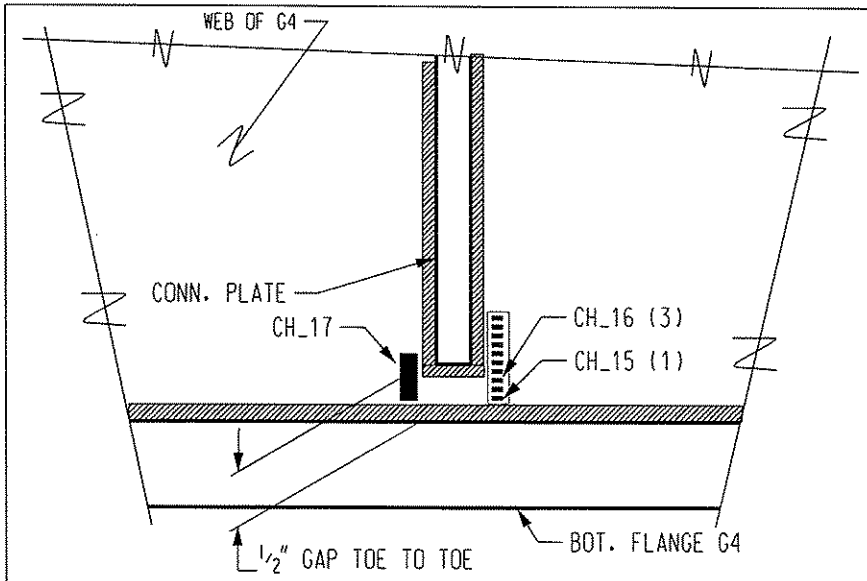

LOOKING NORTH @ G4 - FB 37

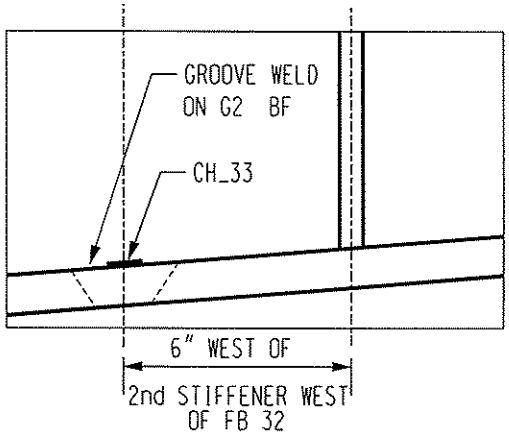

CH_33 ON GROOVE WELD
(LOOKING NORTH @ G2)

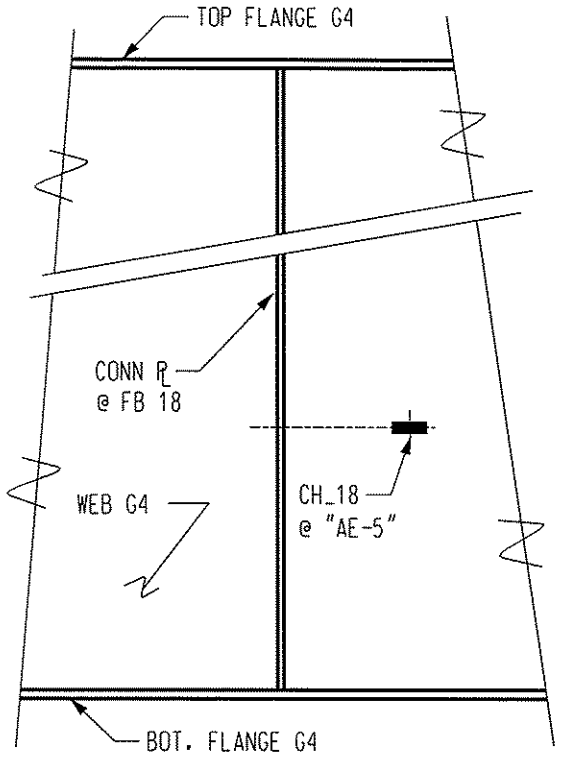

GAGE LOCATED AT "AE-5"
LOOKING SOUTH @ G4 - FB 18

FB 18, FB 33, FB 37 MISC. GAGE DETAILS I-64 OVER THE KANAWAH RIVER South Charleston West Virginia		
Prepared by Lehigh University Bethlehem PA		
Date - 5/10/00	Rev - 1/23/01	
Des- JWF/RJC	Drawn - RJC	8 OF 8

Appendix B

Summary of Permit Load Data

I 64 Over Kanawha River - S. Charleston, WV.

GVW (lbs.)	Total Length (ft.)	# of Axels	Axle Load Max (lbs.)	Date	Direction	Speed (mph)	Comments
96000	75	5	21000	9/27/2000	East	?	Sunday Move
100000	80	5	22500	10/24/2000	West	?	
100000	80	5	22500	10/20/2000	West	?	Sunday Move
102820	65	6	20660	10/19/2000	East	?	
103000	71	5	22750	10/16/2000	West	?	
104000	71	5	23000	10/11/2000	West	?	
105500	65	6	21500	10/19/2000	West	25	
108000	80	6	22500	10/24/2000	West	?	
120000	75	7	18000	10/19/2000	West	10	
122000	72	6	25000	10/6/2000	?	?	
122000	60	7	23000	10/12/2000	East	?	
124000	80	7	18700	11/17/2000	East	20	
125000	85	6	25000	10/10/2000	East	?	Sunday Move
125000	85	6	20000	10/19/2000	West	?	Sunday Move
125000	75	6	25000	10/19/2000	East	?	Sunday Move
125000	75	6	25000	10/19/2000	East	?	Sunday Move
126000	80	7	19000	9/28/2000	East	15	
126000	75	7	20000	11/6/2000	West	?	
127000	70	7	20000	9/20/2000	East	30	
130000	72	7	19167	10/10/2000	West	?	
132000	75	6	30000	10/10/2000	West	?	
132000	75	7	20000	10/11/2000	West	?	Sunday Move
132000	75	7	20000	10/11/2000	West	?	Sunday Move
132000	75	7	20000	10/19/2000	East	?	
133000	110	7	20000	9/27/2000	West	20	
134500	72	8	17500	10/12/2000	West	25	
135000	66	6	24000	11/2/2000	East	25	
140000	72	7	22000	9/27/2000	East	20	
140000	72	7	22000	9/27/2000	East	20	
140000	71	8	19000	10/6/2000	?	?	
142000	66	6	25400	10/6/2000	?	30	
142000	74	8	18750	10/18/2000	?	?	
144000	83	8	19000	9/27/2000	East	?	
144000	90	8	20000	10/3/2000	East	?	
145000	76	7	22333	9/21/2000	East	25	
145000	76	7	22333	9/21/2000	?	25	
145000	79	8	20000	9/25/2000	West	20	
145000	79	8	19000	10/11/2000	West	25	
145000	79	8	19000	10/26/2000	West	30	
145000	80	8	19000	10/26/2000	West	?	
146000	80	8	20000	11/3/2000	West	?	Sunday Move
147000	96.33	8	20000	9/19/2000	East	25	
148000	85	8	20000	10/11/2000	East	?	
148000	88	8	20000	11/1/2000	East	20	
149800	123	7	23400	9/19/2000	East	20	
149800	123	7	23400	11/6/2000	East	?	
149900	123	8	21400	9/19/2000	East	20	
149900	123	8	21400	11/6/2000	East	?	
150000	95	8	20000	9/21/2000	East	25	
150000	78	8	20000	10/17/2000	East	20	
150000	108	8	20000	10/18/2000	East	25	
150000	108	8	20000	10/18/2000	East	25	
150000	81	8	20000	10/27/2000	West	20	
150000	108	8	20000	10/30/2000	East	25	
150000	85	8	20000	11/8/2000	East	20	
150000	80	8	20000	11/9/2000	East	25	
151000	78	7	23000	10/10/2000	West	30	
152000	83	8	20000	9/26/2000	East	25	

152000	95	8	20000	10/5/2000	East	?	
152000	80	8	20000	10/10/2000	?	20	
153000	110	8	20000	9/26/2000	West	25	
153000	110	8	20000	9/26/2000	West	25	
154700	123	8	21400	11/6/2000	East	?	
155000	79	8	21000	10/10/2000	West	20	
155000	79	8	21000	10/13/2000	West	20	
157000	77	8	23550	10/11/2000	West	20	
158100	69.5	8	22275	9/26/2000	East	?	
160000	80	8	23000	9/21/2000	?	?	
160000	78	7	25000	10/18/2000	West	25	
161000	84	8	21250	9/26/2000	West	20	
161000	84	8	21250	9/26/2000	West	20	
161000	85	8	23000	9/26/2000	East	25	
161000	80	8	21000	10/12/2000	West	25	
161000	80	8	21000	10/26/2000	West	25	
163000	74	8	23000	9/21/2000	East	25	
165000	72	7	25000	11/1/2000	East	20	
170000	72	7	25833	10/20/2000	East	?	
171000	102	9	20000	9/21/2000	East	25	
172000	100	9	20000	9/26/2000	West	?	20-77-106.11 Failed
172000	104	9	20000	11/14/2000	West	?	
180500	106	10	18833	10/26/2000	West	?	
186000	98	11	20000	9/19/2000	West?	15	
186000	103	10	21000	10/13/2000	West	?	
188000	110	10	22000	9/26/2000	West	?	
188000	110	10	22000	10/6/2000	West	30	
188000	110	9	22000	10/25/2000	West	30	
189000	108	10	22500	10/30/2000	West	?	
192000	90	10	20000	9/26/2000	East	25	
192000	103	10	22000	10/5/2000	West	20	
192000	104	9	22500	10/13/2000	East	25	
192000	104	9	22500	10/13/2000	West	25	
192000	110	10	22000	10/25/2000	West	25	
192000	110	9	20000	11/13/2000	East	25	
192000	118	10	20000	11/15/2000	West	25	
195000	118	11	20000	9/28/2000	West	?	
195000	100	10	21000	11/8/2000	West	25	
196000	110	10	23000	10/4/2000	West	25	
196000	110	10	23000	10/18/2000	East	25	
196000	110	10	23000	10/18/2000	East	25	
197000	113.5	11	20000	9/29/2000	West	30	
198000	110	10	22000	10/18/2000	West	25	
200000	123	11	18700	10/10/2000	West	?	
206000	110	11	22000	9/21/2000	West	20	
206000	130	11	20000	9/26/2000	East	30	
216000	110	12	20000	11/9/2000	West	15	
216330	122.5	13	17700	9/18/2000	E-W(Return)	25	
216330	122.5	13	17700	9/19/2000	E-W(Return)	20	
217000	124	?	?	9/21/2000	East	?	
217000	116	12	24000	9/26/2000	East	20	
220000	119.5	12	20000	10/5/2000	West	25	
220000	124	12	23000	10/25/2000	East	?	
220000	126	13	20000	10/25/2000	West	25	
220000	126	13	20000	10/25/2000	West	25	
223000	129.75	13	18400	10/26/2000	West	30	
224000	123	13	17666	10/13/2000	West	20	
224000	123	13	17666	10/19/2000	West	20	
228000	126	13	18000	11/1/2000	West	25	
230000	120	13	18000	10/25/2000	East	?	
232000	140	13	18000	11/2/2000	West	25	
240000	135	13	19000	10/26/2000	West	?	
243000	150	13	20000	10/3/2000	West	20	
248200	164	13	20000	11/6/2000	East	20	
298000	164	18	22000	9/22/2000	West	?	